Aus der Klinik für Anaesthesiologie
der Ludwig-Maximilians-Universität München
Direktor: Prof. Dr. med. Bernhard Zwißler

Ketogenic diet enhances human T-cell immunity and reprograms the immunometabolism of Th_{17} and regulatory T cells

Dissertation
zum Erwerb des Doctor of Philosophy (Ph.D.)
an der Medizinischen Fakultät der
Ludwig-Maximilians-Universität München

vorgelegt von
David Effinger
aus Friedrichshafen

2022

Mit Genehmigung der Medizinischen Fakultät der

Ludwig-Maximilians-Universität zu München

First evaluator:	Prof. Dr. Dr. med. Simone Kreth
Second evaluator:	Prof. Dr. Elisabeth Deindl
Third evaluator:	Prof. Dr. Ludger Klein
Fourth evaluator:	Prof. Dr. Anne Krug

Dean:	Prof. Dr. med. Thomas Gudermann

Date of defense:	17.11.2022

Table of contents

1 Abstract

Western dietary habits with excessive consumption of carbohydrates are recognized to evoke chronic inflammatory processes, which in turn contribute to the rising prevalence of many non-communicable diseases in today's society. Ketogenic diets (KD), characterized by a profound reduction in carbohydrate intake, lead to the production of ketone bodies (mainly β-hydroxybutyrate, BHB) as alternative substrates for energy production. Although emerging evidence has highlighted the multifaceted functions of ketone bodies, including potential protective immunomodulatory properties, possible effects on human adaptive immunity have not yet been addressed. Therefore, this thesis aimed at investigating the impact of ketone bodies on human T-cell immune response *in vitro,* using a model mimicking a KD and in a cohort of healthy volunteers enrolled in a first-in-human prospective intervention study following a three-week ketogenic diet. We showed that ketones markedly enhanced human $CD4^+$ and $CD8^+$ T-cell immunity as indicated by substantial transcriptional changes and increased secretion of respective key cytokines which also functionally translated into elevated cell lysis capacity. Furthermore, differentiation of distinct $CD4^+$ T-cell populations was shown to be altered beyond the classical Th_1/Th_2 dichotomy as the reciprocally linked balance of regulatory T cells (T_{reg}) and pro-inflammatory Th_{17} cells was markedly shifted in favor of the anti-inflammatory immunoregulatory phenotype. Concomitantly, the formation of pathogenic Th_{17} cell subsets, closely associated with autoimmune diseases, was reduced. Differentiated metabolic analyses revealed a fundamental and in fact opposite immunometabolic reprogramming of these two $CD4^+$ T helper cell lineages in response to ketone bodies. Mitochondrial respiratory capacity in T_{reg} was significantly elevated, whereas both oxidative phosphorylation and glycolysis in Th_{17} cells were compromised. Taken together, this study proves ketone bodies to be powerful regulators of human adaptive immunity and sheds new light on dietary interventions as feasible and potentially supporting therapeutic tools in modern medicine.

2 Introduction

Over the last two centuries, human life expectancy has experienced a tremendous increase. This is commonly attributed to breakthrough advances in medical care, universal access to public health services, as well as increasing prosperity, a stable food supply and improved working conditions[1–3]. Yet over the last decades, adaptation to our industrialized, comfortable, and mostly sedentary way of life has resulted in the development of a vast set of medical conditions such as obesity, diabetes, and cardiovascular diseases, generally grouped under the rather innocuous-sounding term "lifestyle diseases". This delusive label almost gives the impression that these disorders inevitably belong to our newly gained years of life and therefore cannot be all that bad. However, these non-communicable diseases are accountable for more than half of all deaths worldwide[4,5]. Now that most infectious diseases are manageable, "diseases of lifestyle" have become the new modern scourge of humanity and for the first time in many years life expectancy is predicted to decline[6,7].

Although there is no doubt about a genetic component, environmental, and especially behavioral determinants contribute most to the development of lifestyle-related morbidities. Our Western way of life, characterized by reduced physical activity, alcohol consumption, and increased intake of ultra-processed food high in refined carbohydrates, has become one of the biggest risk factors for our extended lifespan[8,9]. Recent studies have directly linked today's diet to the induction and maintenance of chronic inflammatory processes that set the stage for various immune-mediated diseases[4]. Nutritional interventions, hence, bear a promising potential to counteract these deleterious effects and should be considered and investigated both as preventive and as potentially curative measures.

However, many large observational studies in nutrition research often rely on unverifiable recall-based assessment methods that do not allow conclusions to be drawn about the relationship between diets and health or disease. A large number of these studies therefore are more akin to pseudoscientific reports as evidenced by the sad reality that much of what was once believed to be an established fact in nutrition science has already had to be revised[10,11].

With this in mind, the present thesis discusses for the first time the immunomodulatory impact of a very-low-carbohydrate diet on human T-cell immunity. By providing the long-required immunological scientific background, this may help to redefine nutritional interventions as clinical tools in modern treatment concepts.

2.1 WESTERN DIET AND INFLAMMATION

When reading newspapers or nutrition guides, one increasingly comes across rather lurid phrases such as “Sugar is the new tobacco!” or “Sugar, the secret killer.”. Even if these statements are of course not to be understood literally, there is certainly more than just a small grain of truth in them. The exact composition of macronutrients for a healthy diet has long been the subject of controversy. Although first warnings about the harmful effects of high sugar intake on the development of diseases were issued as early as the 1950s, many studies in the past have successfully cast doubt on the hazards of carbohydrates drawing attention to fat and cholesterol as the real dietary culprits[12,13]. Indeed, the myth that lipids directly clog our arteries, causing coronary heart disease and high blood pressure has persisted in our society for decades. Until today, the German Nutrition Society (Deutsche Gesellschaft für Ernährung e.V. / DGE) considers a diversified and balanced diet to contain only limited amounts of fat and states that more than 50 % of daily dietary energy should be provided by carbohydrates[14]. This perception of macronutrients is clearly reflected in the way we eat today. Although, according to the latest “*Ernährungsreport 2021*” published by the German Federal Ministry of Food and Agriculture (BMEL), 90 % of the consumers attach great importance to health-promoting aspects of food[15], our modern diet is characterized by an excess of calories and an increased consumption of fast-acting carbohydrates[8]. High-energy meals are readily available everywhere and comparatively cheap: On average, a European consumes over 30 kg of added sugar per year[16].

This "Western diet" is increasingly considered to be one of the major causes of many chronic, non-communicable lifestyle diseases. A high carbohydrate intake followed by an increase in plasma glucose and insulin levels triggers erroneous chronic inflammatory processes through activation of the NLRP3 inflammasome[9,17]. Inflammasomes are cytoplasmic multimeric protein complexes that play a pivotal role in the induction of inflammatory responses and can be activated by a plethora of endogenous and exogenous stimuli. Pathogen-associated molecular patterns (PAMPs), highly conserved, characteristic molecules, found on the surface of invading pathogens, or danger-associated molecular patterns (DAMPs), released from damaged or dying cells are recognized by different kinds of pattern-recognition receptors (PRRs) assembled in the inflammasome complex. Upon binding of PAMPs and DAMPs to PRRs, downstream signaling cascades promote proteolytic cleavage and release of pro-inflammatory cytokines interleukin(IL)-1β and interleukin(IL)-18[18,19]. Appropriate activation of inflammasomes is essential for adequate immune protection against exogenous pathogens and promotes tissue repair in response to cellular damage, whereas abnormal, and persistent activation is closely linked to the pathogenesis of a variety of chronic (auto-)inflammatory diseases[19,20].

Recent work has demonstrated that a Western diet is recognized by the organism as a sterile inflammatory stimulus and therefore triggers and maintains chronic systemic inflammation in an NLRP3-dependent manner, reprogramming immune cells toward pro-inflammatory phenotypes[8,17]. A postprandial increase in plasma glucose enhances IL-1β secretion by macrophages, which in turn promotes insulin production. These insulin spikes further stimulate production of IL-1β and reactive oxygen species (ROS), leading to inflammasome activation. Normalizing of blood glucose levels attenuates this self-aggravating loop and is able to prevent the development of feeding-induced inflammation[21].

Acute inflammatory reactions are usually self-limiting and cease after a successful elimination of the trigger (resolution). This is achieved by a well-orchestrated interplay of pro- and anti-inflammatory mediators, eventually resulting in the generation of pro-resolving mediators[22,23]. If this interplay is disturbed, recovery and return to immunological homeostasis may fail to occur, which leads to a chronic low-grade inflammatory environment. Western eating habits appear to constantly fuel such undirected activation of immune cells, which at the beginning progresses in a subclinical manner, but in the long term might cause irreversible tissue damage by promoting potentially harmful autoreactive T cells. As a result, a persistent imbalance between the functional distinct T cell lineages in favor of inflammatory phenotypes paves the ground for various chronic (auto-)inflammatory disorders[4,24].

2.2 ADAPTIVE IMMUNITY AND IMMUNOLOGICAL DISORDERS

There is growing evidence that Western dietary patterns not only trigger innate immune cells but also dysregulate adaptive immunity by promoting $CD4^+$ Th_1 and Th_{17} subsets, closely associated with autoimmunological disorders, while attenuating anti-inflammatory regulatory T cells and Th_2 cell lineages. Given the complex heterogeneity of human T cells, particularly regarding $CD4^+$ T cells, the distinction between targeted immune responses to pathogens and harmful inflammatory processes due to an imbalanced T-cell pool is essential[25–27].

2.2.1 $CD8^+$ T-cell immunity

Acting as an intersection between the innate and adaptive immune system, presentation of pathogenic antigens by antigen presenting cells (APC) leads to the activation of specific T lymphocytes with different and complementary roles. This provides the basis of a targeted immune

reaction against the pathogenic stimulus. Immunization via T-cell receptor-mediated recognition of antigens bound to major histocompatibility complex (MHC) I on APC promotes the induction of a profound $CD8^+$ T-cell response. When in contact with pathogenic or diseased cells, these cytotoxic T cells release their granules which contain perforin and granzymes as their key effector proteins. The former polymerizes and forms pores in the cell membranes of target cells, through which proteases, such as granzyme B, can diffuse in order to initiate apoptotic signaling pathways[28,29]. Moreover, $CD8^+$ T cells secrete IFNγ and TNFα. IFNγ is known to be a multifunctional pro-inflammatory molecule that plays a pivotal role in innate and adaptive immunity. By inducing MHC I and II as well as stimulating the differentiation and migration of cytotoxic T cells and phagocytosing macrophages, it is essential for a profound and effective pathogen clearance[30,31]. TNFα likewise belongs to the group of cytotoxic effector molecules that are released by $CD8^+$ T cells and whose expression is significantly increased upon stimulation[32].

2.2.2 $CD4^+$ T-cell immunity and T helper cell lineages

$CD4^+$ T cells play a crucial role in directing immune responses. Following activation by pathogen-derived peptides presented by MHC II on APC, they differentiate into distinct T helper cell subsets depending on the respective cytokine milieu and antigen stimulation. T helper cells represent a rather heterogeneous pool of cells consisting of different lineages, each with distinct functional patterns. Their immunological features are by no means unidirectional, as the different subgroups also can play even opposing roles in inflammatory processes[33,34]. A well-functioning immune system particularly relies on a balanced equilibrium and an undisturbed interplay between the different T helper cell subpopulations.

For a long time, T helper cells were thought to be restricted to only two major subsets, Th_1 and Th_2. However, this classical two-component model quickly became obsolete as a growing number of $CD4^+$ T-cell types has been recognized over the last years[34].

2.2.2.1 Th_1 / Th_2 cells

T helper cells type 1 (Th_1) mediate cellular host defense against invading intracellular pathogens. In the presence of IFNγ and IL-12, naive T cells increasingly express the transcription

factor T-bet which further drives the development into the Th_1 lineage by enhancing the formation of a Th_1-promoting environment, thereby self-reinforcing lineage differentiation. Th_1 cells are characterized by the secretion of their key cytokine IFNγ. In turn, pro-inflammatory IFNγ promotes differentiation of phagocytic M1 macrophages and enhances pathogen eradication by cytotoxic T cells[34,35].

In contrast, in the presence of IL-4, naive T cell differentiation is polarized toward the Th_2 type which is achieved by increased expression of Th_2 key transcription factor GATA3. Th_2-mediated immunity is part of the humoral immune response and important for eradication of extracellular parasites and bacterial infections. Th_2 cells mainly produce IL-4, IL-5, and IL-10, but do not secret IFNγ, which has long been considered the main distinguishing feature between Th_1 and Th_2 subsets. IL-4 stimulates antibody production by B cells and up-regulates MHC class II production, whereas IL-5 is a key mediator of eosinophil activation. IL-10 exerts pleiotropic functions, but its principal effects are considered to be primarily anti-inflammatory: It suppresses synthesis of various pro-inflammatory cytokines in both innate and adaptive immune cells, inhibits antigen presentation on APC, and directs macrophage differentiation toward M2 macrophages, thus promoting wound healing by dampening inflammatory processes[34,35].

In both lineages, autocrine and paracrine IL-2 acts as a potent growth factor driving clonal expansion, proliferation, and survival, while the respective Th_1 and Th_2 master cytokines subsequently inhibit the differentiation of the opposing lineage[34,36,37].

2.2.2.2 Regulatory T cells and Th_{17} cells

While $CD4^+$ T cells were initially assumed to divide into only two lineages, it has now become clear that various distinct T helper subsets exist beyond the Th_1/Th_2 dichotomy. Among those, regulatory T cells (T_{reg}) and pro-inflammatory Th_{17} cells have emerged as prominent key players in regulating the immunological equilibrium. Although both share some similar requirements during the initial developmental phase, upon differentiated STAT activation they bifurcate into distinct phenotypes with opposite functional properties. Even after differentiation, they retain a certain degree of plasticity, and an imbalance between the two cell lineages is closely associated with the development of autoimmunity[38,39].

Nearly 10 years after the implementation of the Th_1/Th_2 paradigm, Sakaguchi et al. characterized a novel, regulatory $CD4^+$ T cell subset that puts the break on inflammatory processes[40].

Activation of immune cells occurs as a physiological response triggered by various pathogenic and harmful factors and aims at the immediate elimination of the injurious agent. However, without regulation, these initially coordinated processes, as crucial as they are for human host defense, can turn into persistent or recurrent inflammation which drives the development of many inflammatory and autoimmune disorders. Regulatory T cells are capable of attenuating effector T-cell differentiation and function preventing pathological auto-reactivity and are hence indispensable for maintaining a physiological immune homeostasis[4,41].

T_{reg} develop directly in the thymus or may arise from naive $CD4^+$ T cells in the periphery driven by specific cytokines and molecules such as TGFβ, IL-2 or retinoic acid. FOXP3 serves as the lineage-specific master transcription factor. Although the IL-2 receptor α-chain CD25 is not exclusively expressed on T_{reg}, they are generally characterized as $CD4^+$ $FOXP3^+$ $CD25^+$. The suppressive capacity is mediated by the expression of inhibitory cytokines as well as specific surface proteins. Secretion of TGFβ and IL-10 dampens T-cell function and proliferation and also attenuates the expression of antigen presenting MHC II as well as costimulatory molecules on macrophages, thereby impeding signaling pathways vital for T-cell activation[42,43]. Cytotoxic T-lymphocyte-associated protein 4 (CTLA4), constitutively expressed in T_{reg}, acts as an immune checkpoint. Binding of CTLA4 to costimulatory membrane proteins CD80 and CD86 on dendritic cells leads to their internalization by a process known as trogocytosis, which thus compromises CD80/CD86-mediated costimulation via CD28 expressed on effector T cells[44].

The comparatively recent discovery of Th_{17} cells, named after their hallmark cytokine IL-17, has once again broadened the spectrum of T helper cells, and fundamentally changed the understanding of adaptive immunity as Th_{17} cells quickly emerged as powerful adversaries of immunosuppressive T_{reg}[45–47]. The IL-17 family comprises six members, IL-17A to IL-17F, among which IL-17A is the most investigated protein that plays a predominant role in Th_{17}-mediated inflammatory processes. IL-17F is highly homologous to IL-17A but appears to be considerably less potent, and its role in autoimmune models is still controversial[48,49]. The cytokine environment associated with differentiation into Th_{17} cells includes several molecules whose individual roles in human Th_{17} development are not yet as well characterized as in mice and in some cases are not without controversy. IL-1β, IL-6 and TGFβ are generally associated with the conversion of naive $CD4^+$ T cells into Th_{17} cells, while IL-21 and IL-23 seem more vital for maintaining a stable Th_{17} population post-differentiation. However, Th_{17} cells do not represent a homogenous cell compartment but display a substantial functional plasticity. Non-classical IL-17A producing cells, which are able to co-express IFNγ, are named $Th_{17.1}$ as they combine cytokine patterns of both Th_1 and Th_{17} lineages and represent a more inflammatory and disease-driving subpopulation. In contrast, classical Th_{17} cells do not express IFNγ. Shift

to the Th_1-like phenotype is driven by IL-12 and IL-23 as well as by a constant pro-inflammatory cytokine milieu, whereas TGFβ has been discussed as a potential inhibitor of the pathological $Th_{17.1}$ subset[50–52].

Under physiological conditions, Th_{17} cells markedly contribute to the host defense against extracellular bacterial and fungal pathogens. Key cytokines IL-17A and IL-22 maintain mucosal barrier function by promoting granulopoiesis and inducing a chemotactic cytokine gradient for neutrophil recruitment to sites of pathogen invasion. Additionally, both also stimulate production of antimicrobial peptides[38,53]. Although Th_{17} cells undoubtedly exhibit beneficial and essential protective properties, there is clear evidence linking them intimately to autoimmune and inflammatory diseases[51,54].

T_{reg} and Th_{17} cells differ markedly in terms of their functional properties but are also metabolically distinct. While Th_{17} cells mainly rely on glycolysis in order to support differentiation and pathogenicity, T_{reg} meet their energy demands via oxidative phosphorylation (OXPHOS) fueled by oxidation of fatty acids (FAO)[55,56]. It should be pointed out that these pathways not only provide energy required for mere cell survival, but that metabolic reprogramming is increasingly recognized as a crucial mediator of T-cell functionality[39,57].

2.2.3 T-cell immunity and (auto-)inflammatory diseases

Both Th_1 and Th_{17} lineages have been shown to be implicated in the pathogenesis of autoimmune and inflammatory diseases, whereas T_{reg} mediate immunological tolerance. Th_1 cells and their pro-inflammatory cytokines IFNγ and IL-12 were long considered to be the sole scapegoats for the development of autoimmunity. However, over time, several studies have called this dogma into question, as IFNγ- and IL-12-knockout animals were still susceptible to experimentally induced autoimmune disorders, while deficiency of IL-23 appeared to protect against the respective diseases. The subsequent discovery of IL-23-dependent Th_{17} cells has led to a paradigm shift regarding the role and interplay of distinct T helper cells in the onset and maintenance of various medical conditions. In particular, the well-balanced ratio between T_{reg} and Th_{17} cells was found to be crucial for human immune homeostasis (Fig. 1)[46,47].

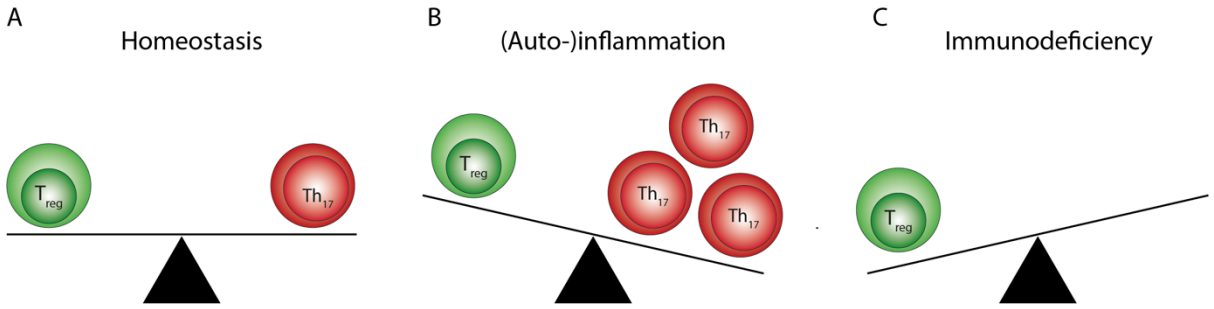

Figure 1: Impact of T_{reg}/Th_{17} balance on immunologic functionality. A balanced equilibrium between both cell lineages is essential for a regulated and efficient immune response (**A**). An imbalance in favor of Th_{17} cells is closely linked to (auto-)inflammatory disorders (**B**), while Th_{17} deficiency markedly compromises human host defense as Th_{17} cells play an essential role in the protection against extracellular pathogens (**C**).

In rheumatoid arthritis (RA), Th_{17} cells are abundantly present in the synovial fluid and in the plasma. Subsequent secretion of IL-17A and IL-22 promotes synovial inflammation leading to destruction of bone and cartilage[58–60]. Concentrations of both cytokines have been shown to significantly correlate with RA disease activity and also might serve as potential biomarkers of therapy response as plasma levels only decrease in therapy-responsive RA patients[61]. In psoriasis, increased secretion of IL-6, IFNγ and IL-23 by pathologically activated dendritic cells (DC) also favors polarization of Th_{17} cells and impairs suppressive activity of T_{reg}. The following cytokine milieu then promotes expression of neutrophil chemoattractants, thereby sustaining a chronic inflammatory microenvironment. Moreover, through activation of STAT3, IL-17A and IL-22 also act directly on epidermal cells inducing aberrant hyperproliferation and hyperplasia of keratinocytes, which further exacerbates severe psoriatic skin lesions[62–64]. On the other side of the balance, T_{reg} from patients with psoriasis were functionally impaired and not able to counteract hyperinflammatory processes[65,66].

Of note, not every Th_{17} phenotype is equally associated with the development of autoimmunological processes. In particular, $Th_{17.1}$ cells have been shown to be closely linked to autoimmune disorders compared to "classical" Th_{17} cells. This subset not only displays a unique pathogenic cytokine pattern by secreting both IL-17A and IFNγ but is also less susceptible to immunosuppressive regulatory T cells[52]. They also appear to be particularly resistant to glucocorticoids and anti-inflammatory IL-10, which further emphasizes their potential as drivers of hyperinflammation[58,67]. $Th_{17.1}$ cells, but not the classical phenotype, have been shown to exacerbate autoimmune encephalomyelitis in mouse models. In colitis and inflammatory bowel disease, together with Th_1 cells, $Th_{17.1}$ cells are also found to be potent inductors and mediators of disease activity[68–70]. Especially Th_{17} cells co-expressing IFNγ are highly enriched in synovial fluids of

patients with RA and juvenile idiopathic arthritis[59,71]. Concurrently, further studies demonstrated that therapy responses in RA correlated significantly with the decrease in $Th_{17.1}$ cells. Moreover, $Th_{17.1}$ cells are also found at high rates at sites of inflammation in patients with sarcoidosis and multiple sclerosis[72,73]. Deciphering the complex mechanisms of how distinct T-cell lineages contribute to the onset and perpetuation of autoreactive disorders, recognizing the prominent role of Th_{17} cells in this context, has recently led to the development of new promising therapeutic options that directly target the Th_{17} axis[64,74]. Furthermore, a recent animal study showed that mice fed a high-carbohydrate diet developed dermatitis-like skin conditions. Notably, this was accompanied by increased levels of IL-17A and IFNγ as well Th_1-associated IL-12 in the psoriatic lesions, linking the pathogenic Th_{17} signaling pathways to Western dietary habits[25].

2.3 CARBOHYDRATE RESTRICTION AND KETOGENIC DIET

The possibly harmful effects of our modern Western eating habits, which usually contain large amounts of carbohydrates, are gaining increasing scientific and public attention[8,75]. As a result, low-carbohydrate, ketogenic(-like) diets and fasting have become increasingly popular in recent years. However, these diets are often marketed as lifestyle trends without the actual molecular biological background being discussed, let alone understood.

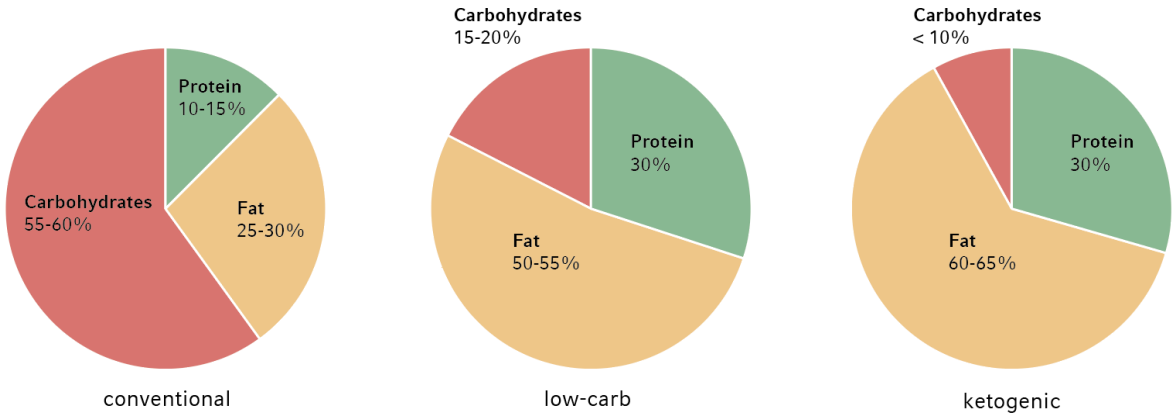

Figure 2: Composition of macronutrients in diets. Representation of typical ratios of carbohydrates, protein, and fat in conventional, low-carb and ketogenic diets[76].

The terms "low-carbohydrate" and "ketogenic" are not clearly defined, so it is always important to pay attention to the respective composition of macronutrients when looking at nutrition studies. Typically, carbohydrates are the main source of energy these days. They usually account for about 55-60 % of daily dietary energy. Many "low-carbohydrate" diets involve a reduction of carbohydrates to about 15-20 % while increasing the proportion of proteins and fats. In ketogenic diets, less than 10 % of daily energy should be provided by carbohydrates (Fig. 2)[76].

Under conditions of carbohydrate restriction, prolonged fasting and extreme physical stress, β-oxidation of fatty acids (FAO) is increasingly used for energy supply. However, the metabolization of fatty acids is not equally possible for all organs as the brain can only utilize ketone bodies but not fatty acids in addition to glucose. Therefore, the synthesis of ketone bodies from fatty acids serves as an evolutionarily conserved mechanism for energy provision, whereas metabolism of ketogenic amino acids accounts for only 4 % of ketone body concentration[77–79].

These approaches not only appear to offer well-known benefits of lower sugar consumption such as loss of body weight, but appear to have far-reaching immunological implications[75,80,81].

2.4 KETONE BODIES

2.4.1 Ketone body metabolism

Acetyl-CoA, the end product of fatty acid degradation, usually enters the Krebs cycle (tricarboxylic acid cycle, TCA) and is oxidized for energy production. Thus, under normal conditions ketone bodies are formed only in very low concentrations, with plasma levels varying between approximately 100 and 250 µM. However, the production of ketone bodies can rapidly increase up to 5 mM in healthy adults during numerous conditions, including starvation, carbohydrate-restricted diets and postexercise[82,83]. Since in these cases, oxaloacetate is being increasingly used for gluconeogenesis, it is no longer available in sufficient form as a substrate for the Krebs cycle, which is thereby significantly slowed down. In order to still be able to meet energy requirements, glycogen, and protein breakdown and in particular fat catabolism are significantly increased. The latter leads to a higher concentration of free fatty acids in the blood followed by an increased fatty acid oxidation in the liver. However, the resulting acetyl-CoA cannot be sufficiently utilized via the decelerated TCA and is therefore used by the liver to synthesize ketone bodies[84].

Synthesis of ketone bodies occurs in the mitochondrial matrix of hepatocytes where fatty acids are broken down into acetyl-CoA via β-oxidation. Subsequently, two molecules of acetyl-CoA are condensed into acetoacetyl-CoA (AcAc-CoA) by the enzyme thiolase. Next, the mitochondrial isoform of 3-hydroxy-3-methylglutaryl-CoA synthase (HMGCS2) catalyzes the rate-determining reaction of acetoacetyl-CoA with another acetyl-CoA and H_20 into β-hydroxy-β-methylglutaryl (HMG)-CoA. HMG-CoA lyase (HMGCL)-mediated cleavage of acetyl-CoA from HMG-CoA results in the formation of the first ketone body acetoacetate (AcAc). Most of the acetoacetate is reduced to β-hydroxybutyrate (BHB), the most abundant ketone body, in an NAD^+/NADH-coupled reaction trough β-hydroxybutyrate dehydrogenase (BDH1). Spontaneous decarboxylation of small amounts of acetoacetate to acetone plays only a minor role under physiological conditions. This gaseous ketone body cannot be further metabolized and is excreted in the urine or exhaled, which is then the source of the characteristic sweet odor, especially during pathological ketoacidosis (Fig. 3A)[85,86].

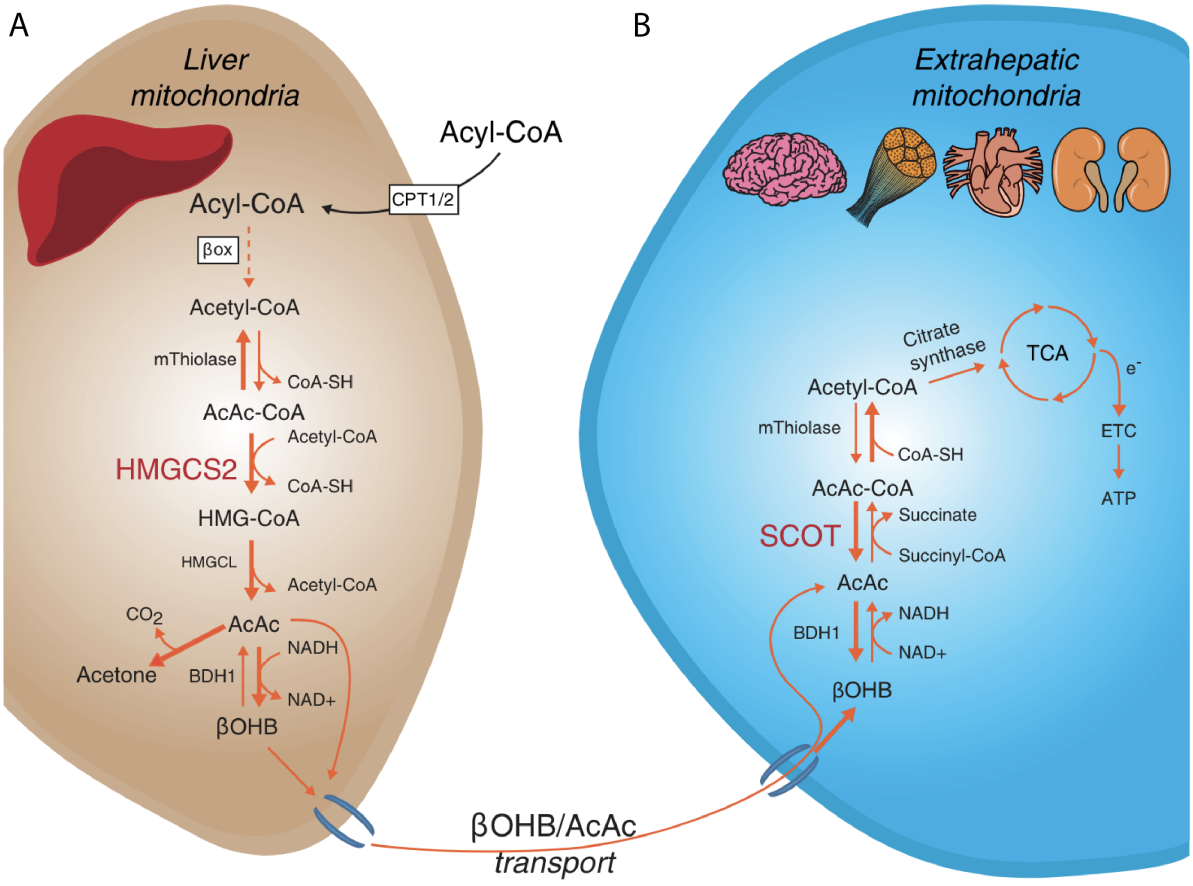

Figure 3: Ketone body metabolism. Schematic diagram of ketogenesis (**A**) and ketone body oxidation (**B**). Modified according to Puchalska et al.[86].

Since the liver cannot utilize ketone bodies for its own energy supply due to the lack of the enzyme succinyl-CoA:3-ketoacid-CoA transferase (SCOT), which is vital for ketone body oxidation, the water-soluble acetoacetate and β-hydroxybutyrate are released into the blood and transferred to extrahepatic tissues. Here, skeletal and cardiac muscle cells as well as the brain can use ketone bodies as an alternative source of energy. Particularly, the brain, which normally prefers glucose as its main fuel, can adapt well to the utilization of ketone bodies and then is able to meet about 75 % of its energy needs from them[78]. Extrahepatic BDH1 converts BHB back into acetoacetate which is subsequently activated to acetoacetyl-CoA by the addition of a coenzyme A (CoA) moiety from succinyl-CoA in a SCOT-catalyzed reaction. The activity of SCOT increases with food abstinence. Alternatively, a free CoA molecule can be directly transferred to acetoacetate in an ATP-dependent manner. In the final step, acetoacetyl-CoA is cleaved by 3-ketothiolase into two molecules of acetyl-CoA, which are then introduced into the TCA (Fig. 3B)[85,86].

Due to the generation of a large number of reducing equivalents for the mitochondrial electron transport chain, the metabolism of ketone bodies is considered to be particularly energetically efficient. Furthermore, BHB increases the redox span within the mitochondrial respiratory chain by keeping mitochondrial ubiquinone in an oxidized state, therefore yielding more ATP per carbon and oxygen molecule consumed compared to the direct utilization of fatty acids[79,87,88].

2.4.2 Function of ketone bodies

Apart from only being an alternative energy source, numerous studies have shown that ketone bodies exert multifaceted effects as important metabolic and signaling mediators (Fig. 4). Among others, BHB is involved in several epigenetic regulatory mechanisms. By inhibiting class I histone deacetylases (HDACs), ubiquitously expressed nuclear enzymes that remove acetyl groups from lysine residues on histones, BHB loosens the compact chromatin structure and facilitates expression of genes such as the transcription factor FOXO3A. This protein is closely associated with the cellular resistance to oxidative stress as it promotes transcription of mitochondrial dismutase 2 (SOD2) and catalase[85,89]. Moreover, direct lysine β-hydroxybutyrylation of histones depicts a new type of histone modification translating distinct metabolic states into rewiring of epigenetic programs[90]. In addition, BHB acts as a ligand for different G-protein-coupled receptors, that have not only been associated with regulatory pathways of fatty acid metabolism in adipocytes, but also seem to mediate intestinal membrane integrity as well as neuroprotective and anti-inflammatory effects, as demonstrated in promising animal stud-

ies[85,91]. In refractory epilepsy in children, ketogenic diet has already become one of the established therapeutic strategies, although the potential underlying anticonvulsant mechanisms remain controversial, with theories ranging from enhanced biosynthesis of inhibitory neurotransmitters to profound changes in gene expression[92,93].

Animal studies have also highlighted possible favorable immunomodulating effects of ketone bodies. At concentrations comparable to those achieved by fasting or carbohydrate reduction, BHB was shown to attenuate NLRP3-mediated inflammation followed by a dampened secretory capacity of pro-inflammatory IL-1β. These effects were mediated directly by BHB, independent of interactions with G-protein-coupled receptors or HDCAs[94]. Through inhibition of both the priming and assembly steps of NLRP3 inflammasome activation in macrophages and neutrophils, ketogenic diets reduced inflammation in a rat model of gout flare, preventing synovial inflammation and joint lesions[95]. First evidence also suggests that carbohydrate-restrictive and similar diets might also affect adaptive immunity. In experimental murine encephalomyelitis (EAE) models, repetitive cycles of fasting periods were able to alleviate and even completely reverse EAE symptoms by reducing the number of specific T-cell lineages implicated in the development of autoimmune disorders and limiting the recruitment of immune cells into the central nervous system[81,96].

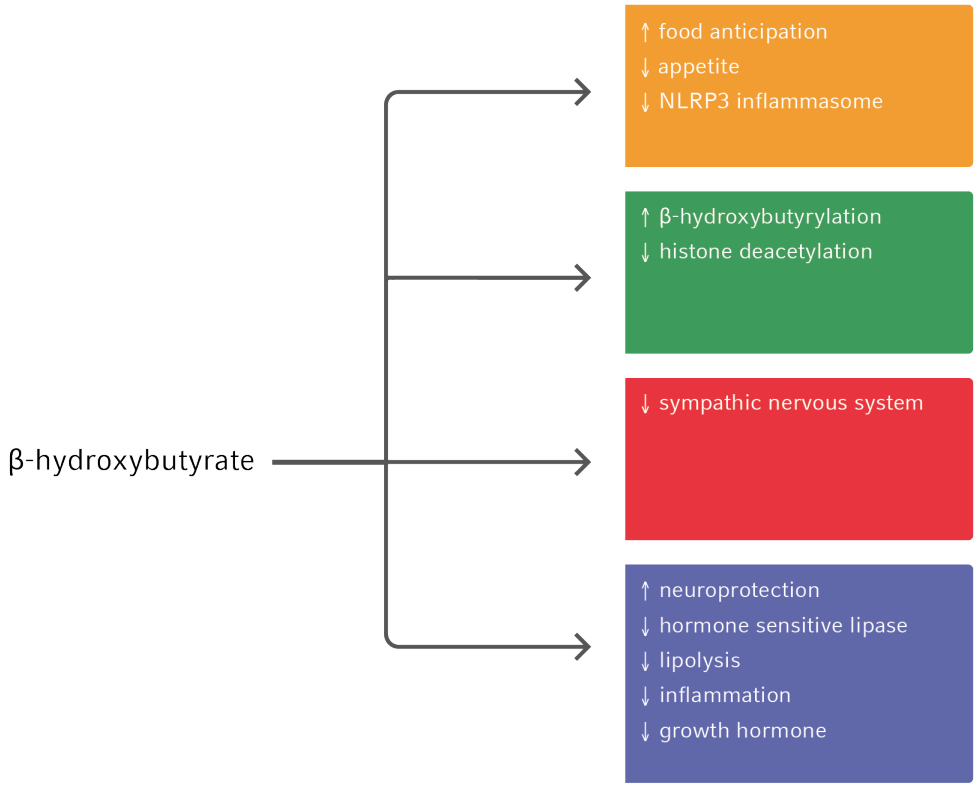

Figure 4: Signaling roles of β-hydroxybutyrate. Illustration of the pleiotropic functions of β-hydroxybutyrate. Modified according to Puchalska et al.[86].

2.5 OBJECTIVE

Although various studies have already discussed positive immunomodulating effects of carbohydrate restriction, highlighting the powerful potential of nutritional interventions, the existing data rely almost exclusively on animal models, and furthermore focus mainly on innate immunity. However, the effects of ketone bodies and ketogenic diets on human adaptive immunity have not yet been adequately addressed.

This thesis sets out to investigate the immunomodulatory effects of BHB and a very-low-carbohydrate diet on human T-cell immunity, taking particular account of the different, functionally distinct and, in some cases, opposing T-cell subsets, since a well-balanced ratio between functionally and metabolically distinct $CD4^+$ T-cell lineages was found to be crucial for human immune homeostasis[46,47].

In order to provide this long-required scientific data, this thesis aims at

(i) analyzing the human $CD4^+$ and $CD8^+$ T-cell response with particular emphasis on the distinct T helper cell lineages and their metabolic function upon incubation with BHB using an *in vitro* model mimicking a ketogenic dietary regime.

(ii) conducting a prospective first-in-human nutritional intervention study enrolling healthy participants who undergo a ketogenic diet for a period of three weeks with comprehensive T-cell analyses prior to and after the intervention.

3 Materials

3.1 LABORATORY EQUIPMENT

(Benchtop) centrifuge	Eppendorf AG, Hamburg
AutoMACSPro Separator	Miltenyi Biotec GmbH, Bergisch Gladbach
Incubator (Kendro BB6220)	BINDER GmbH, Tuttlingen
Cell Separation Magnet	Becton Dickinson GmbH, Heidelberg
FilterMax F3 MultiMode Microplate Reader	Molecular Devices, USA
Fridge	Liebherr-International GmbH, Biberach
Freezer	Liebherr-International GmbH, Biberach
LightCycler® 480 Instrument	Roche Diagnostics GmbH, Mannheim
Micropipettes	Eppendorf AG, Hamburg
NanoDrop™ Spectrophotometer	Peqlab Biotechnologie GmbH Erlangen
Pipette boy (Easypet)	Eppendorf AG, Hamburg
Laminar flow cabinet	Heraeus Holding GmbH, Hanau
Nitrogen tank	Cryotherm GmbH & Co. KG, Kirchen (Sieg)
Thermocycler (Mastercycler)	Eppendorf AG, Hamburg
Thermoshaker	Thermo Scientific Inc., USA
ViCell XR Cell Viability Analyzer	Beckman Coulter Inc., USA
Vortex mixer	Thermo Scientific Inc., USA
Analytical balance	Sartorius AG, Göttingen
Laboratory water bath	Julabo GmbH, Seelbach
Flow cytometer, BD FACSCanto II	Becton Dickinson GmbH, Heidelberg
Seahorse XFe96 Analyzer	Agilent Technologies, USA
Glucomen Areo 2K ketone monitor	Berlin-Chemie AG, Berlin

3.2 CONSUMABLES

15 ml / 50 ml tubes	Greiner Bio-One International GmbH, Österreich
Micro tubes 0.5 ml, 1.6 ml, 2.0 ml	Eppendorf AG, Hamburg
Safe-lock tubes	Eppendorf AG, Hamburg
50 ml Leucosep tubes	Greiner Bio-One International GmbH, Österreich
Polystyrene tubes, 5 ml	Sarstedt AG & Co., Nümbrecht
Cell culture plates 25/75 cm^2	Sarstedt AG & Co., Nümbrecht
Pipette tips	Eppendorf AG, Hamburg
Filter pipette tips	Biozym Scientific GmbH & Co. KG, Hessisch Oldendorf
Serological pipettes	Eppendorf AG, Hamburg
96-well plate	Life technologies, USA
Multiwell plates 6 – 96 well	Greiner Bio-One International GmbH, Österreich
S-Monovette, lithium-heparin, 7.5 ml	Sarstedt AG & Co., Nümbrecht
TruCulture tubes	RulesBasedMedicine, USA
Safety-Multifly™- needle	Sarstedt AG & Co., Nümbrecht
β-Ketone test strips	Berlin-Chemie AG, Berlin

3.3 CHEMICALS AND REAGENTS

RPMI-1640 medium	Biochrom AG, Berlin
Fetal bovine serum	Biochrom AG, Berlin
L-glutamine (200 mM)	Biochrom AG, Berlin
Penicillin-Streptomycin	Biochrom AG, Berlin
Phosphate buffered saline (PBS)	Biochrom AG, Berlin
Sodium pyruvate (100nM)	Thermo Fisher Scientific Inc., USA
D-(+)-Glucose	Merck Millipore, USA
D/L-β-hydroxybutyric acid	Merck Millipore, USA
Aqua ad injectabilia	B. Braun SE, Melsungen

Poly-L-Lysine	Biochrom AG, Berlin
Ficoll-Histopaque®-1077	Sigma-Aldrich, USA
Calcein-AM	Sigma-Aldrich, USA
Triton X-100 (1%)	Thermo Fisher Scientific Inc., USA
LEGEND MAX™ Human ELISA Kits	BioLegend, USA
TexMACS™ medium	Miltenyi Biotec GmbH, Bergisch Gladbach
Ultra-LEAF™ Purified anti-human CD3 antibody	BioLegend, USA
Ultra-LEAF™ Purified anti-human CD28 antibody	BioLegend, USA
T Cell TransAct™, human	Miltenyi Biotec GmbH, Bergisch Gladbach
Recombinant human IL-1β	Miltenyi Biotec GmbH, Bergisch Gladbach
Recombinant human IL-2	Miltenyi Biotec GmbH, Bergisch Gladbach
Recombinant human IL-4	Miltenyi Biotec GmbH, Bergisch Gladbach
Recombinant human IL-6	Miltenyi Biotec GmbH, Bergisch Gladbach
Recombinant human IL-12	Miltenyi Biotec GmbH, Bergisch Gladbach
Recombinant human IL-23	Miltenyi Biotec GmbH, Bergisch Gladbach
Recombinant human TGFβ1	Miltenyi Biotec GmbH, Bergisch Gladbach
Anti-IFNγ	Miltenyi Biotec GmbH, Bergisch Gladbach
Anti-IL-4	Miltenyi Biotec GmbH, Bergisch Gladbach
Anti-IL-12	Miltenyi Biotec GmbH, Bergisch Gladbach
Retinoic acid	Merck Millipore, USA
Seahorse XFe96 FluxPaks	Agilent Technologies, USA
XF RPMI Medium pH 7.4	Agilent Technologies, USA
Seahorse XF Cell Mito Stress Test Kit	Agilent Technologies, USA
Seahorse XF Glycolytic Rate Assay Kit	Agilent Technologies, USA
Dynabeads™ Human T-Activator CD3/CD28	Thermo Fisher Scientific; USA
autoMACS Running Buffer – MACS Separation Buffer	Miltenyi Biotec GmbH, Bergisch Gladbach

autoMACS Washing Buffer – MACS Separation Buffer	Miltenyi Biotec GmbH, Bergisch Gladbach
autoMACS Rinsing Solution	Miltenyi Biotec GmbH, Bergisch Gladbach
CD4 MicroBeads, human	Miltenyi Biotec GmbH, Bergisch Gladbach
CD8 MicroBeads, human	Miltenyi Biotec GmbH, Bergisch Gladbach
Pan T Cell Isolation Kit, human	Miltenyi Biotec GmbH, Bergisch Gladbach
$CD4^{+}CD25^{+}CD127^{dim/-}$ Regulatory T Cell Isolation Kit II, human	Miltenyi Biotec GmbH, Bergisch Gladbach
IL-17 Secretion Assay – Cell Enrichment and Detection Kit (PE), human	Miltenyi Biotec GmbH, Bergisch Gladbach
Transcriptor First Strand cDNA Synthesis Kit	Roche Diagnostics GmbH, Mannheim
Universal ProbeLibrary (UPL)	Roche Diagnostics GmbH, Mannheim
Real Time Ready IL-8 Single Assay	Roche Diagnostics GmbH, Mannheim
Oligonucleotide primer (qRT-PCR)	Metabion, Martinsried, München
Lightcycler 480 Probes Master	Roche Diagnostics GmbH, Mannheim
miRNeasy Mini Kit (50)	Qiagen, Hilden
QIAzol Lysis Reagent	Qiagen, Hilden
Chloroform	Sigma-Aldrich, USA
MitoTracker™ Green FM	Thermo Fisher Scientific; USA
Cell Activation Cocktail (without Brefeldin A)	BioLegend, USA
Brefeldin A Solution (1,000X)	BioLegend, USA
Antibodies for flow cytometry	BioLegend, USA
Human TruStain FcX™ (Fc Receptor Blocking Solution)	BioLegend, USA
Bovine serum albumin, "Fraction V"	Sigma-Aldrich, USA
Invitrogen™ eBioscience™ Foxp3/Transcription Factor Staining Buffer Set	Thermo Fisher Scientific; USA

3.4 SOFTWARE

FilterMax F3 MultiMode Microplate Reader:

SoftMax Pro 7.1 GxP data acquisition and analysis software, Molecular Devices, USA

LightCycler® 480:

LightCycler® 480 Instrument (96 wells) and Relative Quantification Software, Roche Diagnostics GmbH, Mannheim

Flow cytometry data analyses:

FlowJo v10, FlowJo, USA

Statistics:

GraphPad PRISM 9, GraphPad Software, Inc., USA

References:

Mendeley - Reference Manager, Mendeley Ltd (Elsevier), UK

4 Methods

4.1 BLOOD SAMPLING AND IMMUNE CELL ISOLATION

4.1.1 Blood sampling

Blood from healthy volunteers was collected by sterile puncture of a peripheral vein using winged butterfly needles. Blood was drawn into S-Monovettes containing lithium heparin for subsequent isolation of peripheral blood mononuclear cells (PBMC), or into serum monovettes and TruCulture tubes for analyses of cytokine secretion patterns. After an incubation period of 20 minutes at room temperature, during which the whole blood clotted, serum monovettes were centrifuged at 3000 rpm. Afterwards serum was pipetted off as supernatant and further processed or stored at -80 °C. For PBMC isolation and TruCulture analysis see 4.1.2 or 4.5.2.

4.1.2 Isolation of peripheral blood mononuclear cells (PBMC)

Leucosep tubes with a porous polyethylene separation barrier were filled with 15 ml of Ficoll (1.077 g/ml). After centrifugation at 2000 rpm for 5 minutes, Ficoll resided below the separation membrane preventing blood and Ficoll from mixing, minimizing the risk of contamination by erythrocytes and granulocytes. Heparinized whole blood from subjects were diluted with phosphate-buffered saline solution (PBS), and 25 ml was transferred into prepared Leucosep tubes. Density gradient centrifugation at 2000 rpm for 17 min without brake, was carried out in order to separate the whole blood based on the differences in density of the cell populations. The PBMC-containing interphase was subsequently removed, washed several times in PBS, and eventually the cell number was determined via ViCell analyzer.

4.1.3 T-cell isolation

T-cell isolation from PBMC was performed via microbead-based separation in the AutoMACSPro Separator according to the manufacturer's protocol. Positive cell selection using microbead separation is based on labeling the desired antigen target structure with specific monoclonal antibodies coupled to superparamagnetic nanoparticles. Subsequently, the cell suspension passes through a column with ferromagnetic coating within a magnetic field in the AutoMACSPro separator. The microbead-labeled cells are thus retained within the column, whereas unlabeled cells pass through. Next, the labeled cells are automatically eluted and recovered separately (positive selection). To isolate a specific cell type in non-labeled form, all non-target cells are magnetically labeled with microbeads. During the separation process, the

unlabeled target cells are collected in the flow-through fraction. All magnetically labeled non-target cells are retained in the column. Antibody-antigen binding does not activate the cell or affect the surface structure or cell functionality[97]. In preparation for isolation, the required centrifuge was cooled down to 4 °C and the buffer was gently thawed on ice. For antigen labeling, PBMC are incubated in buffer for 15 minutes at 4 °C with the respective microbeads. PBMC are then washed and processed in the AutoMACSPro separator for T-cell isolation.

4.2 CELL CULTURE

4.2.1 *In vitro* stimulation of PBMC

Peripheral blood mononuclear cells (PBMC) from healthy subjects were isolated as described above. PBMC were cultured in RPMI 1640 containing 80 mg/dl glucose supplemented with 10 % heat-inactivated fetal calf serum (FCS), 1 % HEPES, 1 % L-glutamine, 100 U/ml penicillin, and 100 U/ml streptomycin. For incubation with β-hydroxybutyrate (BHB), D/L-BHB was added to the prepared medium at a final concentration of 10 mM. PBMC were incubated at 37 °C and 5 % CO_2. T-cell activation was performed using 50 U/ml IL-2 and CD3/CD28 Dynabeads at a bead-cell ratio of 1:8 for 48 hours.

4.2.2 Differentiation of Th_1 and Th_2 cells

For differentiation into T helper cell subsets Th_1 and Th_2, $CD4^+$ T cells were separated from PBMC and seeded into cell culture plates for seven days. T-cell activation and expansion was performed using T Cell TransAct™. For polarization of naive T cells into the Th_1 subset, TexMACS™ growth medium was supplemented with IL-12 (50 ng/µl) and anti-IL-4 (20 ng/µl), while for differentiation of Th_2 cells IL-2 (100 U/ml), IL-4 (50 ng/ml), anti-IFNγ (50 ng/ml) and anti-IL-12 (50 ng/ml) were added. Cells were cultured at 37 °C and 5 % CO_2. Medium was changed after four days; the respective supplementation was maintained.

4.2.3 Differentiation of regulatory T cells

In order to differentiate regulatory T cells (T_{reg}), $CD4^+$ T cells were incubated for seven days in TexMACS™ growth medium, stimulated with T Cell TransActTM and supplemented with TGFβ1 (5 ng/ml), anti-IFNγ (1 µg/ml), anti-IL-4 (1 µg/ml), IL-2 (100 U/ml) and retinoic acid (10 mM). Cells were cultured at 37 °C and 5 % CO_2. Medium was changed after four days; the respective supplementation was maintained.

4.2.4 Differentiation of Th_{17} cells

For differentiation into Th_{17} cells, $CD4^+$ T cells were seeded into cell culture plates, pre-coated with CD3 antibodies. TexMACS™ growth medium was supplemented with CD28 antibodies (1 µg/ml), IL-1β (10 ng/ml), IL-6 (10 ng/ml), IL-23 (10 ng/ml), TGFβ1 (5 ng/ml), in addition to anti-IFNγ (10 µg/ml) and anti-IL-4 (10 µg/ml). Cells were cultured for seven days at 37 °C and 5 % CO_2. Medium was changed after four days; the respective supplementation was maintained.

4.3 PROSPECTIVE *IN VIVO* INTERVENTION STUDY

4.3.1 Study design

Healthy adult volunteers were enrolled in a prospective nutritional intervention study to investigate the effects of a ketogenic diet (KD) on human T-cell immunity. Women during pregnancy and lactation as well as subjects with current administration of glucocorticoids or suffering from severe metabolic disorders or autoimmune diseases were not included. Characteristics of healthy volunteers are depicted in 4.3.2. After comprehensive nutritional counseling, participants conducted a ketogenic diet for three weeks, consuming less than 30 g of carbohydrates per day. Prior to (T0) and after (T1) the dietary intervention, blood was collected and stimulated *ex vivo* for 24 hours for subsequently conducted immunological analyses. During KD, endogenous ketone body levels were quantified on a regular basis using the Glucomen Areo 2K ketone monitor for point-of-care quantification. Serum glucose levels were measured at the Institute of Laboratory Medicine via the hexokinase method using the GLUC3 kit (Roche Diagnostics, Cat.# 05168791 190) on a Cobas 8000/c702 (Roche Diagnostics, Penzberg, Germany).

Informed consent was obtained from all volunteers. The study was performed after review and positive evaluation by the Ethics Committee of the Medical Faculty at the University of Munich (project no. 19-523), according to the Declaration of Helsinki with its revisions and amendments (Tokyo/1975, Venice/1983, Hong Kong/1989, Somerset West/1996, Edinburgh/2000, Seoul/2008, and Fortaleza/2013).

4.3.2 Patients' characteristics

Age, years (mean ± SD)	35.56 (± 11.56)
Sex (female / male)	f = 25 / m = 19
Fasting blood glucose T0, mg/dl (mean ± SEM)	93.67 (± 4.04)
Fasting blood glucose T1, mg/dl (mean ± SEM)	98.61 (± 4.65)
BMI T0, kg/m^2 (mean ± SEM)	22.59 (± 0.401)
BMI T1, kg/m^2 (mean ± SEM)	21.99 (± 1.022)

Table 1: Characteristics of healthy participants conducting a ketogenic diet.

4.4 QUANTIFICATION OF GENE EXPRESSION

4.4.1 RNA isolation

T cells were harvested and lysed in QIAzol Lysis Reagent. After addition of chloroform, separation into an aqueous and an organic phase was performed by centrifugation. RNA molecules remained in the aqueous phase, whereas denatured proteins and lipids were dissolved in the organic phase. The upper aqueous phase was pipetted off, ethanol was added, and the solution was placed on the silica membrane of RNA isolation tubes. After multiple washing steps, RNA was dissolved from the membrane using elution solution and transferred to nuclease-free tubes. The amount of extracted RNA (ng/µl) and the degree of purity were determined on the NanoDrop™ 2000/2000c spectrophotometer.

4.4.2 cDNA synthesis

Prior to transcription, RNA samples were diluted with nuclease-free water to a concentration of 1000 ng/µl in 10 µl. If only smaller amounts of RNA were available, the lowest concentration was chosen as the final concentration. To each of the diluted RNA samples, 1 µl Oligo-dt Primer 0.4 µg/µl, 1 µl dNTP Mix 10 nM, and 1 µl Random Hexamer Primer 0.4 µg/µl were added and the RNA was denatured in a thermal cycler for 5 minutes at 65 °C. Afterwards, samples were cooled down on ice for one minute. For the subsequent cDNA synthesis, 4 µl of 5x First Strand Buffer, 1 µl of 0.1M DTT, 1 µl of RNaseOUT Recombinant Ribonuclease Inhibitor (40 U/µl), and 1 µl of SuperScript® III Reverse Transcriptase (200 U/µl) were added respectively, and the

sample was mixed well. The cDNA synthesis was performed in the Thermocycler using three incubation phases: 5 minutes at 25 °C, 45 minutes at 50 °C and 15 minutes at 70 °C. cDNA was immediately stored at -20 °C.

4.4.3 Real-time quantitative reverse transcriptase polymerase chain reaction (qRT-PCR)

Real-time quantitative reverse transcriptase polymerase chain reaction (qRT-PCR) enables simultaneous quantification of the desired and amplified gene segment. In addition to PCR amplification, this is based on the labeling of known target regions using UPL oligonucleotide probes. Those contain a reporter dye at the 5' end of the probe. Based on Förster resonance energy transfer (FRET), fluorescence emission is suppressed by a dark quencher located at the 3'. If the dark quencher is hydrolytically cleaved by Taq polymerase during the elongation phase, the unquenched fluorescence signal can be detected in real time after excitation by a light source of specific wavelength. The qRT-PCR is performed in the LightCycler®480 in three phases. First, the sample is brought to 95 °C in order to cause denaturation and separation of the dsDNA. The subsequent annealing phase at 50 °C, allows the binding of primers and probes to the DNA template. The actual amplification of the cDNA takes place during the final elongation phase at 72 °C. Fluorescence intensity increases proportionally to the amount of the PCR amplicon. cDNA quantification occurs in the exponential phase of amplification, when template, primer and polymerase are present at an optimal concentration. The cycle at which the fluorescence first exceeds the threshold value of the background fluorescence (Cp value = crossing point) is determined.

For qRT-PCR, first, the cDNA samples were diluted with nuclease-free water to a concentration of 2 ng/ml. From this, 5 µl per well were pipetted into a 96-multiwell plate (10 ng cDNA / well). Subsequently, 15 µl of the master mix consisting of 4.4 µl PCR-grade nuclease-free water, 0.2 µl forward primer (20 µM), 0.2 µl reverse primer (20 µM), 0.2 µl fluorescent UPL probe (10 µM) and 10 µl DNA Probes Master were added. The plate was sealed with a foil, centrifuged and the qRT-PCR was started in the LightCycler480. After qRT-PCR, the LightCycler® RelativeQuantification Software was used to determine the mRNA expression of the target genes in relation to the expression of the housekeeping genes β-actin and TBP. The expression was determined for target genes and reference genes (housekeepers) in duplicates. For primer sequences see Table 2.

Target mRNA	Primer sequence - forward	Primer sequence - reverse
PRF1	5‘-CAC TCA CAG GCA GCC AAC T -3‘	5‘- GGG AGT GTG TAC CAC ATG -3‘
IFNγ	5‘- GGC ATT TTG AAG AAT TGG AAA -3‘	5‘- TTT GGA TGC TCT GGT CAT CTT -3‘
GZMB	5‘- GGG GGA CCC AGA GAT TAA -3‘	5‘- CCA TTG TTT CGT CCA TAG -3‘
TNFα	5‘- CAG CCT CTT CTC CTT CCT GAT -3‘	5‘- GCC AGA GGG CTG ATT AGA GA -3‘
IL-2	5‘- AAG TTT TAC ATG CCC AAG AAG G -3‘	5‘- AAG TGA AAG TTT TTG CTT TGA GCT -3‘
IL-4	5‘- TGC CTC ACA TTG TCA CTG C -3‘	5‘- GCA CAT GCT AGC AGG AAG AAC -3‘
IL-10	5‘- TGC CTT CAG CAG AGT GAA GA -3‘	5‘- GCA ACC CAG GTA ACC CTT AAA -3‘
IL-17A	5‘- TGG GAA GAC CTC ATT GGT GT -3‘	5‘- GGA TTT CGT GGG ATT GTG AT -3‘
IL-22	5‘- CAA CAG GCT AAG CAC ATG TCA -3‘	5‘- ACT GTG TCC TTC AGC TTT TGC -3‘
TGFβ1	5‘- ACT ACT ACG CCA AGG AGG TCA -3‘	5‘- TGC TTG AAC TTG TCA TAG ATT TCG -3‘
Tbet	5‘- TGG GTG CAG TGT GGA AAG -3‘	5‘- TCC TGT GTT GGG GGA GTC -3‘
GATA3	5‘- CTC ATT AAG CCC AAG CGA AG -3‘	5‘-TCT GAC AGT TCG CAC AGG AC -3‘
FOXP3	5‘- CCT TGC CCC ACT TAC AGG -3‘	5‘- CCA CCG TTG AGA GCT GGT -3‘
RORc	5‘- CAG CGC TCC AAC ATC TTC T -3‘	5‘-CCA CAT CTC CCA CAT GGA C -3‘
CTLA4	5‘- TCA CAG CTG TTT CTT TGA GCA -3‘	5‘- AGG CTG AAA TTG CTT TTC ACA -3‘
β-actin	5‘- CCA ACC GCG AGA TGA -3‘	5‘- CCA GAG GCG TAC AGG GAT AG -3‘
TBP	5‘- GAA CAT CAT GGA TCA GAA CAA CA -3‘	5‘- ATA GGG ATT CCG GGA GTC AT -3‘

Table 2: Primer sequences for qRT-PCR.

4.4.4 Next-generation sequencing

Transcriptome profiling of human $CD4^+$ and $CD8^+$ T cells was performed by the Helmholtz Zentrum München, Deutsches Forschungszentrum für Gesundheit und Umwelt (GmbH), Munich, Germany using 30-RNA next-generation sequencing. The following description is based on information kindly provided by the working group. Illumina compatible sequencing libraries were generated via QuantSeq 3' mRNA-Seq Library Prep Kit FWD for Illumina (Lexogen GmbH, Austria). PCR Add-on Kit for Illumina (Lexogen GmbH, Austria) was utilized for determination of optimal number of cycles for endpoint PCR following the manufacturer's protocol. Quantification of dsDNA and quality control of libraries were carried out using the Quant-iT PicoGreen dsDNA Assay Kit (Invitrogen, USA) and the Bioanalyzer High Sensitivity DNA Analysis Kit (Agilent Technologies, Inc., USA). Sequencing of prepared libraries was conducted on an Illumina HiSeq 4000 sequencer (Illumina, Inc., USA). After pooling, the individually barcoded libraries were distributed across lanes of the same flow-cell aiming for approximately 10 million paired-end reads per sample. After removing the adapter sequencing using BBDUk (https://jgi.doe.gov/data-and-tools/bbtools), raw forward reads (stored as fastq files) were aligned against the hg38 human reference genome via STAR (Dobin et al., 2013). htseq-count was used for quantification of the aligned reads, while quality of both, aligned and unaligned reads was analyzed via FastQC (https://www.bioinformatics.babraham.ac.uk/projects/fa stqc/). All resulting reports were summarized using the multiQC tool (https://multiqc.info). Only genes for which the number of reads for the entire data set was five times the number of samples were included. In order to verify the plausibility of the data, expression of the sex specific XIST gene was analyzed with an expected high expression in females compared to a low expression in males. Data consistency was assessed by creating a correlation heat map, allowing the detection of technical outliers. DESeq2 was used for conducting differential expression analysis. Statistical significance was accepted for corrected p-values (false discovery rate, FDR) below 25 % (Love et al., 2014). Gene set enrichment analysis (GSEA) was performed including all genes kept in the analysis ranked after shrinked (apeglm) log2-fold-change using the command-line version of the GSEA software (version 4.0.3) (Subramanian et al., 2005). 11 545 genes remained in the dataset after quality control (CD4 T0/T1 n = 5667/5878; CD8 T0/T1 n = 5799/5746). $CD4^+$ T-cell expression patterns of two patients were identified as technical outliers by correlation heatmap analysis (significant genes: CD4 T0/T1 $p < 0.05$: n = 294/346, with FDR < 25 % n = 7/3; CD8 T0/T1 $p < 0.05$: n = 325/252, with FDR < 25 % n = 7/2). Final data set containing expression profiles of 13 (CD4) and 15 (CD8) subjects.

4.5 FUNCTIONAL ASSAYS

4.5.1 Enzyme-Linked Immunosorbent Assay (ELISA)

The concentrations of cytokines in the supernatant were determined by Enzyme-Linked Immunosorbent Assays (ELISA). Supernatants from cell culture plates were harvested and immediately stored at -80 °C until further analyses. Frozen supernatants were slowly thawed on ice and centrifuged to remove debris prior to running the assay. All ELISA kit assays were "sandwich" ELISA on 96-well plates, and assays were performed according to the manufacturer's protocol. One day prior to the analysis, the 96-well plate was coated with the respective anti-human capture antibody that binds and retains the target protein. To each well, 100 µl of the supernatant (pure or pre-diluted) was added and incubated for two hours at room temperature with shaking at 200 rpm. The supernatant was then discarded, the plate washed several times, and the biotinylated detection antibody was added to each well. After one hour of incubation at room temperature under shaking, the contents were discarded again. After washing the plate, Avidin-HRP D solution was added, and the plate was incubated for 30 minutes. Substrate solution F was filled into each well and incubated in the dark for 30 minutes. Wells containing the human target protein turned blue. The reaction was stopped by adding a stop solution, causing the solution to turn from blue to yellow, with an intensity proportional to the protein concentration. Absorbance was measured using a FilterMax F3 MultiMode Microplate Reader and values were evaluated using a kit-specific standard curve. All samples were run in duplicates and mean values were taken for analysis. For further information see Table 3.

ELISA Kit	Catalogue #	Company
LEGEND MAX™ Human IFN-γ ELISA Kit	430107	Biolegend
LEGEND MAX™ Human TNF-α ELISA Kit	430207	Biolegend
LEGEND MAX™ Human IL-2 ELISA Kit	431807	Biolegend
LEGEND MAX™ Human IL-4 ELISA Kit	430307	Biolegend
LEGEND MAX™ Human IL-8 ELISA Kit	431507	Biolegend
LEGEND MAX™ Human IL-10 ELISA Kit	430607	Biolegend
LEGEND MAX™ Total TGF-β1 ELISA Kit	436707	Biolegend
LEGEND MAX™ Human IL-17A ELISA Kit	435707	Biolegend
LEGEND MAX™ Human IL-22 ELISA Kit	434507	Biolegend

Table 3: ELISA kits used for quantification of cytokines.

4.5.2 Whole blood multiplex protein analysis (TruCulture)

For multiplex protein analyses, whole blood from healthy volunteers was drawn directly into special TruCulture tubes containing medium and lipopolysaccharide (LPS). According to the manufacturer's protocol, the tubes were inverted three times and incubated at 37 °C. After 24 hours, valve separators were inserted into the tubes in order to separate immune cells from the supernatant. Multiplex analyses were performed by RulesBasedMedicine (RBM, Austin, Texas, USA).

4.5.3 Calcein-acetoxymethyl (AM) cytotoxicity assay

Analysis of $CD8^+$ T cell-mediated cytotoxicity was performed using a calcein-acetoxymethyl (AM) lysis assay in which U87 glioblastoma (GBM) cells served as target cells. Following the uptake of the non-fluorescent calcein-AM into live and metabolically active target cells, acetoxymethyl ester (AM) is enzymatically cleaved by intracellular esterases, removing the acetoxymethyl group. The remaining calcein molecules now bind calcium ions within the cell, which results in a green, fluorescent signal. This complex can no longer pass the cell membrane and remains in the intact cell. When calcein-labeled target cells are lysed by cytotoxic cells, the emitting dye is released into the cell medium and can be quantified in the supernatant. The fluorescence intensity is proportional to the number of lysed target cells and is thus a measure of the toxicity. As target cells, U87 GBM cells were seeded at a concentration of 20 000 cells per well on a 96-well plate in 200 µl of culture medium on the day before the assay. After 24 hours of incubation, fluorescence labeling was performed. For this, medium was removed, and the adherent cells incubated for 60 minutes in 8 µM Calcein-AM solution (dissolved in DMSO, diluted in PBS). Subsequently, the wells were washed several times with PBS to remove possible calcein residues. Stimulated PBMC were harvested, washed, and the CD3/CD28 beads were magnetically removed. After separation, isolated T cells were now added to the calcein-labeled U87 cells at a ratio of 1:10. In addition, the basal autolysis rate of tumor cells (spontaneous release) was determined by incubating labeled GBM cells alone. To determine the maximum lysis rate, U87 cells were incubated in medium containing 1 % Triton X (maximum release). Several wells were filled with medium only acting as blanks. After 8 hours incubation, the plate was centrifuged, the supernatant removed, and the fluorescence intensity (relative fluorescence units, RFU) determined on the FilterMax F3 MultiMode Microplate Reader at an excitation wavelength of 490 nm and an emission measurement at 520 nm. The lysis rate was calculated using the following formula:

$$lysis\ rate\ [\%] = \frac{RFU_{sample} - RFU_{\text{spontaneous release}}}{RFU_{\text{maximum release}} - RFU_{\text{spontaneous release}}} * 100$$

4.6 FLOW CYTOMETRY

Intra- and extracellular antibody staining for flow cytometric (FACS, fluorescence-activated cell scanning) analyses was carried out according to the manufacturer's protocols. Cell numbers of immune cells were adjusted to a concentration of 0.2 x 10^6 cells in 100 µl ice cold FACS buffer (PBS with 5 % BSA) and collected in 5 ml polystyrene tubes. PBMC were pre-incubated with Human TruStain FcX™ for Fc receptor blocking prior to antibody staining. For staining extracellular antigens, antibodies were added at the concentration recommended by the manufacturer and the cells were incubated on ice, protected from light for 30 minutes. Cells were then washed twice with FACS buffer and resuspended in 500 µl buffer for analysis. For intracellular staining, the Invitrogen™ eBioscience™ Foxp3/Transcription Factor Staining Buffer Set was used according to the manufacturer's instructions for permeabilization and fixation of immune cells prior to staining. Fixation/Permeabilization working solution was prepared by mixing Foxp3 Fixation/Permeabilization Concentrate with the provided diluent at a ratio of 1 to 3. For the 1X Permeabilization Buffer, 10X Permeabilization Buffer was diluted with distilled water. 1 ml of the Fixation/Permeabilization working solution was added and the cells were mixed thoroughly using a vortex mixer before being incubated for 45 minutes at room temperature protected from light. Before adding the antibody, cells were washed twice with 1X Permeabilization Buffer and the supernatant was discarded.

Analyses of T helper cell lineages were performed after microbead-based isolation of $CD4^+$ T cells. Th_1 and Th_2 cells were assessed by expression patterns of CXCR3, CCR4 and CCR6. Regulatory T cells were characterized by staining with antibodies against CD25 and FOXP3. Staining of $CD4^+$ T cells with IL-17A and IFNγ antibodies was used for differentiation between distinct Th_{17} lineages. Isotype and single-stained controls for compensation were carried out for each experimental setting. Flow cytometric analyses were run on a FACS Canto II and data were analyzed using FlowJo v10 software. Information on the antibodies used can be found in Table 4.

Target antigen	Clone	Fluorophore	Catalogue #	Company
CXCR3	G025H7	PE	353705	BioLegend
CCR4	L291H4	Brilliant Violet 421™	359413	BioLegend
CCR6	G034E3	FITC	353411	BioLegend
CD25	BC96	PE	302605	BioLegend
FOXP3	206D	Alexa Fluor® 488	320111	BioLegend
IL-17A	BL168	APC	512333	BioLegend

IFNγ	4S.B3	Brilliant Violet 421™	502531	BioLegend
CD4	RPA-T4	PerCP	300527	BioLegend
CD8a	RPA-T8	Brilliant Violet 421™	301035	BioLegend

Table 4: List of antibodies used for flow cytometric analyses.

4.7 MITOCHONDRIAL ANALYSES

4.7.1 Oxygen consumption rate (OCR) and extracellular acidification rate (ECAR)

Mitochondrial respiration, glycolytic capacity and ATP production were assessed in real-time using a Seahorse XF96 Analyzer according to the manufacturer's protocol. Prior to analysis, regulatory T cells or Th_{17} cells were seeded into the wells of a poly-L-lysine-coated XF96 cell culture microplate. Seahorse XF RPMI Medium supplemented with 1 mM pyruvate, 2 mM glutamine, and 5 mM glucose served as assay medium. All analyses were run in triplicates at a concentration of 200 000 cells in 180 µl assay medium per well. The oxygen consumption rate (OCR), a key indicator of mitochondrial oxidative phosphorylation, was determined using the Agilent Seahorse XF Cell Mito Stress Test Kit. Compounds were prepared with final well concentration of 1 µM Oligomycin, 0.75 µM FCCP and 0.5 µM Rotenone/Antimycin A and loaded to the XF96 sensor cartridge. Extracellular acidification rate (ECAR), surrogate parameter for glycolysis was assessed by performing the Agilent Seahorse XF Glycolytic Rate Assay with 0.5 µM Rotenone/Antimycin A and 50 mM 2-deoxy-glucose preloaded in drug delivery ports. All values shown in graphs represent individual experiments performed in 3 technical replicates.

4.7.2 Analysis of mitochondrial mass

Mitochondrial mass was assessed flow cytometrically using MitoTracker Green. 100 000 cells were incubated with 200 nM MitoTracker solution at 37 °C for 15 min, protected from light. Subsequently, mitochondrial mass was quantified by flow cytometry indicated by mean fluorescence intensity (MFI) using a FACS Canto II flow cytometer.

4.8 STATISTICS

Data are presented as mean ± standard error of the mean (SEM) or as box plots with median, 25th and 75th percentiles and range, unless not specified otherwise. All data sets were analyzed using the Kolmogorov Smirnov and D'Agostino & Pearson test for normal distribution and the p-values using t-test, Wilcoxon's Sign Rank test or Mann-Whitney U test for statistical significance. Statistical significance was assumed at a p-value of < 0.05, with $*p < 0.05$, $**p < 0.01$, $***p < 0.001$ and $****p < 0.0001$. All experiments were performed in duplicates and at least repeated three times.

5 Results

5.1 BHB DOES NOT ACTIVATE UNSTIMULATED T CELLS

First, in order to evaluate the impact of ketone bodies on human adaptive immunity, peripheral mononuclear cells (PBMC) from healthy subjects were cultivated in RPMI containing 80 mg/dl glucose in the presence or absence of 10 mM β-hydroxybutyrate (BHB) without any further T-cell specific stimulation. After 48 hours, PBMC were harvested for pan T-cell isolation. Subsequently, gene expression of classical $CD4^+$ and $CD8^+$ cytokines as well as transcription factors were quantified.

As shown in Figure 5, mRNA expression of $CD8^+$ cytokines perforin (PRF1) and granzyme B (GZMB) as well as IFNγ remained unaltered after incubation with BHB. Additionally, BHB alone was not able to modulate gene expression of $CD4^+$ cytokines IL-2, IL-4, and IL-10 (Figure 6 A-C). Regarding T helper cell subsets, neither changes of regulatory T cell- (T_{reg}) or Th_{17}-related transcription factors FOXP3 and RORc, nor of the respective master cytokines IL-17A and TGFβ1 (TGFB1) could be detected (Figure 6 D-G).

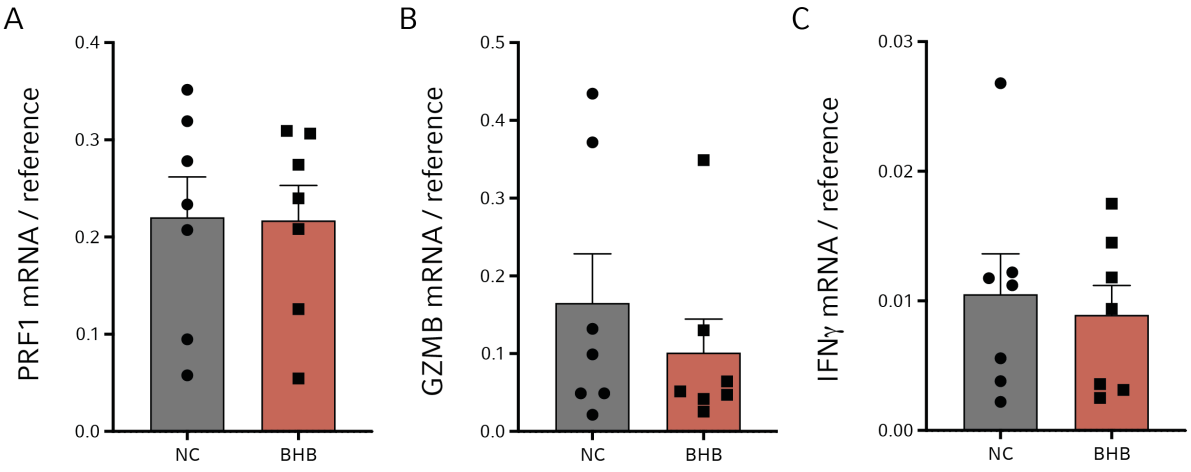

Figure 5: mRNA expression of $CD8^+$ T-cell cytokines in unstimulated T cells. PBMC from healthy subjects were incubated in RPMI containing 80 mg/dl glucose in the absence (NC) or presence of β-hydroxybutyrate (BHB) for 48 hours. Pan T cells were isolated and gene expression of $CD8^+$ cytokines PRF1, GZMB and IFNγ (**A-C**) was quantified via qRT-PCR relative to reference genes. n = 7.

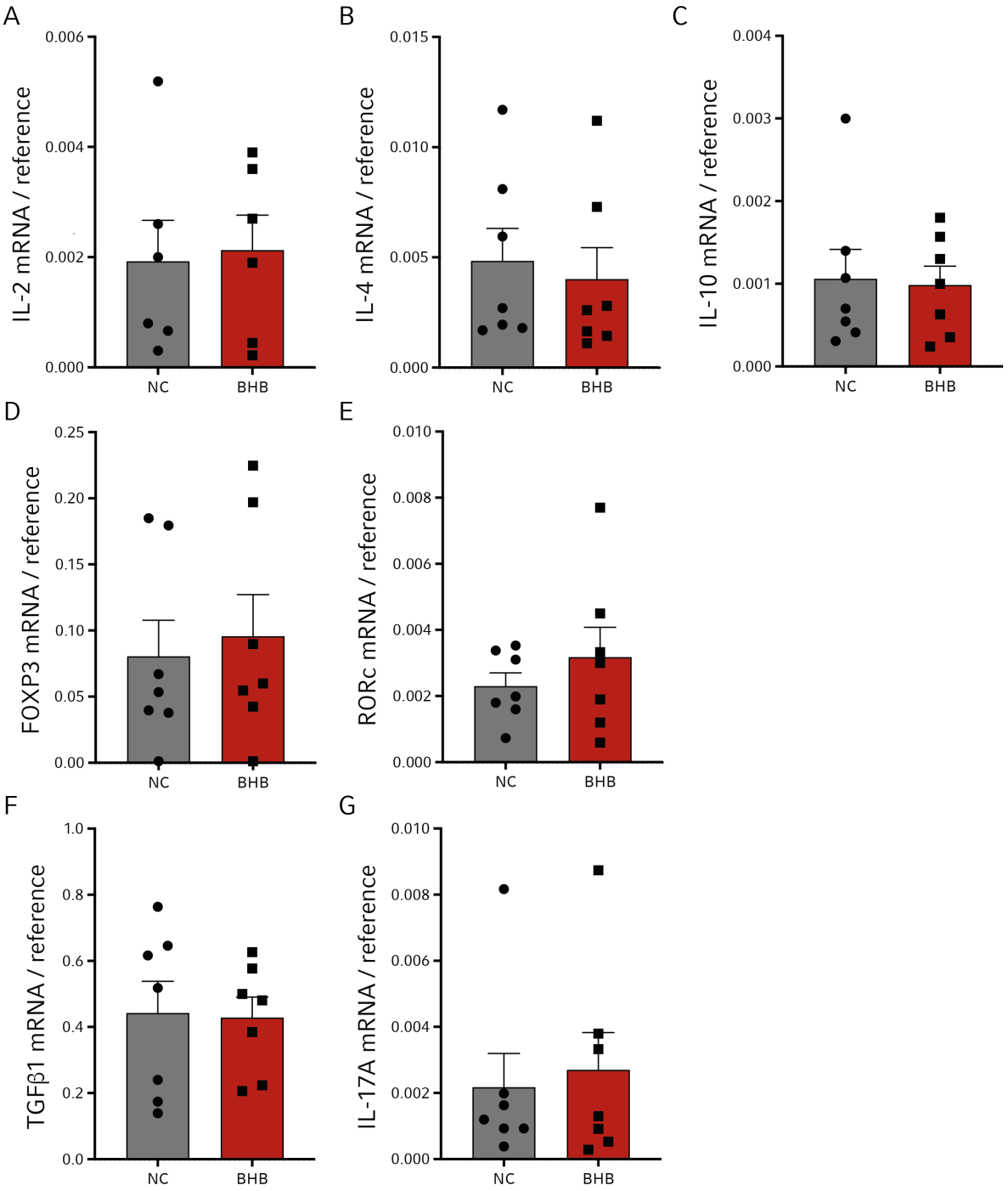

Figure 6: mRNA expression of CD4⁺ T-cell cytokines and transcription factors in unstimulated T cells. PBMC from healthy subjects were incubated in RPMI containing 80 mg/dl glucose in the absence (NC) or presence of β-hydroxybutyrate (BHB) for 48 hours. Pan T cells were isolated and gene expression of CD4⁺ cytokines IL-2, IL-4 and IL-10 (**A-C**), T_{reg}/Th_{17} transcription factors FOXP3 and RORc (**D, E**) as well as the respective master cytokines TGFβ1 and IL-17A (**F, G**) was quantified via qRT-PCR relative to reference genes. n = 7.

5.2 BHB ENHANCES IMMUNE CAPACITY OF STIMULATED T CELLS

Since incubation of human immune cells with BHB had no significant impact on T-cell gene expression in the absence of any further T cell specific stimulus, PBMC were now incubated under T cell stimulating conditions using CD3/CD28 Dynabeads, mimicking a physiological T-cell activation. RPMI media contained 80 mg/dl glucose and was supplemented with 10 mM BHB. After 48 hours, pan T cells were isolated, and the supernatant was collected for further analyses.

5.2.1 Analysis of CD8⁺ T-cell immunity

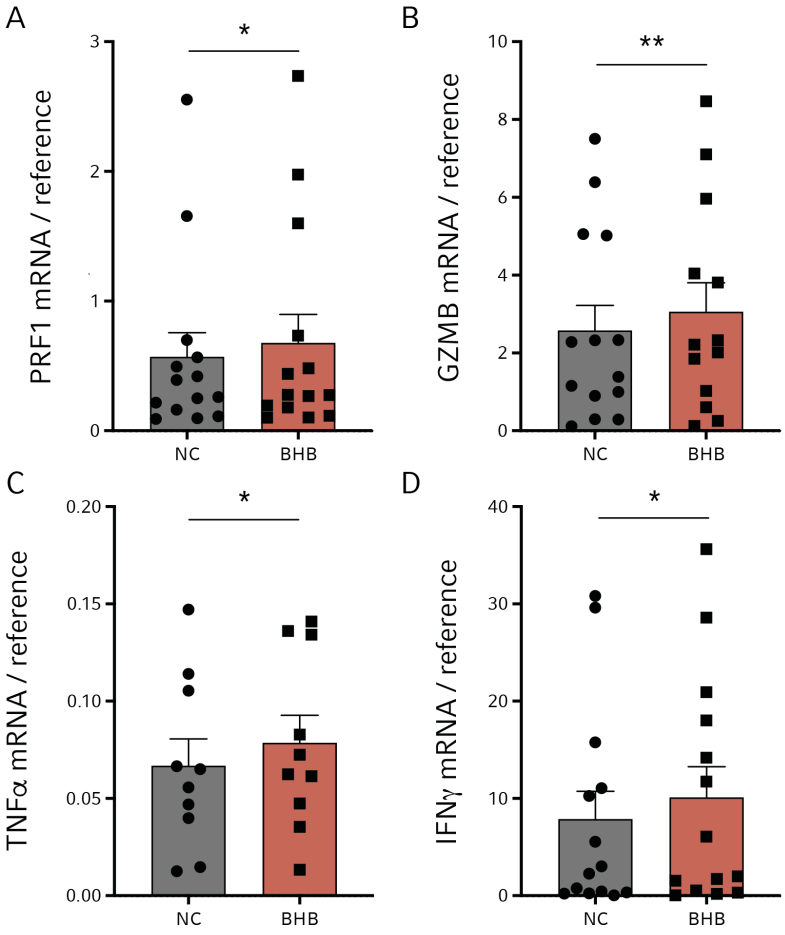

Figure 7: mRNA expression of CD8⁺ T-cell cytokines in stimulated T cells. PBMC from healthy subjects were incubated in RPMI containing 80 mg/dl glucose in the absence (NC) or presence of β-hydroxybutyrate (BHB) for 48 hours under T cell stimulating conditions. Pan T cells were isolated and gene expression of CD8⁺ cytokines PRF1, GZMB, TNFα and IFNγ (**A-D**) was quantified via qRT-PCR relative to reference genes. n = 14/13/10/14, *p < 0.05, **p < 0.01.

In stimulated T cells, BHB led to a significant upregulated gene expression of $CD8^+$ T-cell cytokines PRF1 (+18.87 % ± 12.11 %; p = 0.041), GZMB (+39.44 % ± 7.99 %; p = 0.007) and TNFα (+17.72 % ± 5.87 %; p = 0.014) as well as IFNγ (+28.19 % ± 10.52 %; p = 0.002) (Fig. 7). Protein secretion of IFNγ and TNFα was also increased after incubation with BHB (IFNγ: +29.00 % ± 10.62 %; p = 0.029, TNFα: +90.97 % ± 20.88 %; p = 0.0005, Fig. 8). The upregulated secretion of $CD8^+$ effector cytokines in T cells was also functionally evident as T cells displayed a markedly elevated cell lysis capacity upon incubation with BHB (+15.84 % ± 6.68 %; p = 0.045, Fig. 9).

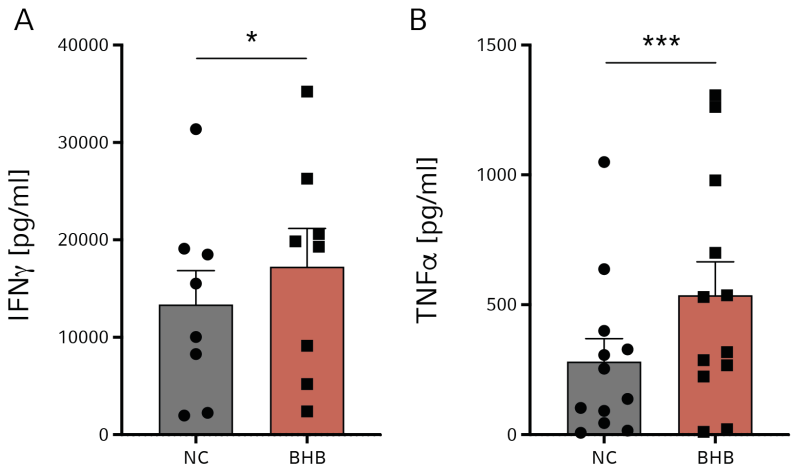

Figure 8: Secretion of $CD8^+$ cytokines. PBMC from healthy subjects were incubated in RPMI containing 80 mg/dl glucose in the absence (NC) or presence of β-hydroxybutyrate (BHB) for 48 hours under T cell stimulating conditions. Protein concentrations of IFNγ (**A**) and TNFα (**B**) in the supernatant were quantified by ELISA. n = 8/12, *p < 0.05, ***p < 0.001.

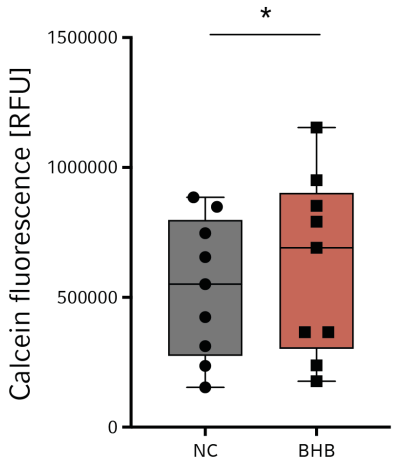

Figure 9: Evaluation of T cell specific cytotoxic capacity. PBMC from healthy subjects were incubated in RPMI containing 80 mg/dl glucose in the absence (NC) or presence of β-hydroxybutyrate (BHB) for 48 hours under T cell stimulating conditions. Subsequently, isolated T cells were co-cultivated with calcein-labeled glioblastoma cells and lysis-dependent fluorescence in the supernatant was quantified. RFU = Relative fluorescence units. n = 9, *p < 0.05.

5.2.2 Analysis of CD4⁺ T-cell immunity

Following incubation with BHB, qRT-PCR analyses revealed a significant transcriptional up-regulation of CD4⁺ cytokines IL-2 (+70.81 % ± 33.46 %; p = 0.007), IL-4 (+17.46 % ± 10.81 %; p = 0.026) and IL-8 (+33.64 % ± 15.45 %; p = 0.044) (Fig. 10) as well elevated protein levels of the respective cytokines in the supernatant (IL-2: +13.76 % ± 3.70 %; p = 0.005, IL-4: +44.30 % ± 15.78 %; p = 0.017 and IL-8: +40.09 % ± 12.49 %; p = 0.009, Fig. 11).

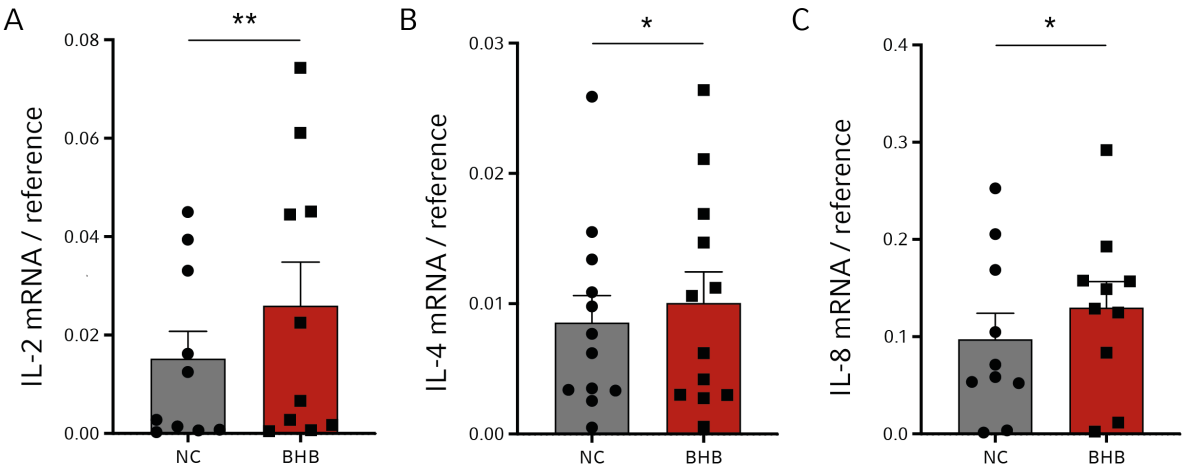

Figure 10: mRNA expression of CD4⁺ T-cell cytokines in stimulated T cells. PBMC from healthy subjects were incubated in RPMI containing 80 mg/dl glucose in the absence (NC) or presence of β-hydroxybutyrate (BHB) for 48 hours. Pan T cells were isolated and gene expression of CD4⁺ cytokines IL-2, IL-4 and IL-8 was quantified via qRT-PCR relative to reference genes (**A-C**). n = 10/12/10, *p < 0.05, **p < 0.01.

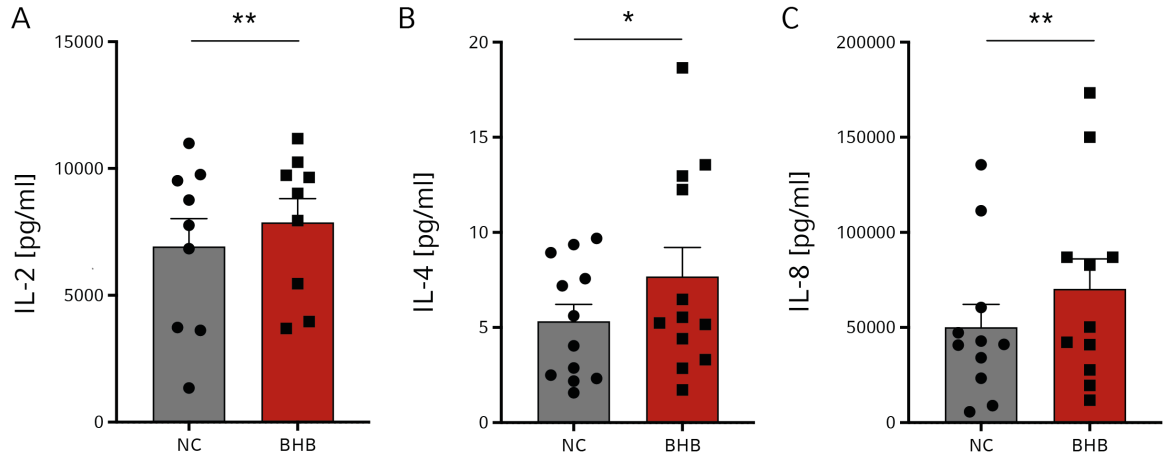

Figure 11: Secretion of CD4⁺ cytokines. PBMC from healthy subjects were incubated in RPMI containing 80 mg/dl glucose in the absence (NC) or presence of β-hydroxybutyrate (BHB) for 48 hours under T cell stimulating conditions. Protein concentrations of CD4⁺ cytokines IL-2, IL-4 and IL-8 in the supernatant were quantified by ELISA (**A-C**). n = 9/12/11, *p < 0.05, **p < 0.01.

5.3 BHB MODULATES DIFFERENTIATION OF TH_1 / TH_2 CELLS

$CD4^+$ T cells represent a heterogeneous cell population consisting of different subsets, each with a distinct functional profile. Among those, for a long time, T helper cells type 1 and 2 (Th_1 and Th_2 cells) have been the most commonly described T helper subsets. Following seven days of incubation under lineage specific conditions for differentiation, supplementation with BHB led to an attenuated gene expression of Th_1 transcription factor Tbet (-27.76 % ± 6.71 %; p = 0.009), whereas no changes of Th_2 transcription factor GATA3 could be depicted (Fig. 12 A, B). In line with the respective transcriptional changes, flow cytometric analysis revealed a considerable decrease of pro-inflammatory Th_1 cells (-17.06 % ± 5.49 %; p = 0.054), whereas differentiation of Th_2 cells remained unaltered (Fig. 12 C, D).

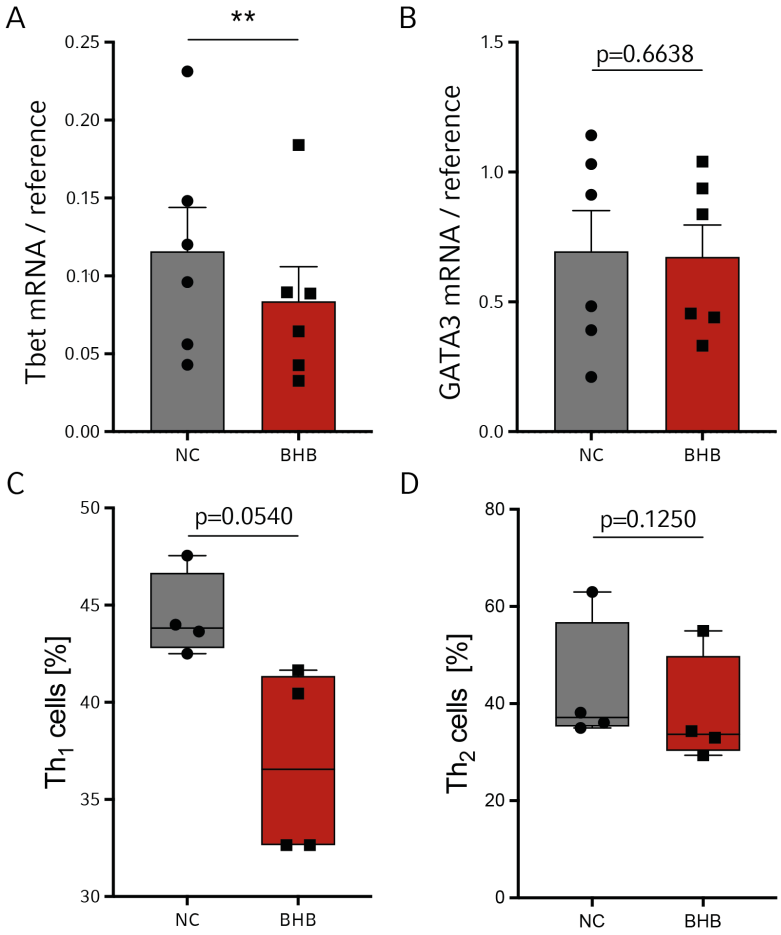

Figure 12: Analysis of Th_1/Th_2 T-cell differentiation. $CD4^+$ T cells of healthy subjects were incubated under Th_1 or Th_2-skewing conditions in the absence (NC) or presence of β-hydroxybutyrate (BHB) for seven days. mRNA expression of Th_1/Th_2 transcription factors Tbet and GATA3 was quantified via qRT-PCR relative to reference genes (**A, B**). Frequencies of Th_1/Th_2 subsets were assessed by flow cytometry (**C, D**). n = 6/6/4/4, **p < 0.01.

5.4 T_{REG} / TH_{17} CELL BALANCE IS REGULATED BY BHB

The next step was to investigate the effects of ketone bodies on regulatory T cells (T_{reg}) and pro-inflammatory Th_{17} cells, which are considered essential opponents in T cell-mediated immunity beyond the established Th_1/Th_2 paradigm.

5.4.1 Analysis of T_{reg} and Th_{17} cell differentiation after 48 hours of incubation

Gene expression of T_{reg} transcription factor FOXP3 as well as master cytokines IL-10 and TGFβ1 was analyzed in $CD4^+$ T cells after being isolated from PBMC following 48 hours incubation in the absences or presence of BHB. Here, no BHB-mediated impact on T_{reg} specific gene expression was detectable (Fig. 13).

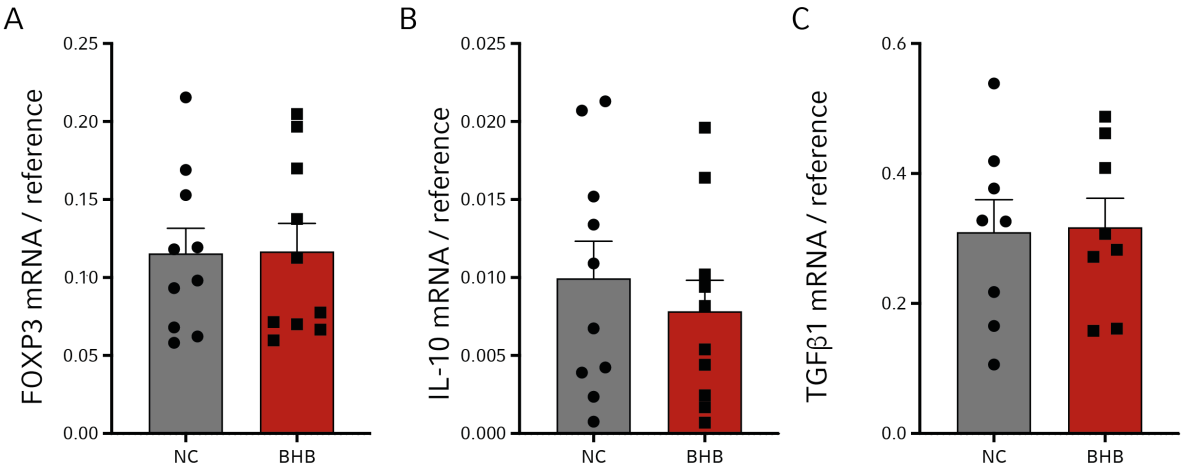

Figure 13: Analysis of T_{reg} specific gene expression after 48 hours incubation. PBMC from healthy subjects were incubated in RPMI containing 80 mg/dl glucose in the absence (NC) or presence of β-hydroxybutyrate (BHB) for 48 hours. $CD4^+$ T cells were isolated and mRNA expression of T_{reg} transcription factor FOXP3 and cytokines IL-10 and TGFβ1 was quantified via qRT-PCR relative to reference genes. n = 10/10/8.

After 48 hours, BHB led to an upregulation of Th_{17} transcription factor RORc (+33.58 % ± 9.06 %; p = 0.004, Fig. 14 A). Although mRNA expression of Th_{17} key cytokine IL-17A remained unaltered, protein secretion was significantly increased (+20.16 % ± 4.69 %; p =0.001, Fig. 14 B, F). Subsequently conducted differential flow cytometry analysis displayed a significant increase of both general IL-$17A^+$ $CD4^+$ T cells (+34.94 % ± 7.96 %; p = 0.021) as well as classical IL-17^+ IFNγ^- Th_{17} cells (+13.94 % ± 3.92 %; p = 0.037). Frequency of non-classical IL-$17A^+$ IFNγ^+ $Th_{17.1}$ cells was also elevated but without reaching statistical significance (+37.94 % ± 13.94 %; p = 0.072) (Fig. 14 C-E).

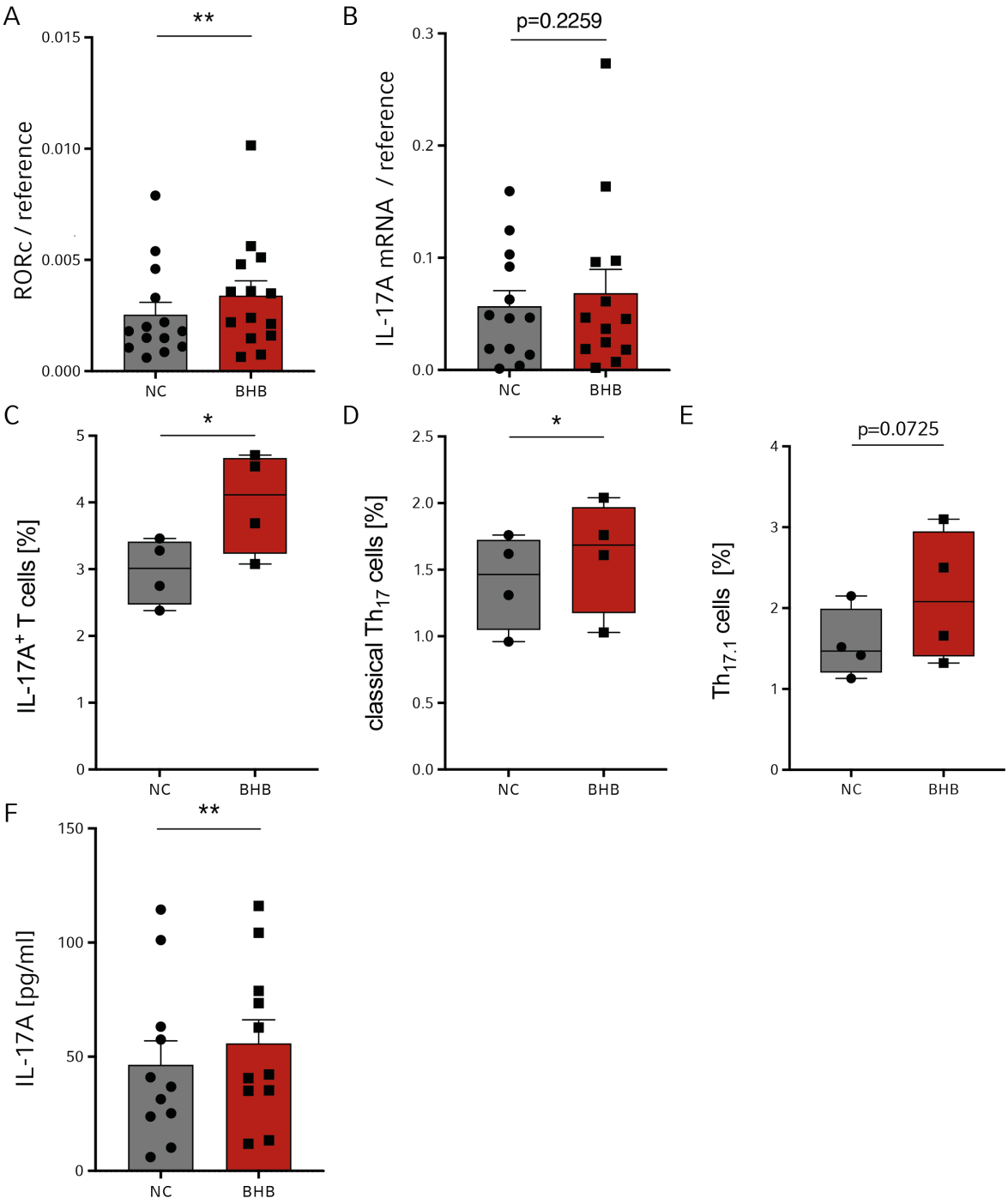

Figure 14: Analysis of Th_{17} differentiation after 48 hours incubation. PBMC from healthy subjects were incubated in RPMI containing 80 mg/dl glucose in the absence (NC) or presence of β-hydroxy-butyrate (BHB) for 48 hours. $CD4^+$ T cells were isolated and mRNA expression of Th_{17} transcription factor RORc and key cytokine IL-17A was quantified via qRT-PCR relative to reference genes (**A, B**). Frequencies of Th_{17} subsets were assessed via flow cytometry (**C-E**) and cytokine concentration of IL-17A in the supernatant was quantified by ELISA (**F**) n = 14/13/4/4/4/11, *$p < 0.05$, **$p < 0.01$.

5.4.2 Analysis of T_{reg} and Th_{17} cell differentiation after five days of incubation

Polarization of T cells toward distinct subsets is a process that normally requires several days. Therefore, in order to assess possible long-term effects of BHB on T_{reg} and Th_{17} cell differentiation, the incubation period was extended to five days in the absence or presence of BHB. Again, BHB did not alter gene expression of FOXP3 or IL-10 in $CD4^+$ T cells after five days of incubation. Likewise, neither changes in the total abundance of T_{reg} nor in IL-10 secretion were detectable (Fig. 15).

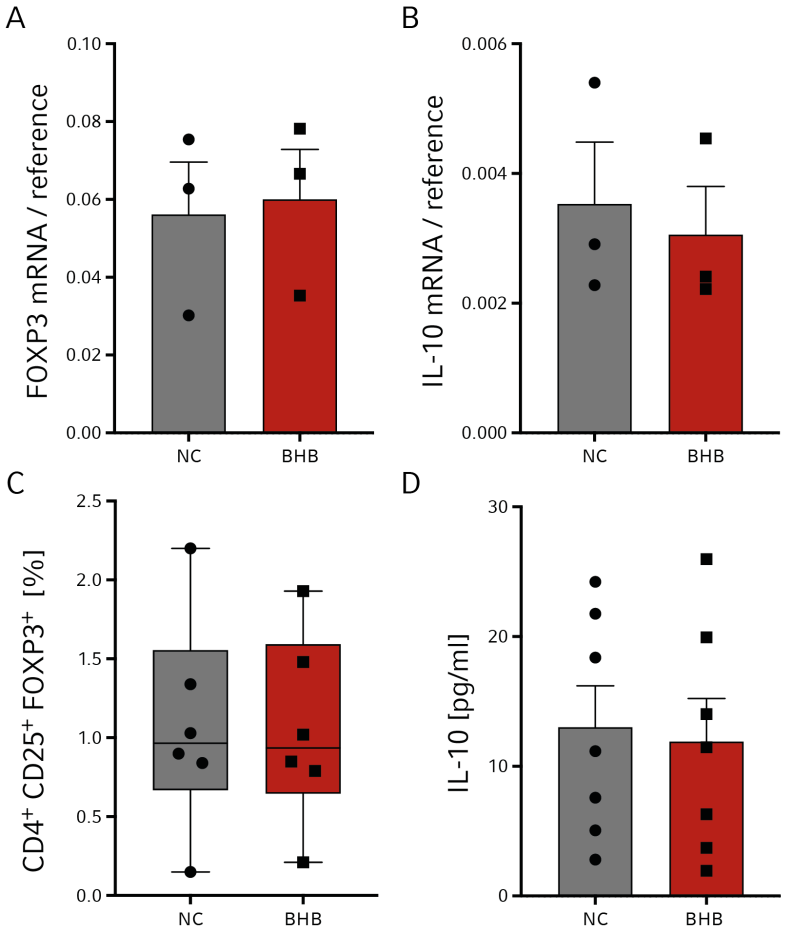

Figure 15: Analysis of T_{reg} differentiation after five days of incubation. PBMC from healthy subjects were incubated in RPMI containing 80 mg/dl glucose in the absence (NC) or presence of β-hydroxybutyrate (BHB) for five days. $CD4^+$ T cells were isolated and mRNA expression of T_{reg} transcription factor FOXP3 and cytokine IL-10 was quantified via qRT-PCR relative to reference genes (**A, B**). Frequency of T_{reg} was assessed by flow cytometry (**C**) and cytokine concentration of IL-10 in the supernatant was quantified by ELISA (**D**). n = 3/3/5/7.

Regarding Th_{17} cell differentiation, although no changes in RORc were detectable and IL-17A gene expression was even increased (+41.55 % ± 12.51 %; p = 0.045, Fig. 16 A, B), differential flow cytometric analysis revealed a significantly decreased frequency of $IL\text{-}17A^+$ $CD4^+$ T cells in response to BHB (-5.85 % ± 1.66 %; p = 0.038). Interestingly, differentiation of non-classical

$Th_{17.1}$ cells in particular was significantly attenuated (-10.60 % ± 1.84 %; p = 0.010), whereas the amount of classical IL-17A$^+$ IFN$^-$ Th_{17} cells as well as the IL-17A secretion capacity remained unaltered (Fig. 16 D-F).

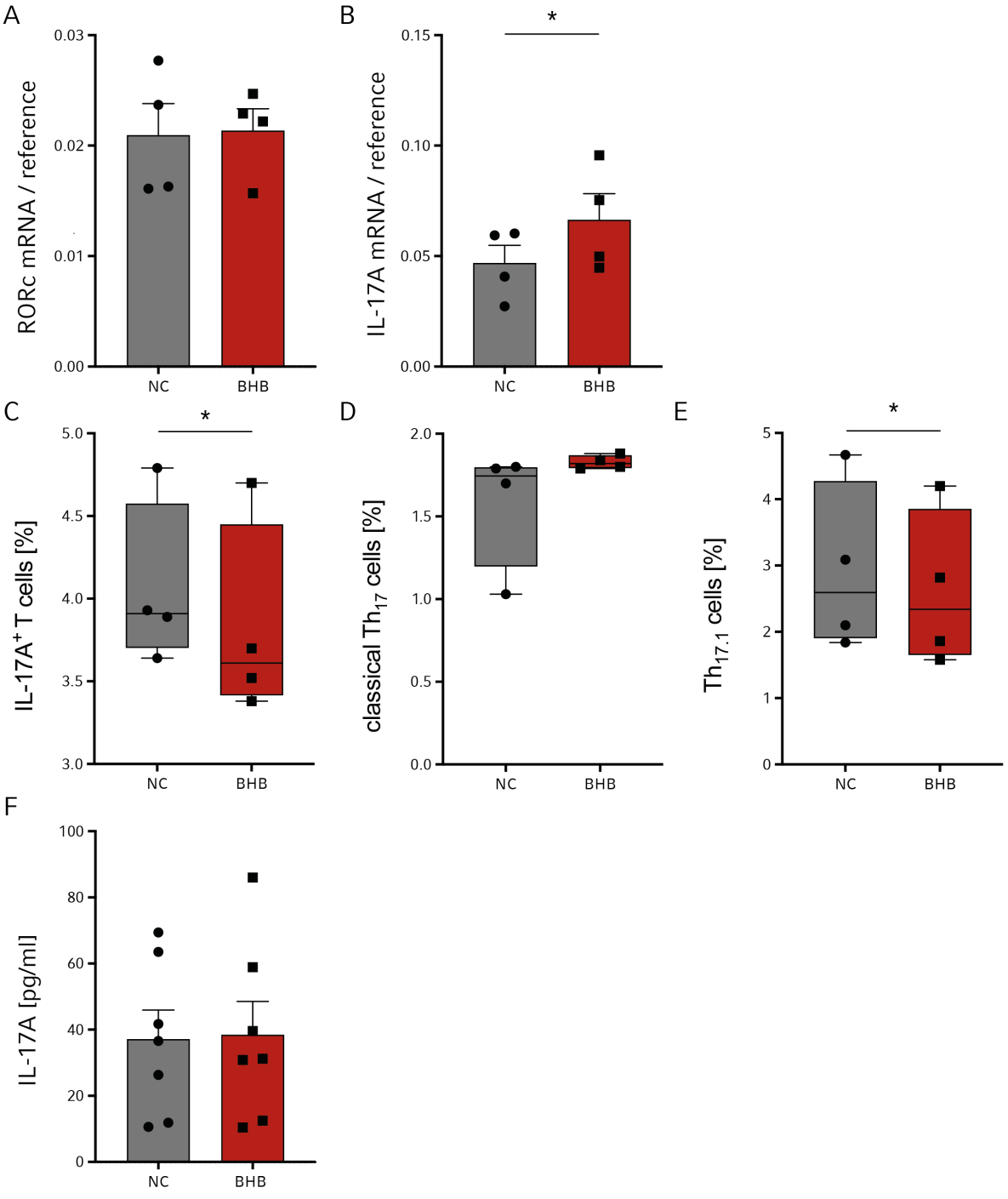

Figure 16: Analysis of Th_{17} cells after five days of incubation. PBMC from healthy subjects were incubated in RPMI containing 80 mg/dl glucose in the absence (NC) or presence of β-hydroxybutyrate (BHB) for five days. CD4$^+$ T cells were isolated and mRNA expression of Th_{17} transcription factor RORc and key cytokine IL-17A was quantified via qRT-PCR relative to reference genes (**A, B**). Frequencies of Th_{17} subsets were assessed via flow cytometry (**C-E**) and cytokine concentration of IL-17A in the supernatant was quantified by ELISA (**F**). n = 4/4/4/4/4/7, *p < 0.05.

5.4.3 Analysis of T_{reg} and Th_{17} cells under respective subset polarizing conditions

In addition to activation by antigen-presenting cells (APC), further differentiation of $CD4^+$ T cells into distinct subsets substantially depends on the respective cytokine microenvironment. Hence, BHB's capacity to regulate differentiation of T_{reg} and Th_{17} cells within a lineage-skewing cytokine milieu was assessed. Therefore, native $CD4^+$ T cells were cultured under specific subset-polarizing conditions. After seven days, gene expression, cell frequencies and cytokine secretion were analyzed.

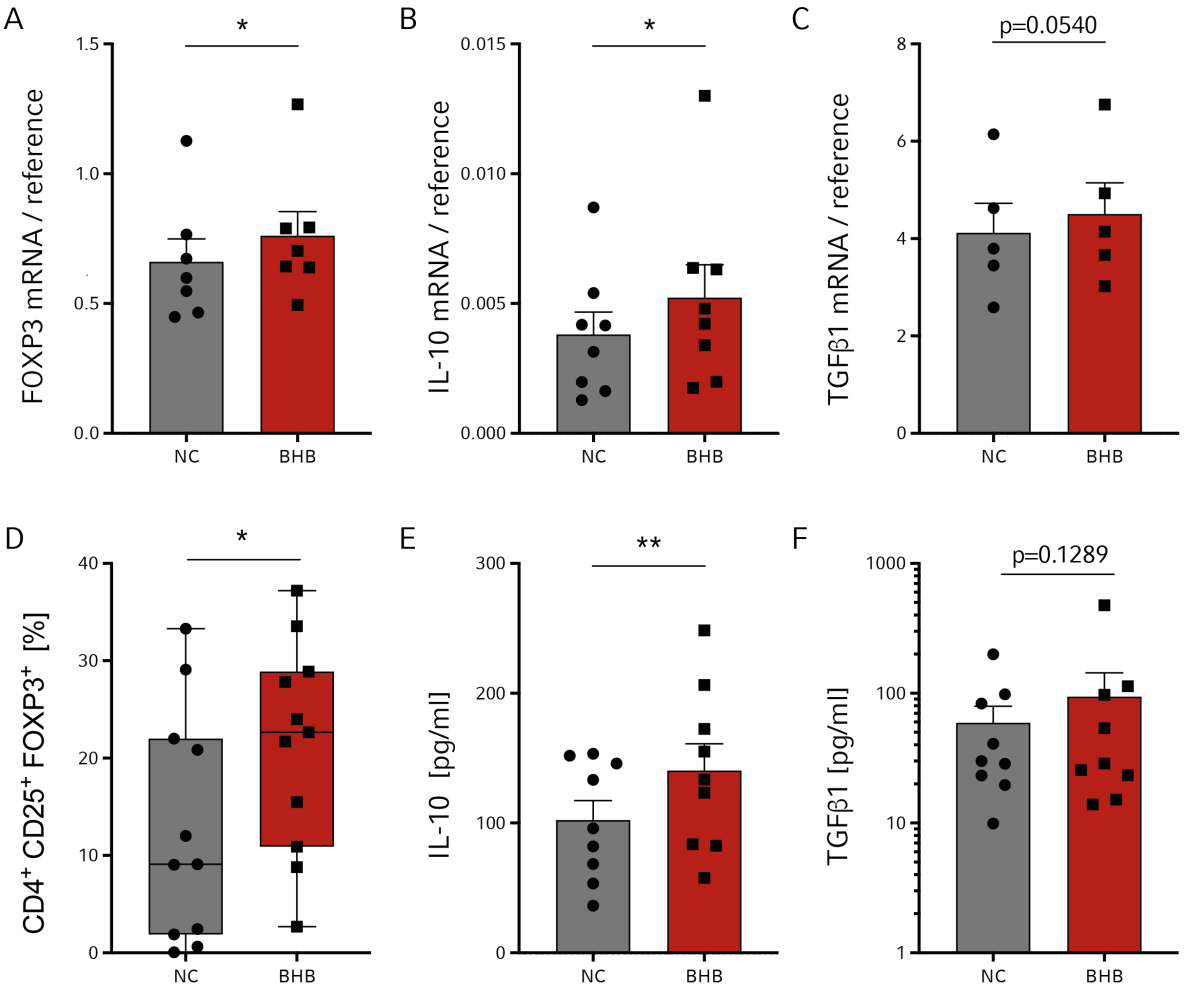

Figure 17: Analysis of T_{reg} differentiation under polarizing conditions. $CD4^+$ T cells of healthy subjects were incubated under T_{reg}-skewing conditions in the absence (NC) or presence of β-hydroxybutyrate (BHB) for seven days. mRNA expression of T_{reg} transcription factor FOXP3 and cytokines IL-10 and TGFβ1 was quantified via qRT-PCR relative to reference genes (**A-C**). Frequency of T_{reg} was assessed by flow cytometry (**D**) and cytokine concentration of IL-10 and TGFβ1 in the supernatant was quantified by ELISA (**E, F**). n = 7/8/5/11/9/9, *p < 0.05, **p < 0.01.

Incubation of BHB^+ $CD4^+$ T cells under T_{reg}-skewing condition led to a transcriptional upregulation of T_{reg} transcription factor FOXP3 (+15.22 % ± 4.71 %; p = 0.017, Fig. 17 A). Consequently, frequency of T_{reg} cells was significantly elevated (+66.41 % ± 22.44 %; p = 0.014, Fig. 17 D). Higher abundance of T_{reg} was followed by enhanced mRNA expression and protein secretion of effector cytokines IL-10 (mRNA: +37.33 % ± 14.74 %; p = 0.039, protein: +37.24 % ± 8.34 %; p = 0.002, Fig. 17 B, E) and TGFβ1 (mRNA: +9.27 % ± 3.52 %; p = 0.054, protein: +59.15 % ± 30.48 %; p = 0.128, Fig. 17 C, F).

Upon incubation in a cytokine milieu promoting Th_{17} cell differentiation, supplementation with BHB did not evoke significant changes in gene expression of RORc and IL-17A (Fig. 18 A, B). Analysis by flow cytometry, however, revealed a significantly decreased total number of overall $IL\text{-}17A^+$ $CD4^+$ T cells (-41.06 % ± 10.94 %; p = 0.005). Further subset analysis depicted a substantially reduced differentiation of both classical Th_{17} (-41.51 % ± 14.32 %; p = 0.027) as well as non-classical $Th_{17.1}$ cells (-42.42 % ± 10.43 %; p = 0.006) (Fig. 18 C-E). Reduction of Th_{17} cells was also reflected by a reduced secretion capacity of IL-17A (-13.52 % ± 4.10 %; p = 0.016, Fig. 18 F).

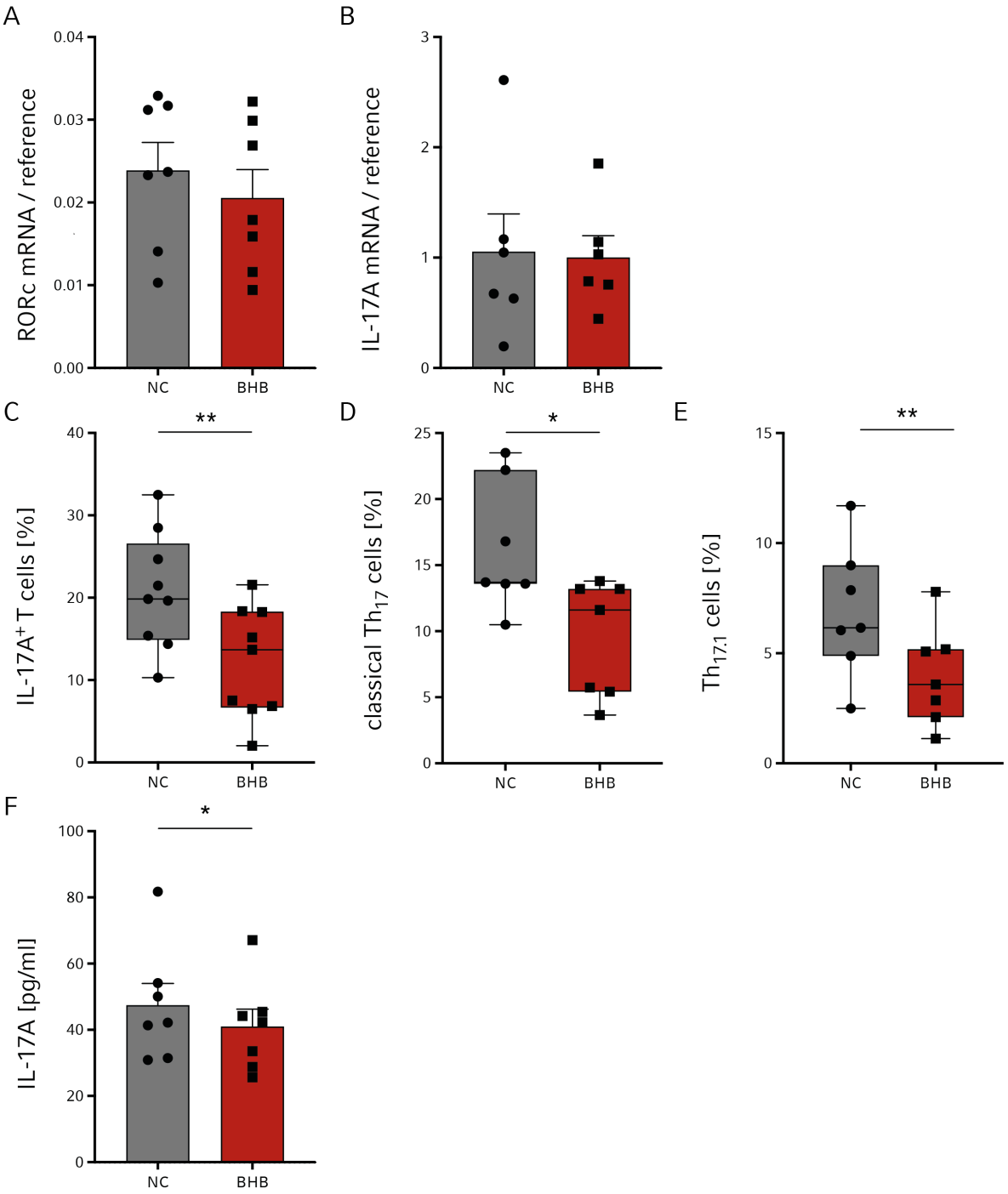

Figure 18: Analysis of Th_{17} subset differentiation under polarizing conditions. $CD4^+$ T cells of healthy subjects were incubated under Th_{17}-skewing conditions in the absence (NC) or presence of β-hydroxybutyrate (BHB) for seven days. mRNA expression of Th_{17} transcription factor RORc and key cytokine IL-17A was quantified via qRT-PCR relative to reference genes (**A, B**). Frequencies of Th_{17} subsets were assessed via flow cytometry (**C-E**) and cytokine concentration of IL-17A in the supernatant was quantified by ELISA (**F**). n = 7/6/9/7/7/7, *p < 0.05, **p < 0.01.

5.5 BHB LEADS TO OPPOSITE METABOLIC CHANGES IN T_{REG} AND TH_{17} CELLS

To this point, we were able to provide first evidence that ketone bodies differentially regulate the development of opponent T_{reg} and Th_{17} cells in favor of a more anti-inflammatory T helper cell phenotype. We next sought to characterize the possible underlying mechanisms accountable for this observed effect. Each lineage of the heterogeneous T helper cell compartment relies on unique metabolic pathways which are closely associated with cell differentiation and the functional capacity of the respective cell line. Of note, immunosuppressive T_{reg} take on a metabolic signature that is profoundly distinct from that of their pro-inflammatory Th_{17} counterpart[55,98].

We thus hypothesized that the observed opposite changes in T_{reg} and Th_{17} cell frequencies and cytokine secretion might be due to different metabolic alterations in these opposing cell lines in response to BHB. Therefore, following five days of cultivation in the absence or presence of BHB, T_{reg} and Th_{17} cells were isolated from PBMC, and metabolic analyses were conducted in order to characterize the energy pathways in each subset separately.

5.5.1 Mitochondrial analysis of T_{reg}

Regulatory T cells displayed a significant enhancement of basal (+18.40 % ± 3.26 %; $p = 0.0003$) and maximal respiratory rates (+15.82 % ± 5.24 %; $p = 0.009$) as well as a marked increase in spare respiratory capacity (+38.59 % ± 10.06 %; $p = 0.048$) upon five-day incubation with BHB, quantified via Seahorse analyses (Fig. 19 A-E). Consistent with these results, mitochondrial mass in BHB^+ T_{reg} was also markedly increased (+34.38 % ± 12.97 %; $p = 0.019$), which was demonstrated by flow cytometry (Fig. 19 F). However, this shift toward oxidative respiration did not attenuate the glycolytic capacity as the extracellular acidification rate (ECAR) remained unaltered (Fig. 20).

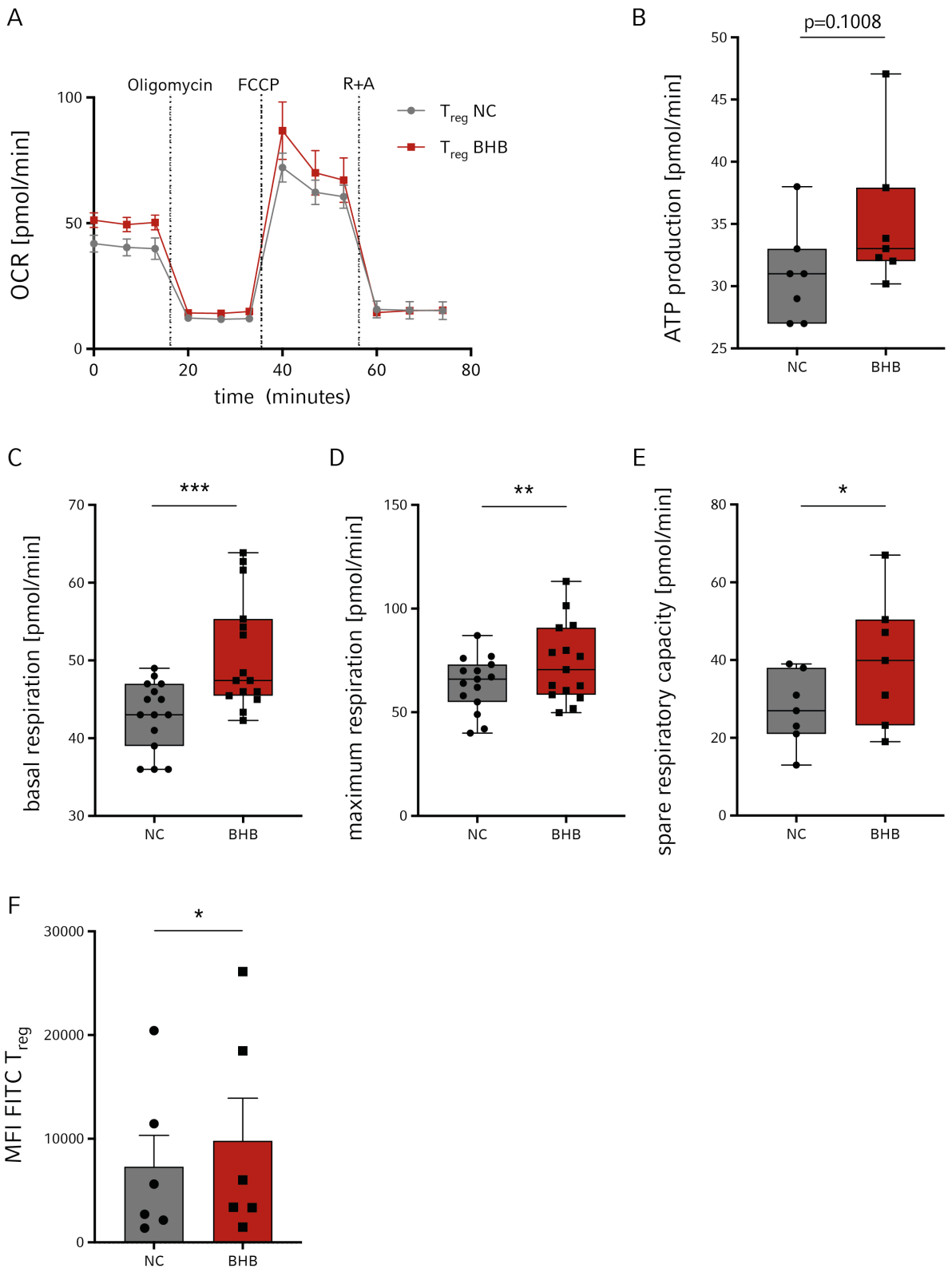

Figure 19: Analysis of mitochondrial metabolism of T_{reg}. PBMC from healthy subjects were incubated in RPMI containing 80 mg/dl glucose in the absence (NC) or presence of β-hydroxybutyrate (BHB) for five days. T_{reg} were isolated and oxygen consumption rate (OCR, **A**), ATP production (**B**), basal (**C**), and maximal respiration (**D**) as well as spare respiratory capacity (**E**) were assessed in a Seahorse XF96 Analyzer using the Mito Stress Kit. Mitochondrial mass **(F)** was quantified by flow cytometry using MitoTrackerGreen dye indicated by MFI FITC. R + A = rotenone + antimycin A, MFI = mean fluorescence intensity, n = 3/6, *p < 0.05, **p < 0.01, ***p < 0.001.

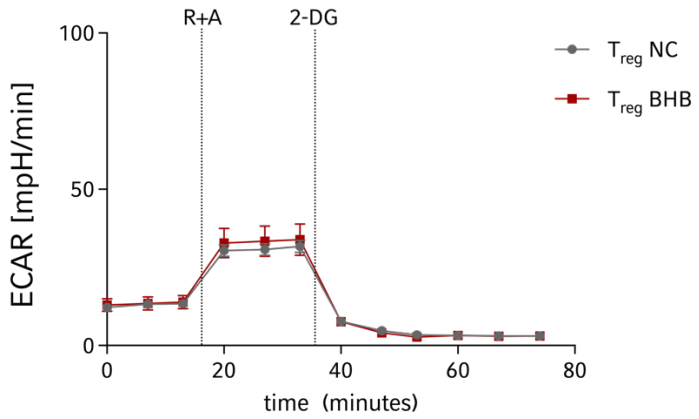

Figure 20: Analysis of glycolytic capacity of T_{reg}. PBMC from healthy subjects were incubated in RPMI containing 80 mg/dl glucose in the absence (NC) or presence of β-hydroxybutyrate (BHB) for five days. T_{reg} were isolated and extracellular acidification rate (ECAR) was assessed in a Seahorse XF96 Analyzer using the Glycolytic Rate Assay. R + A = rotenone + antimycin A, 2-DG = 2-Desoxyglucose, n = 3.

5.5.2 Mitochondrial analysis of Th_{17} cells

However, in Th_{17} cells, analysis of oxygen consumption rate revealed that following BHB supplementation, basal (-16.58 % ± 3.19 %; p = 0.0002), maximum (-30.89 % ± 5.87 %; p < 0.0001) and spare respiratory capacity (-38.11 % ± 15.56 %; p = 0.049) were markedly decreased (Fig. 21 A-E). Consistent with this, mitochondrial mass was reduced in Th_{17} cells but without reaching statistical significance yet (-36.41 % ± 18.68 %; p = 0.063, Fig. 21 F). Notably, BHB^+ Th_{17} cells – unlike T_{reg} – displayed a compromised capacity of glycolysis as seen in decreased ECAR (Fig. 22).

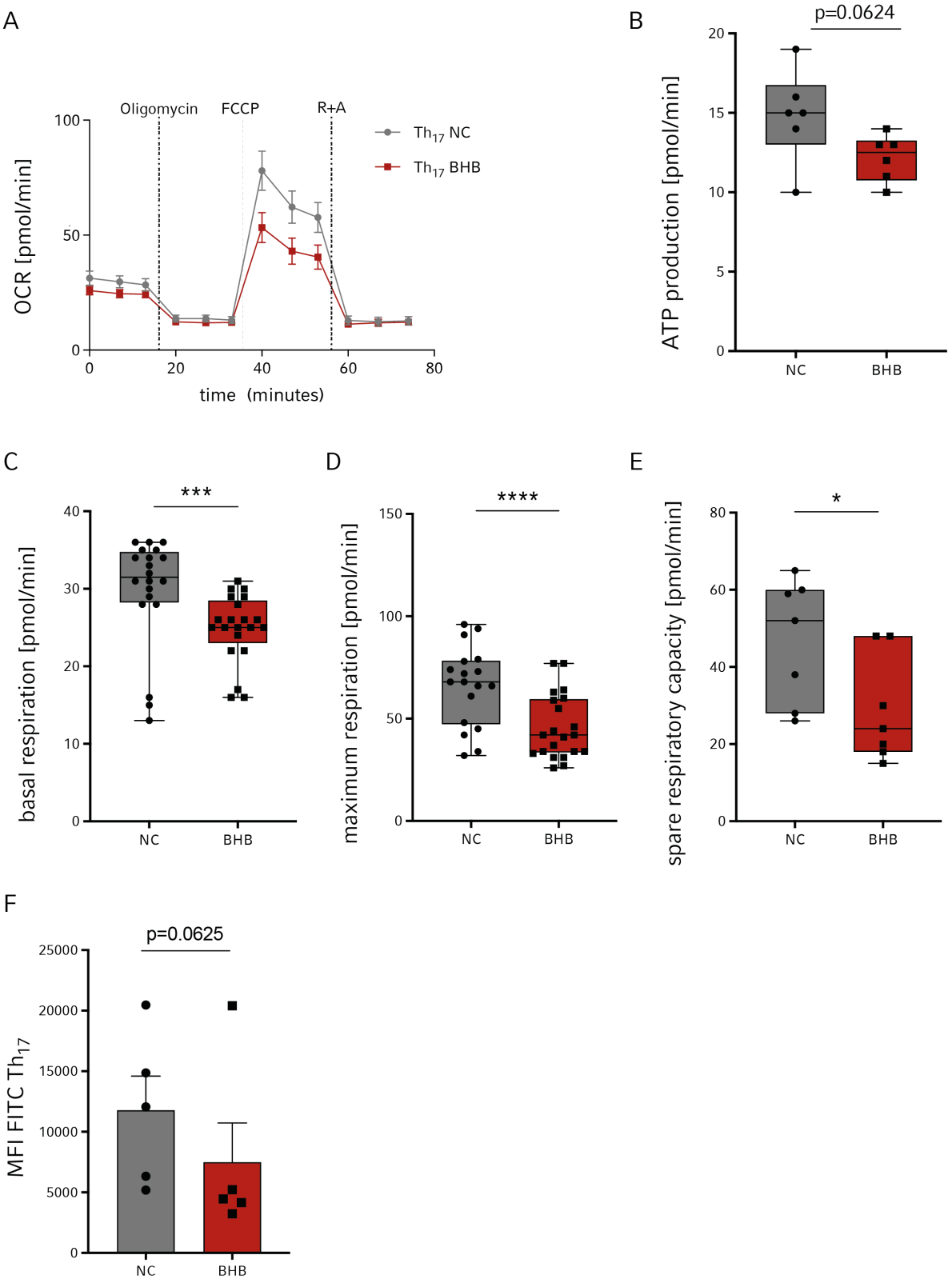

Figure 21: Analysis of mitochondrial metabolism of Th_{17} cells. PBMC from healthy subjects were incubated in RPMI containing 80 mg/dl glucose in the absence (NC) or presence of β-hydroxybutyrate (BHB) for five days. Th_{17} cells were isolated and oxygen consumption rate (OCR, **A**), ATP production (**B**), basal (**C**), and maximal respiration (**D**) as well as spare respiratory capacity (**E**) were assessed in a Seahorse XF96 Analyzer using the Mito Stress Kit. Mitochondrial mass **(F)** was quantified by flow cytometry using MitoTrackerGreen dye indicated by MFI FITC R + A= rotenone + antimycin A, n = 3/4, *p < 0.05, ***p < 0.001, ****p < 0.0001.

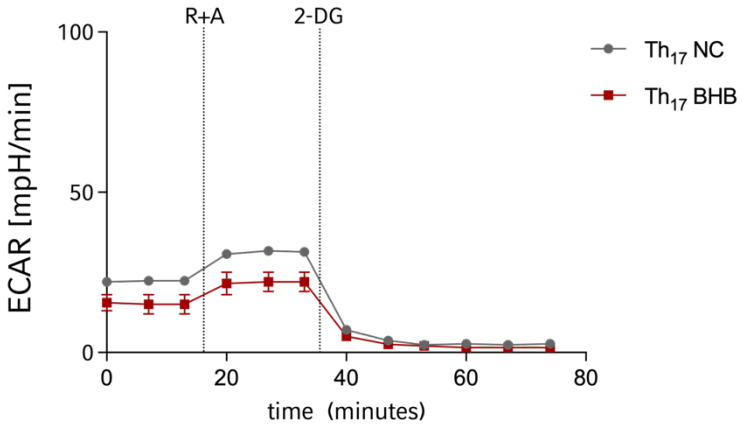

Figure 22: Analysis of glycolytic capacity of Th_{17} cells. PBMC from healthy subjects were incubated in RPMI containing 80 mg/dl glucose in the absence (NC) or presence of β-hydroxybutyrate (BHB) for 5 days. Th_{17} cells were isolated and extracellular acidification rate (ECAR) was assessed in a Seahorse XF96 Analyzer using the Glycolytic Rate Assay. R + A= rotenone + antimycin A, 2-DG = 2-Desoxyglucose, n = 3.

Taken together, BHB appeared to differentially reprogram metabolic pathways in T helper cells in a subset-dependent manner. In T_{reg} cells, BHB significantly increased mitochondrial respiration without affecting glycolytic capacity, whereas in Th_{17} cells, both OXPHOS and glycolysis were severely impaired.

5.6 KETOGENIC DIET – PROSPECTIVE *IN VIVO* INTERVENTION STUDY

In vitro results displayed substantial transcriptional, functional, and metabolic alterations in human T cells upon incubation with BHB.

In order to validate these promising findings and to translate the previous *in vitro* approaches into clinical practice, a prospective nutritional intervention study was initiated, in which healthy volunteers were to follow a three-week diet with restricted carbohydrate consumption.

5.6.1 *In vivo* study design

As depicted in Figure 23, healthy volunteers were asked to perform a three-week ad libitum ketogenic diet, limiting total carbohydrate intake to less than 30 g per day. Prior to (T0) and after (T1) the dietary intervention blood was collected and stimulated *ex vivo* for 24 hours for subsequently conducted immunological analyses of separated $CD4^+$ and $CD8^+$ T cells and monitoring of blood glucose levels. For assessment of whole blood cytokine expression, blood was directly drawn into TruCulture tubes. Throughout the study, endogenous ketone body levels were quantified on a regular basis using point-of-care quantification.

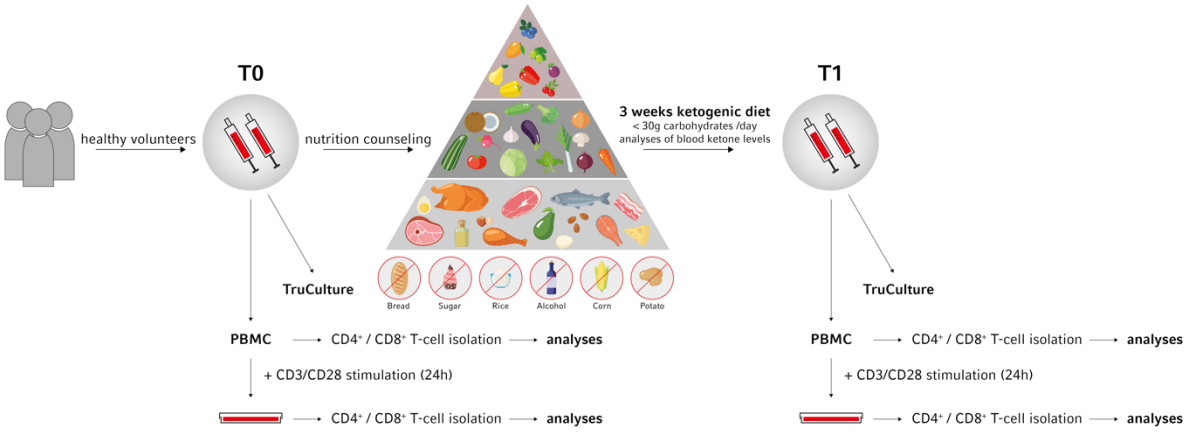

Figure 23: Schematic layout of study flow. Healthy volunteers underwent a ketogenic diet, consuming less than 30 g carbohydrates per day for a duration of three weeks. Prior to (T0) and after (T1) the dietary intervention blood was collected and stimulated *ex vivo* for 24 hours or directly drawn into TruCulture tubes for analysis of whole blood cytokine secretion. Subsequently, immunological analyses were performed, and blood glucose levels were determined. Ketone body levels were monitored regularly throughout the study by point-of-care-testing[99].

5.6.2 Plasma ketone body and glucose levels during KD

KD resulted in markedly increased blood ketone levels ranging between 1.0 and 1.5 mM with a maximum of 3.1 mM (Fig. 24 A), whilst fasting blood glucose levels remained stable and within normal range (Fig. 24 B).

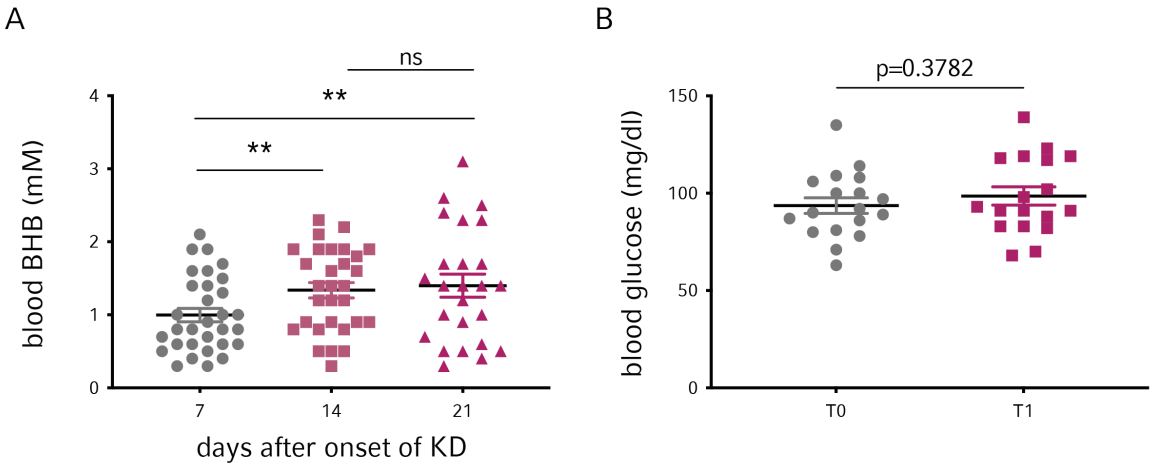

Figure 24: Ketone bodies and fasting serum glucose. Healthy volunteers conducted a three-week ketogenic diet. β-hydroxybutyrate (BHB) levels were monitored by point-of-care-measurements (**A**). Prior to (T0) and after (T1) the dietary intervention fasting plasma glucose levels were determined via laboratory tests (**B**). n = 30/18. ns = not significant, **p < 0.01.

5.7 KETOGENIC DIET ALONE DOES NOT ACTIVATE HUMAN T CELLS

In accordance with the previous *in vitro* experiments, a ketogenic diet did not alter gene expression patterns in unstimulated $CD8^+$ (Fig. 25) and $CD4^+$ T cells (Fig. 26). Particularly, no changes of T_{reg} and Th_{17} specific transcription factors and key cytokines were observed (Fig. 26 F-H)

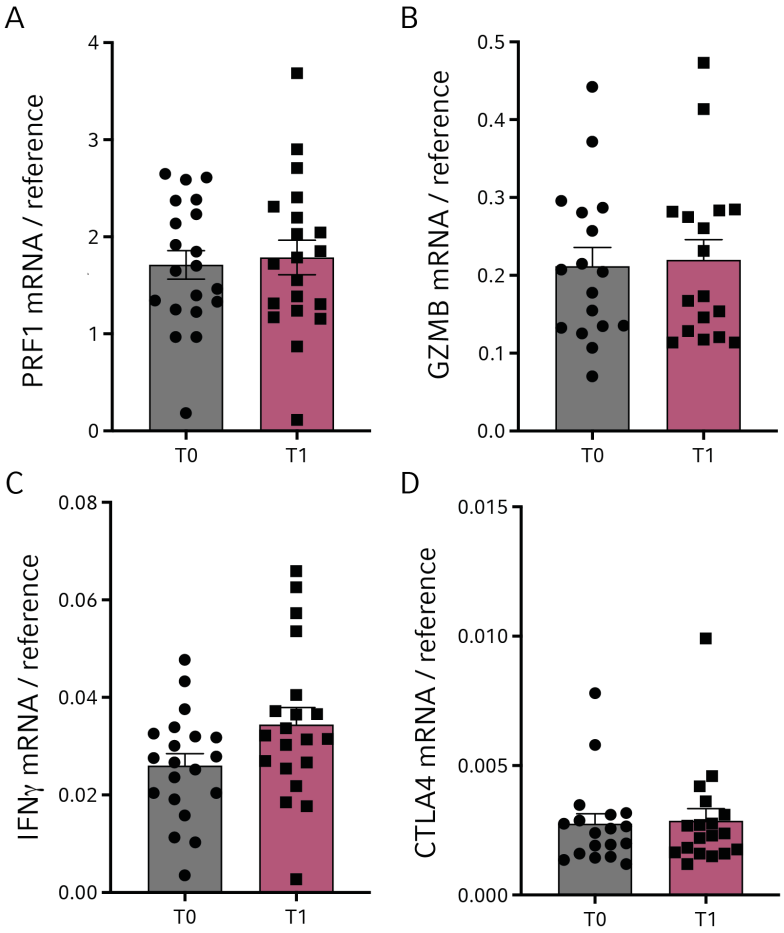

Figure 25: mRNA expression in unstimulated $CD8^+$ T cells in response to KD. Healthy volunteers conducted a three-week ketogenic diet. Prior to (T0) and after (T1) the dietary intervention $CD8^+$ T cells were isolated and gene expression of PRF1, GZMB, IFNγ and CTLA4 was quantified via qRT-PCR relative to reference genes. n = 20/17/20/18.

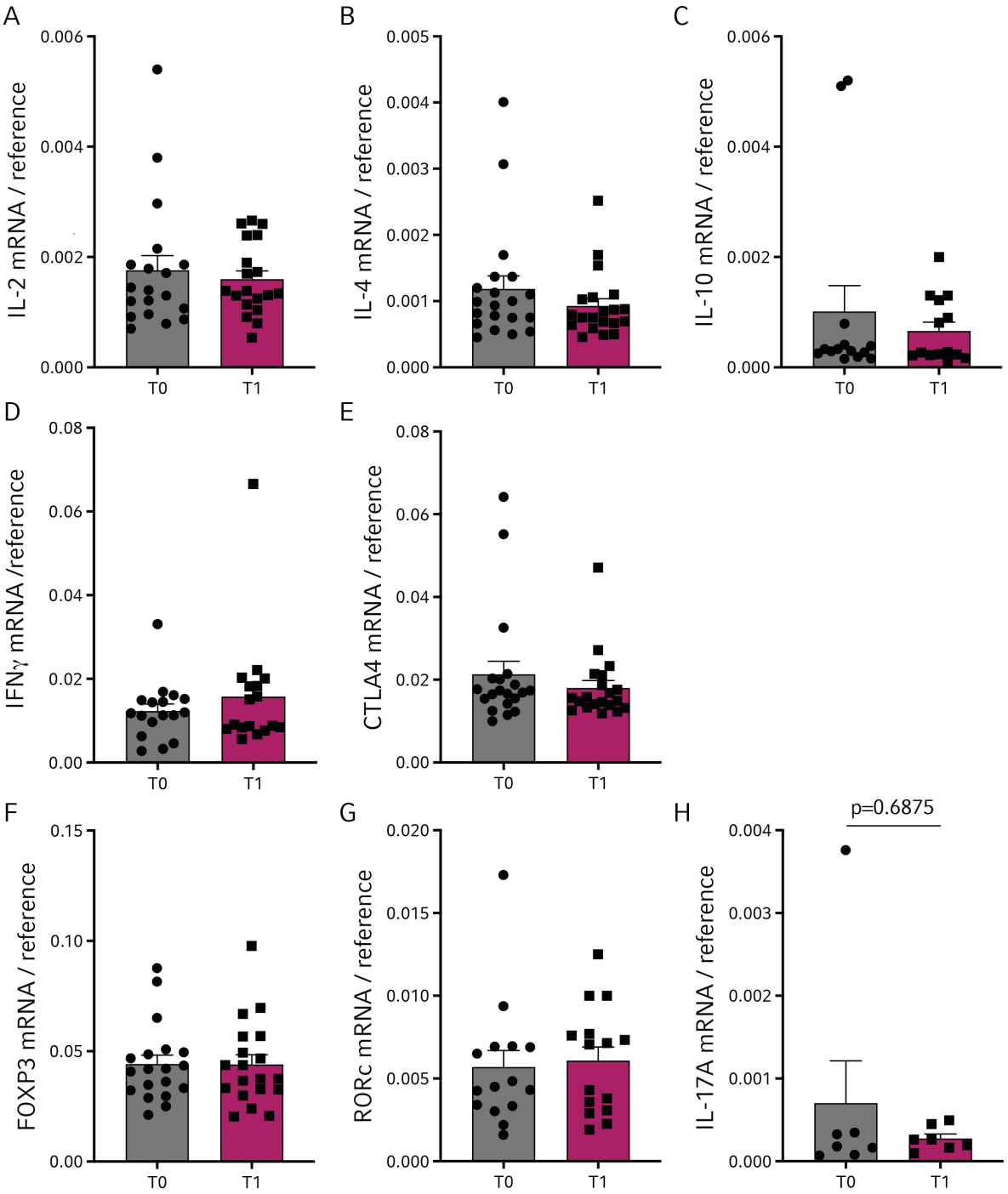

Figure 26: mRNA expression in unstimulated CD4⁺ T cells in response to KD. Healthy volunteers conducted a three-week ketogenic diet. Prior to (T0) and after (T1) the dietary intervention CD4⁺ T cells were isolated and gene expression of IL-2, IL-4, IL-10, IFNγ, CTLA (**A-E**), T_{reg}/Th_{17} transcription factors RORc and FOXP3 (**F, G**) as well as the Th_{17} key cytokine IL-17A (**H**) were quantified via qRT-PCR relative to reference genes, n = 19/20/14/17/20/20/15/7.

.

5.8 T-CELL DIFFERENTIATION AND TRANSCRIPTOMIC PHENOTYPING

KD did not lead to transcriptomic alteration in T cells without further T cell specific stimulation. Therefore, next, PBMC from volunteers conducting a KD were stimulated *ex vivo* for 24 hours prior to subsequent analyses. Analogous to the *in vitro* approaches T-cell stimulation was performed by using CD3/CD28 Dynabeads, mimicking a T-cell immune activation by APC.

5.8.1 $CD4^+$ / $CD8^+$ T-cell ratio

First, the overall frequency of $CD4^+$ and $CD8^+$ T cells was determined. Here, an increase in $CD8^+$ T cells (+10.63 % ± 3.93 %; p = 0.019) could be detected, while the number of $CD4^+$ T cells remained unchanged after KD, leading to a significant decrease of the $CD4^+/CD8^+$ T-cell ratio (-10.15 % ± 3.66 %; p = 0.018) (Fig. 27).

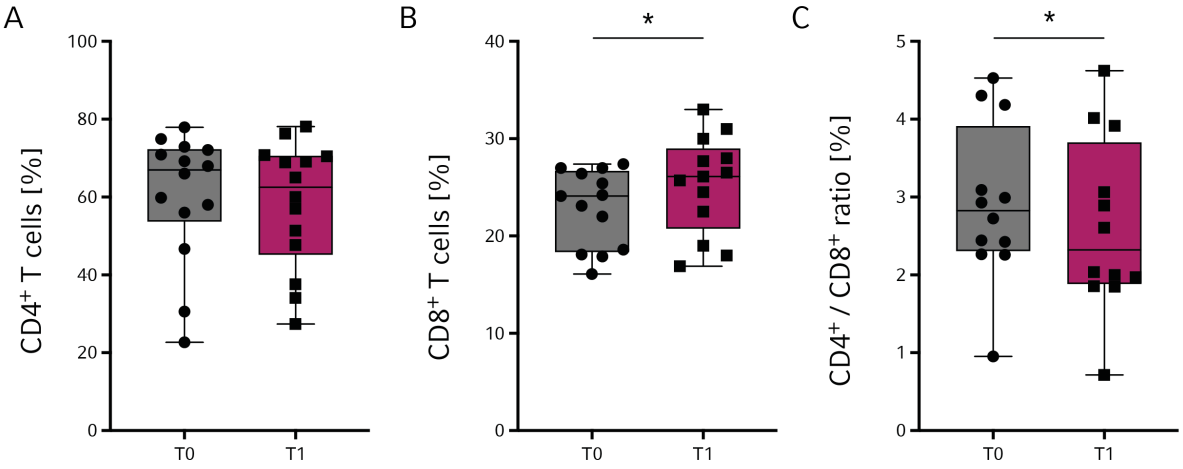

Figure 27: Flow cytometric quantification of $CD4^+$ and $CD8^+$ T cells in response to KD. Healthy volunteers conducted a three-week ketogenic diet. Prior to (T0) and after (T1) the dietary intervention PBMC were isolated and stimulated *ex vivo* for 24 hours. Frequencies of $CD4^+$ (**A**) and $CD8^+$ T cells (**B**) as well as the $CD4^+/CD8^+$ ratio (**C**) were quantified via flow cytometer. n = 14/13/12, *p < 0.05.

5.8.2 Transcriptome and gene set enrichment analysis of CD4+ and CD8+ T cells

Incubation with BHB significantly enhanced T-cell immune capacity and affected both the differentiation of various $CD4^+$ T helper cell subsets and the metabolic processes of the respective cell lines. We next sought to identify yet unknown gene expression patterns and signaling pathways in human T cells that are directly altered in response to carbohydrate restriction.

Therefore, differential gene expression in $CD4^+$ and $CD8^+$ T cells from healthy participants was analyzed in RNA-samples taken prior to and after the nutritional intervention. T1/T0 transcriptome analysis revealed a significant regulation of genes known to be associated with T-cell activation and differentiation (NR4A1, NFKBID, TNF, TNFRSF9, CRTAM, DUSP4, TRAV30), but also of those associated with T-cell regulation (EGR2) as well as of genes involved in fatty acid metabolism and mitochondrial pathways (ACSL6, TOMM7)[100] (Fig. 28 A, B). Transcriptome profiling showed that expression of NR4A1 (nuclear receptor 4A1, Nur77) in particular was considerably enhanced in response to KD. Overexpression of this immediate early response gene has recently been reported to impair both Th_1 and Th_{17} cell differentiation, whereas knockdown of NR4A1 in an EAE mouse model resulted in accelerated and more severe disease activity accompanied by an increase in IFNγ- and IL-17A-secreting $CD4^+$ T cells[101,102]. These fundamental changes were also evident in the gene set enrichment analyses depicting the significantly regulated signaling pathways in both T-cell lineages. Gene set enrichment analyses showed significant changes regarding T-cell function and different metabolic pathways (Fig. 28 C).

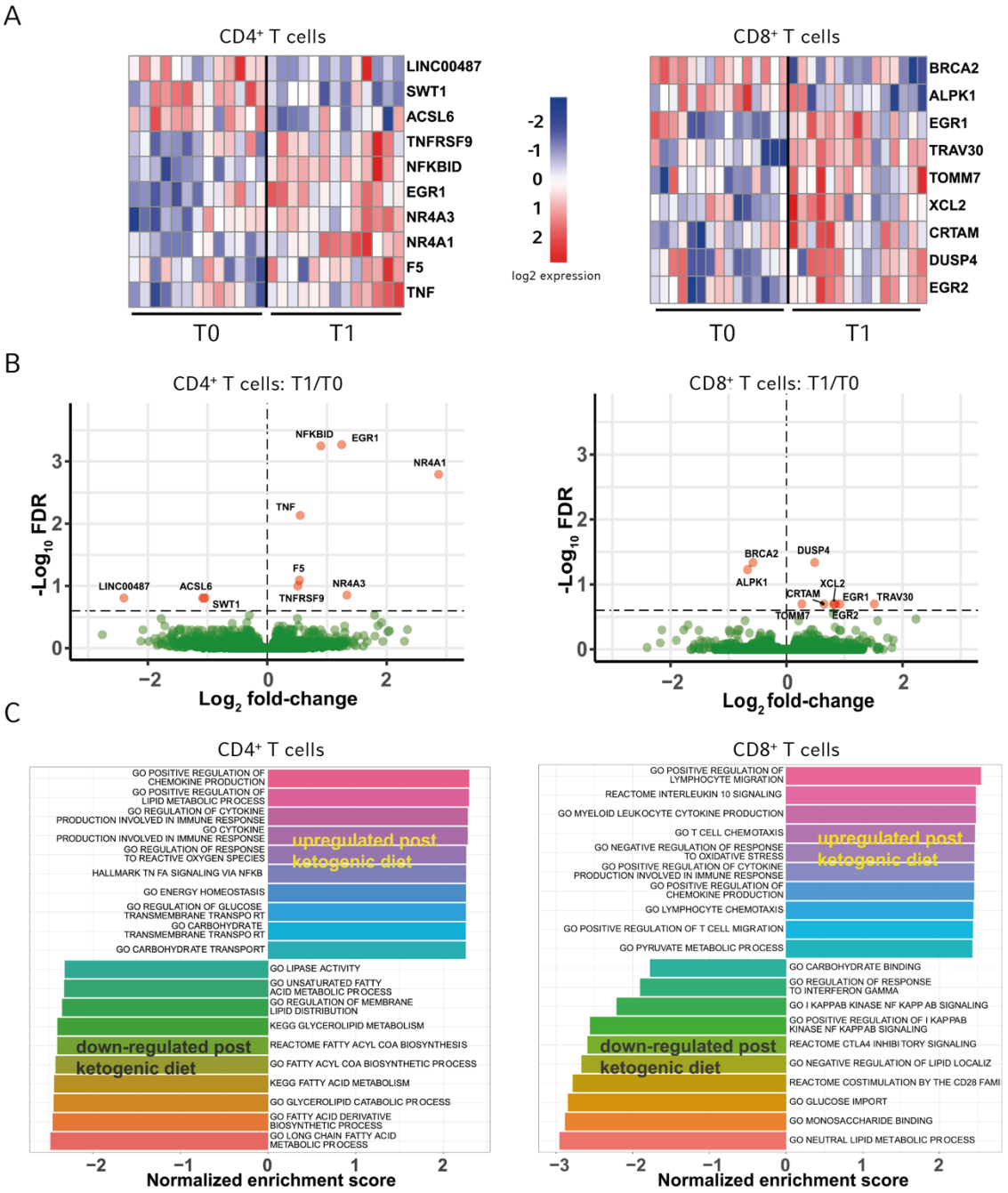

Figure 28: Next-generation sequencing of CD4⁺ and CD8⁺ T cells in response to KD. Healthy volunteers conducted a three-week ketogenic diet. Prior to (T0) and after (T1) the dietary intervention PBMC were isolated and stimulated *ex vivo* for 24 hours. Afterwards, CD4⁺ and CD8⁺ T cells were separated for gene expression analyses. Heatmaps of significantly differentially regulated genes in CD4⁺ (left) and CD8⁺ T cells (right) in response to KD. The color and intensity of the boxes illustrate upregulation (red) or downregulation (blue) of genes after KD (**A**). Representation of T1/T0 differential gene expression in human CD4⁺ (left) and CD8⁺ T cells (right) using Volcano plots. Each point represents a gene as a function of fold change (Log_2 fold-change, x-axis) and statistical significance (Log_{10} FDR-corrected p-values, y-axis). The dashed horizontal line depicts the FDR threshold of 25%, red points highlight significantly regulated genes (**B**). Gene set enrichment analysis for visualization of the ten most highly regulated pathways in CD4⁺ (left) and CD8⁺ T cells (right). Positive (normalized) enrichment scores indicate upregulation, negative (normalized) enrichment scores indicate downregulation upon KD (**C**). FDR = false discovery rate, log = logarithm, GO = Gene Ontology, n = 13/15.

5.9 KETOGENIC DIET ENHANCES CD8⁺ T-CELL IMMUNE CAPACITY

Initial qRT-PCR *in vitro* analyses of CD8⁺ T cells confirmed the considerable KD-induced effects on human T cells. Here, key cytokines of cytotoxic T cells GZMB (+31.38 % ± 12.31 %; p = 0.034) and IFNγ (+55.94 % ± 17.83 %; p = 0.029) were significantly increased by KD. Perforin gene expression (PRF1) was also elevated but did not reach statistical significance (+12.75 % ± 10.43 %; p = 0.329). Furthermore, immune checkpoint protein cytotoxic T-lymphocyte-associated protein 4 (CTLA4) expression was upregulated (+37.63 % ± 15.27 %; p = 0.035) (Fig. 29). In line with the observed induction of CD8-related effector cytokines, CD8⁺ T cells displayed a significantly increased cell lysis capacity after KD (+167.20 % ± 37.34 %; p = 0.020, Fig. 30).

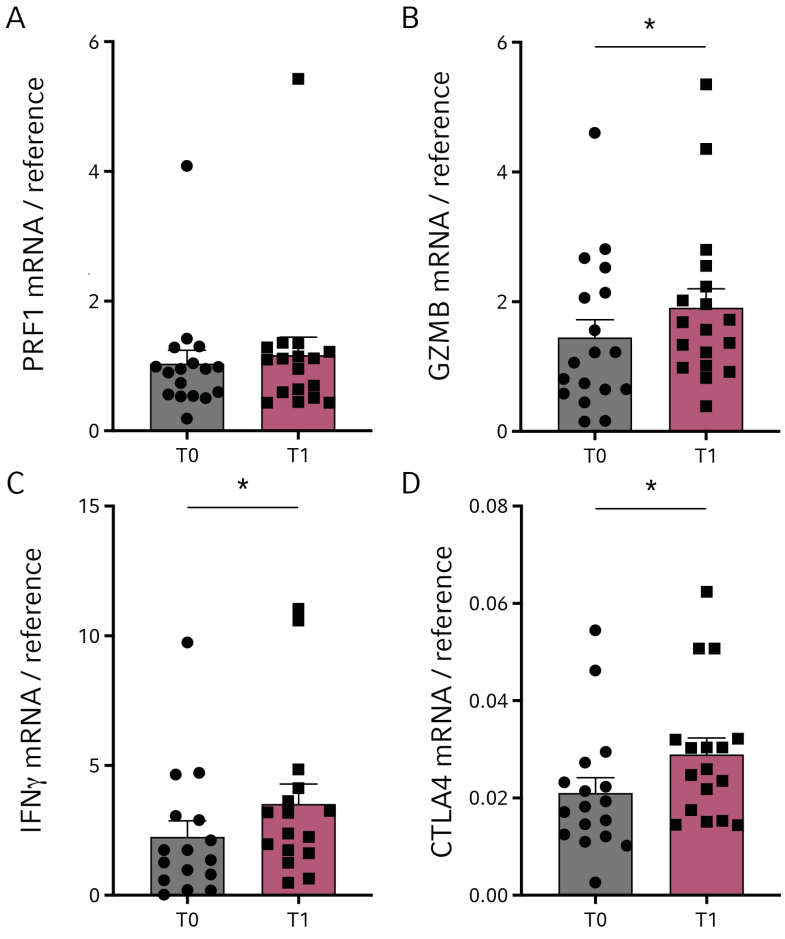

Figure 29: mRNA expression in stimulated CD8⁺ T cells in response to KD. Healthy volunteers conducted a three-week ketogenic diet. Prior to (T0) and after (T1) the dietary intervention PBMC were isolated and stimulated *ex vivo* for 24 hours. Afterwards, CD8⁺ T cells were separated and gene expression of PRF1, GZMB, IFNγ and CTLA4 was quantified via qRT-PCR relative to reference genes. n = 17/18/16/17, *p < 0.05.

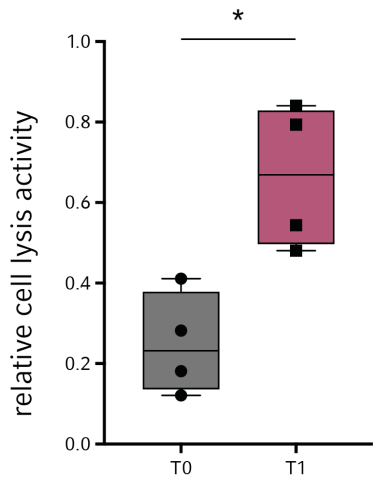

Figure 30: Evaluation of CD8⁺ T cell specific cytotoxic capacity in response to KD. Healthy volunteers conducted a three-week ketogenic diet. Prior to (T0) and after (T1) the dietary intervention PBMC were isolated and stimulated *ex vivo* for 24 hours. Afterwards, separated CD8⁺ T cells were cultivated with calcein-labeled glioblastoma cells and lysis-dependent fluorescence in the supernatant was quantified. $n = 4$, $*p < 0.05$.

5.10 KETOGENIC DIET ENHANCES CD4⁺ T-CELL IMMUNE CAPACITY

Analogous to the *in vitro* approaches, *ex vivo* stimulated CD4⁺ T cells from participants displayed a significant regulation of gene expression following three-week KD diet, as mRNA expression of IL-2 (+226.83 % ± 84.15 %; p = 0.015) and IL-4 (+50.94 % ± 19.25 %; p = 0.023) was markedly increased. Moreover, post-KD, CD4⁺ T cells displayed enhanced levels of CTLA4 (+13.80 % ± 6.28 %; p = 0.043), whereas, in contrast to CD8⁺ T cells, IFNγ expression remained unchanged in the CD4⁺ T-cell subpopulation (Fig. 31).

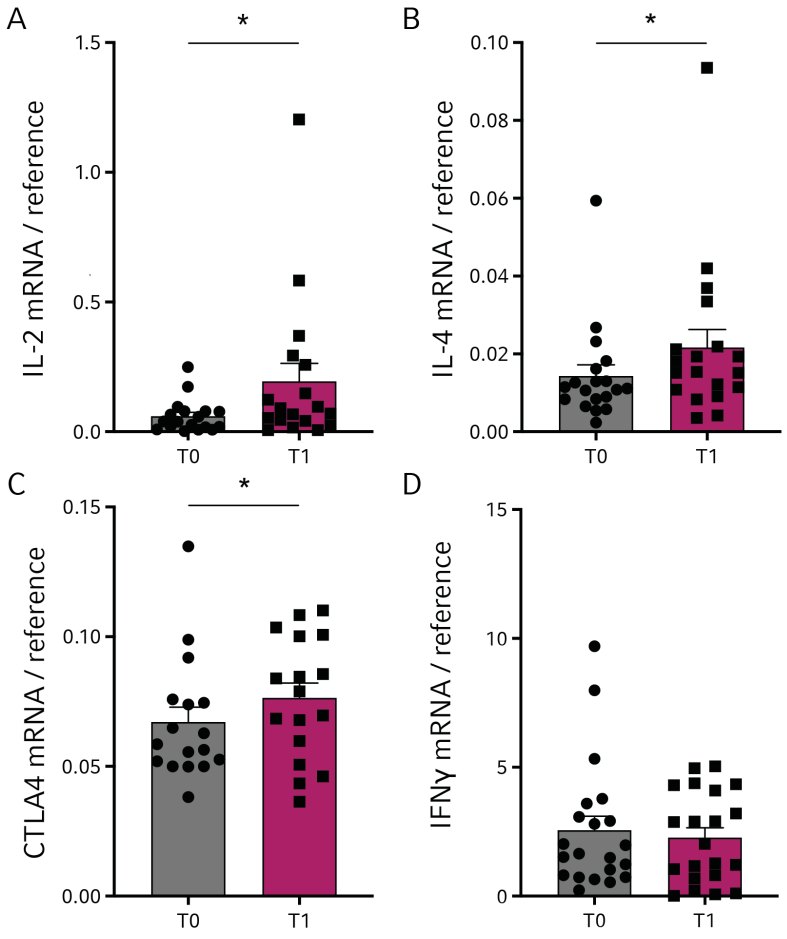

Figure 31: mRNA expression in stimulated CD4⁺ T cells in response to KD. Healthy volunteers conducted a three-week ketogenic diet. Prior to (T0) and after (T1) the dietary intervention PBMC were isolated and stimulated *ex vivo* for 24 hours. Afterwards, CD4⁺ T cells were separated and gene expression of IL-2, IL-4, CTLA4 and IFNγ was quantified via qRT-PCR relative to reference genes. n = 18/19/17/21, *p < 0.05.

5.11 KETOGENIC DIET REGULATES TH_1/TH_2 CELL DIFFERENTIATION

In vitro approaches have already highlighted the potential ability of BHB to alter the differentiation of distinct T helper cell subsets. Therefore, possible effects on T-cell subpopulations in response to a three-week KD were subsequently investigated.

KD led to an elevation of Th_2 transcription factor GATA3 (+21.34 % ± 8.32 %; p = 0.042), and concomitantly, Th_2 T helper cell subset was indeed significantly enriched (+30.39 % ± 5.23 %; p = 0.015). Gene expression of Th_1 transcription factor Tbet was not altered, yet there was an apparent decrease in Th_1 cell frequency after KD (-25.61 % ± 12.01 %; p = 0.077), resulting in an overall significantly reduced Th_1/Th_2 cell ratio (-48.64 % ± 16.49 %; p = 0.046) (Fig. 32).

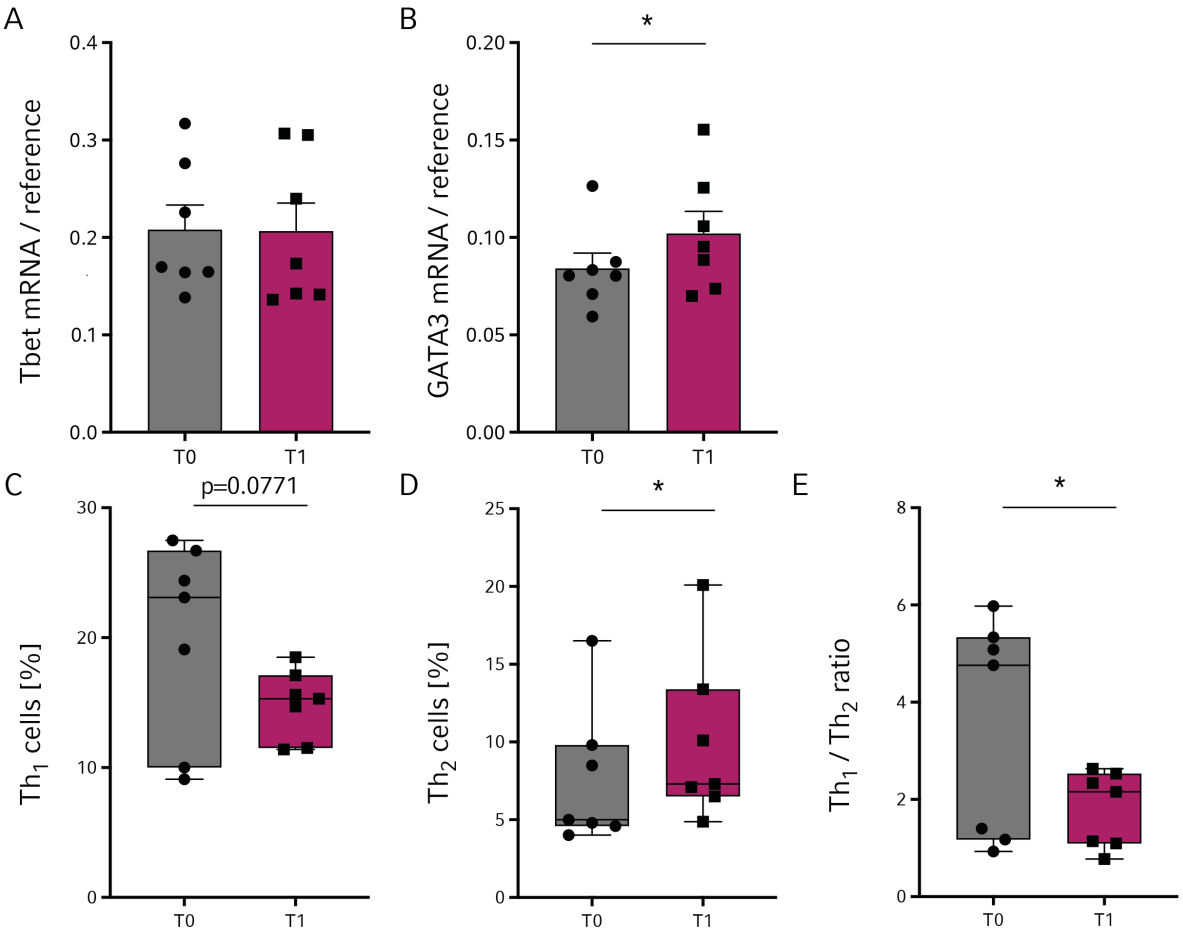

Figure 32: Analysis of Th_1/Th_2 cell differentiation in response to KD. Healthy volunteers conducted a three-week ketogenic diet. Prior to (T0) and after (T1) the dietary intervention PBMC were isolated and stimulated *ex vivo* for 24 hours. $CD4^+$ T cells were separated and mRNA expression of Th_1/Th_2 transcription factor Tbet and GATA3 was quantified via qRT-PCR relative to reference genes (**A-B**). Frequencies of Th_1 (**C**) and Th_2 (**D**) cells as well as the Th_1/Th_2 ratio (**E**) were assessed by flow cytometry**.** n = 7. *p < 0.05.

5.12 KETOGENIC DIET ALTERS T_{REG} / TH_{17} CELL BALANCE

5.12.1 Analysis of T_{reg} and Th_{17} cell differentiation in response to KD

Since our data demonstrated that supplementation with β-hydroxybutyrate exerts distinctive impact on $CD4^+$ T helper cells beyond the well-known Th_1/Th_2 balance, we next set out to examine the effect of KD on the immunological balance between anti-inflammatory regulatory T cells (T_{reg}) and pro-inflammatory Th_{17} cells.

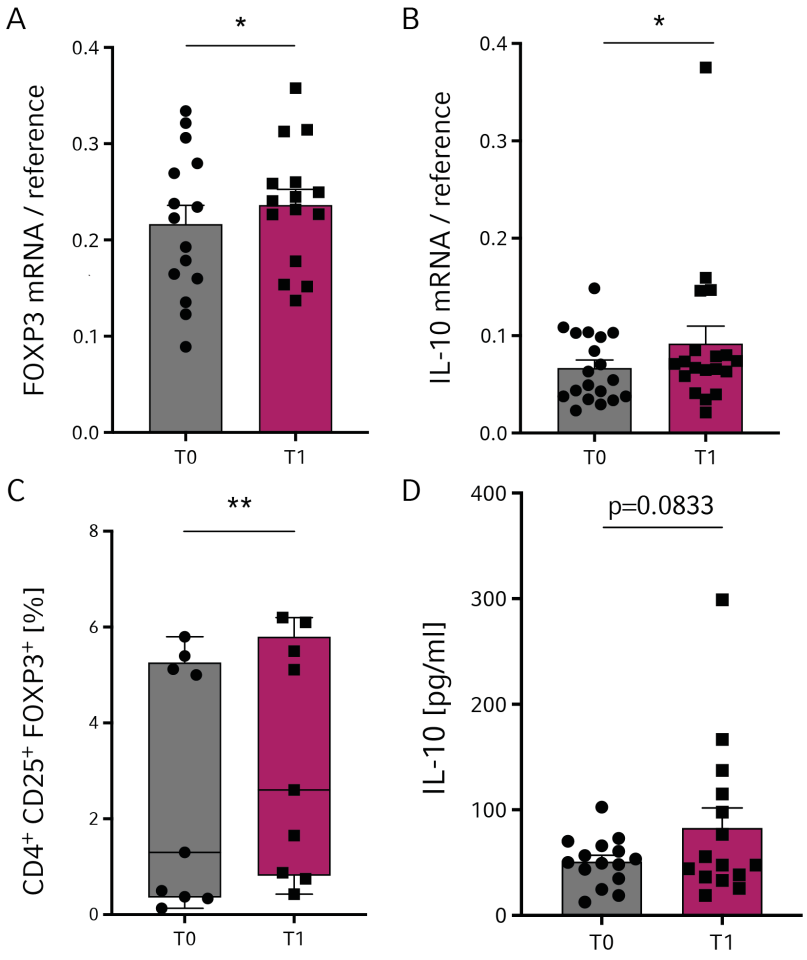

Figure 33: Analysis of T_{reg} differentiation in response to KD. Healthy volunteers conducted a three-week ketogenic diet. Prior to (T0) and after (T1) the dietary intervention PBMC were isolated and stimulated *ex vivo* for 24 hours. $CD4^+$ T cells were separated and mRNA expression of T_{reg} transcription factor FOXP3 and cytokine IL-10 was quantified via qRT-PCR relative to reference genes (**A-B**). Frequency of T_{reg} was assessed by flow cytometry (**C**) and cytokine concentration of IL-10 in the supernatant was quantified by ELISA (**D**). n = 15/19/9/15, *p < 0.05, **p < 0.01.

Indeed, as shown in previous *in vitro* results, carbohydrate restriction led to an increased gene expression of T_{reg} transcription factor FOXP3 (+9.20 % ± 4.29 %; p = 0.049), which was followed by an enhanced fraction of $CD4^+$ $CD25^+$ $FOXP3^+$ T_{reg} (+21.89 % ± 5.68 %; p = 0.008). Moreover, mRNA expression (+37.43 % ± 19.46 %; p = 0.041) and protein secretion (+62.22 % ± 30.41 %; p = 0.083) of T_{reg} cytokine IL-10 were upregulated in response to KD (Fig. 33).

Analyzing Th_{17} specific gene expression after KD, Th_{17} transcription factor RORc as well as key cytokines IL-17A and IL-22 remained stable (Fig. 34 A-C). However, quantification of Th_{17} subsets via flow cytometry revealed a significant decrease in total IL-17^+ T cells (-17.23 % ± 6.97 %; p = 0.019) and in particular, a lower abundance of the non-classical IL-$17A^+$ IFNγ^+ $Th_{17.1}$ subpopulation (-25.60 % ± 8.55 %; p = 0.015), whereas KD did not affect the frequency of classical IL-$17A^+$ IFNγ^- Th_{17} cells (Fig. 34 D-F). This resulted in a significantly reduced ratio of $Th_{17.1}$/classical Th_{17} cells (-21.02 % ± 6.25 %; p = 0.006, Fig. 34 G). Compromised differentiation of Th_{17} cell lineages subsequently led to attenuated secretion of Th_{17} key cytokines IL-17A (-46.64 % ± 12.09 %; p = 0.001) and IL-22 (-23.12 % ± 9.23 %; p = 0.014) (Fig. 34 H, I).

Taken together, the immunomodulatory capacity of ketone bodies on the T_{reg}/Th_{17} balance, already demonstrated *in vitro*, was confirmed in human volunteers after KD.

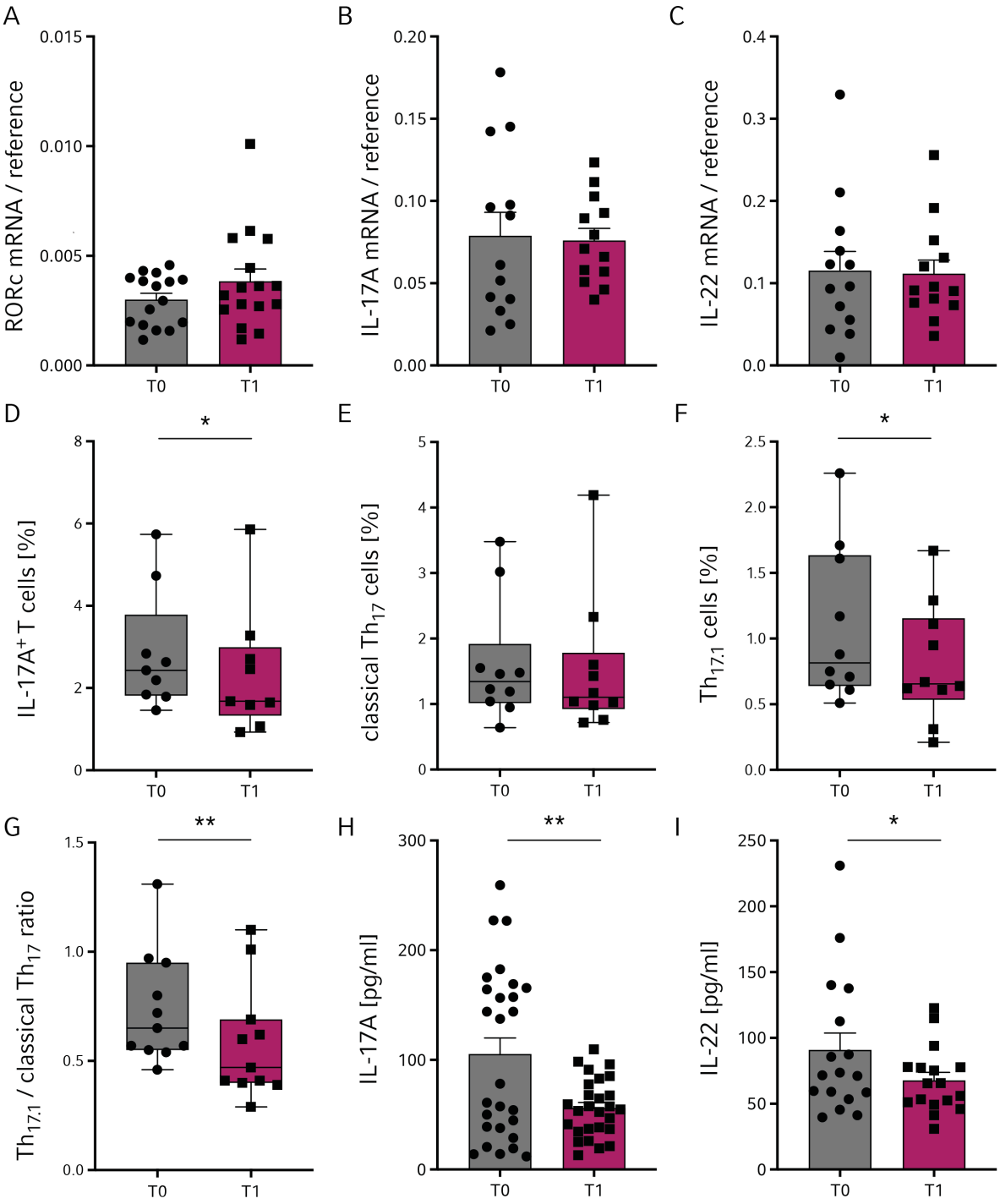

Figure 34: Analysis of Th_{17} subset differentiation in response to KD. Healthy volunteers conducted a three-week ketogenic diet. Prior to (T0) and after (T1) the dietary intervention PBMC were isolated and stimulated *ex vivo* for 24 hours. $CD4^+$ T cells were separated and mRNA expression of Th_{17} transcription factor RORc as well as key cytokines IL-17A and IL-22 was quantified via qRT-PCR relative to reference genes (**A-C**). Frequency of Th_{17} subsets (**D-F**) and the $Th_{17.1}$/classical Th_{17} ratio (**G**) were assessed by flow cytometry and cytokine concentrations of IL-17A (**H**) and IL-22 (**I**) in the supernatant were quantified by ELISA. n = 16/13/13/9/10/10/11/27/17. *$p < 0.05$, **$p < 0.01$.

5.12.2 KD-mediated effects on IL-17A as a function of pre-diet baseline levels

Total IL-17A mRNA expression did not appear to be altered by KD (Fig. 35 A). However, further analysis revealed that changes in IL-17A expression seemed to depend on baseline (T0) levels (Fig. 35 B). In subjects depicting a higher IL-17A mRNA baseline, KD significantly attenuated IL-17A gene expression (-31.53 % ± 11.98 %; p = 0.046, Fig. 35 C), whereas in $CD4^+$ T cells from subjects with comparatively lower mRNA levels prior to KD, IL-17A mRNA expression was elevated but without reaching statistical significance (+72.70 % ± 38.01 %; p = 0.104, Fig. 35 D).

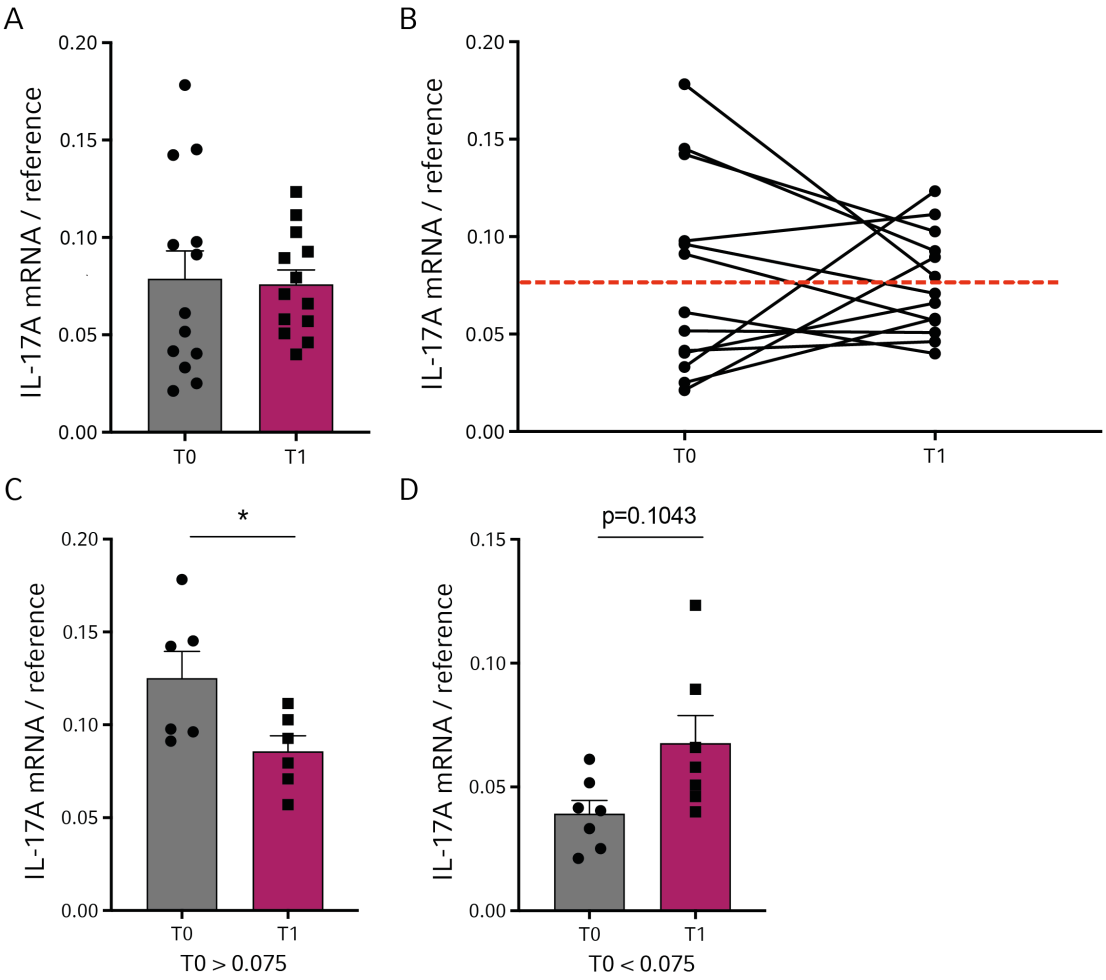

Figure 35: Baseline-dependent analysis of IL-17A gene expression in response to KD. Healthy volunteers conducted a three-week ketogenic diet. Prior to (T0) and after (T1) the dietary intervention PBMC were isolated and stimulated *ex vivo* for 24 hours. $CD4^+$ T cells were separated, and IL-17A mRNA expression was quantified via qRT-PCR relative to reference genes. Depicted are overall gene expression (**A, B**) as well as gene expression in subjects with IL-17A baseline expression above (**C**) and below (**D**) the threshold prior to KD. n = 13/6/7. *p < 0.05.

This baseline-dependent modulation of IL-17A was even more evident when looking at the IL-17A cytokine secretion (Fig. 36 B). Here, T cells from participants with IL-17A concentrations above 100 pg/ml displayed a significantly dampened IL-17A secretion capacity after KD (-59.42 % ± 5.79 %; $p < 0.0001$, Fig. 36 C). However, in subjects with baseline concentration below the threshold, IL-17A cytokine secretion remained stable (Fig. 36 D).

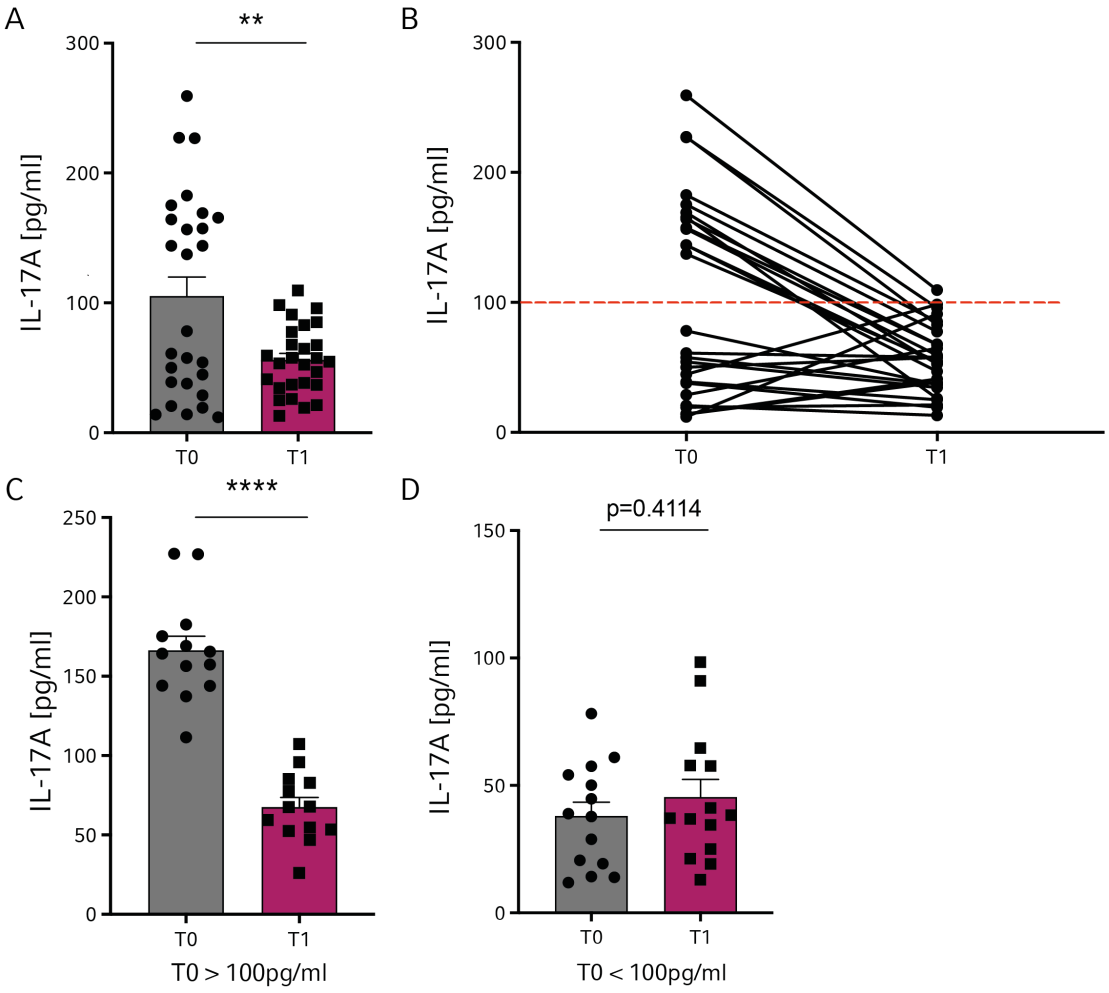

Figure 36: Baseline-dependent analysis of IL-17A cytokine secretion in response to KD. Healthy volunteers conducted a three-week ketogenic diet. Prior to (T0) and after (T1) the dietary intervention PBMC were isolated and stimulated *ex vivo* for 24 hours. Cytokine concentration of IL-17A in the supernatant was quantified by ELISA. Depicted are overall protein secretion (**A, B**) as well as secretion levels in subjects with IL-17A baseline levels above (**C**) and below (**D**) the threshold prior to KD. n = 27/13/14. **$p < 0.01$, ****$p < 0.0001$.

5.13 KETOGENIC DIET IMPROVES OVERALL IMMUNE RESPONSE

The balanced interplay of innate and adaptive immunity is an indispensable prerequisite for efficient and successful host defense against invading pathogens. In order to investigate how a KD modulates overall immune capacity, whole blood samples were obtained in TruCulture tubes which contained lipopolysaccharide (LPS), thereby mimicking pathogen encounter. Subsequently, cytokine concentrations were quantified. Here, KD resulted in a significant increase of IFNγ (+121.38 % ± 99.98 %; $p = 0.048$,), TNFα (+30.75 % ± 13.27 %; $p = 0.043$), IL-4 (+13.96 % ± 6.32 %; $p = 0.046$), and IL-12sub40 (+25.28 % ± 9.83 %; $p = 0.028$). However, secretion of IL-17A remained constant (Fig 37). These data again confirmed the immune enhancement induced by ketone bodies and emphasized the potential of KD as a booster for the overall immune response.

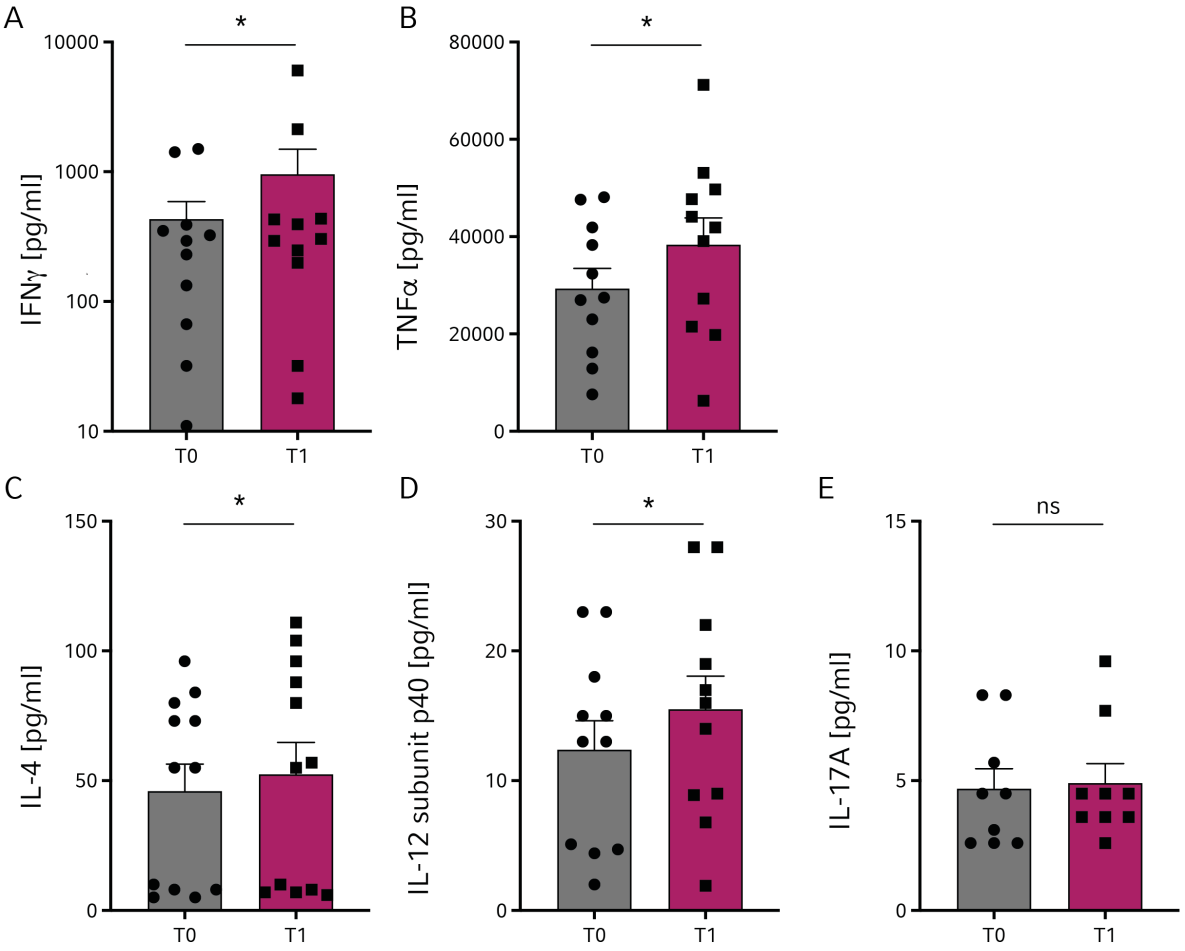

Figure 37: Secretion of CD4⁺ and CD8⁺ cytokines in LPS-stimulated whole blood samples. Healthy volunteers conducted a three-week ketogenic diet. Prior to (T0) and after (T1) the dietary intervention whole blood samples were obtained using TruCulture tubes, containing medium and LPS and incubated for 24 hours. Cytokine secretion was assessed via multiplex analysis. n = 11/11/12/11/9. *$p < 0.05$, ns = not significant.

6 Discussion

Due to modern medicine and universal access to public health measures, life expectancy has steadily increased over the past 200 years and is now significantly higher than ever before. But these newly gained years of life are increasingly accompanied by a range of diseases such as obesity, diabetes, cardiovascular diseases, and autoimmune disorders, commonly glossed over and trivialized as "diseases of civilization"[9,103]. Over the years, these non-communicable diseases have become the leading cause of death worldwide and have reached epidemic proportions[5]. Not only do they pose devastating consequences for individuals, but also threaten to overwhelm our healthcare system. If nothing changes, the constant rise in life expectancy may come to an end sooner or later[6,7].

Emerging evidence suggests the common pathophysiological basis of many life-style related pathologies to be an erroneous chronic immune activation which can be triggered by a high carbohydrate uptake with subsequent spikes in plasma glucose and insulin. These noxious dietary habits induce systemic low-grade inflammation through activation of NLRP3 inflammasomes, followed by a reprogramming of innate immune cells toward pro-inflammatory phenotypes[17,21,104].

Indeed, nutritional patterns in today's Western societies are characterized by a high consumption of ultra-processed food, predominantly containing high amounts of added sugar and refined carbohydrates[8,105]. Nutritional interventions therefore appear to bear great potential to counteract these deleterious effects on human immunity and could serve not only as preventive but also as complementary curative measures.

With dietary strategies being increasingly recognized as new therapeutic tools, the ketogenic diet (KD) has attracted great interest and is the subject of much endeavor and debate[106–108]. Carbohydrate restriction results in an enhanced synthesis of ketone bodies within hepatic mitochondria, among which β-hydroxybutyrate (BHB) is the most abundant, in order to provide an alternate source of energy from the liver to peripheral tissues[85]. Apart from only being a major substrate for ATP production, BHB has emerged as a multifunctional molecule, exerting pleiotropic effects as a vital metabolic and signaling mediator[82,86].

Recent animal studies have highlighted its beneficial immunomodulating effects, as BHB was shown to dampen NLRP3-mediated inflammation and to counteract associated diseases, while fasting diets were able to reduce autoimmunity in experimental murine encephalomyelitis models[81,96].

Yet, these studies on BHB and ketogenic(-like) diets, mainly focus on innate immunity and mostly use rather unphysiological animal models. However, the possible effects on human adaptive immunity have not yet been sufficiently addressed.

Thus, in order to investigate possible immunomodulatory properties of BHB and carbohydrate restriction in humans, we decided to adopt a two-step approach:

First, we established an *in vitro* model mimicking a ketogenic nutrition regime and analyzed human T-cell responses. For this purpose, peripheral mononuclear cells (PBMC) from healthy subjects were incubated in medium supplemented with β-hydroxybutyrate under T cell specific stimulation and immunological analyses were performed subsequently. In order to substantiate and confirm the obtained *in vitro* results, next, we carried out a prospective nutritional intervention study, recruiting healthy participants who conducted a ketogenic diet with a very limited carbohydrate intake of less than 30 g per day for a period of three weeks. PBMC were isolated and stimulated *ex vivo* for 24 hours before (T0) and after (T1) the dietary adjustment to assess changes in T-cell immunity.

Both, *in vitro* and *in vivo* results, revealed comprehensive immunometabolic reprogramming of human $CD4^+$ and $CD8^+$ T cells in response to BHB and following a very-low-carbohydrate diet, respectively.

6.1 BETA-HYDROXYBUTYRATE MODULATES HUMAN T-CELL IMMUNITY

In unstimulated T cells isolated from healthy participants, BHB did not evoke any significant transcriptional changes of $CD4^+$ or $CD8^+$ T cell associated cytokines or transcription factors. Activation and expansion of human T cells require recognition of the respective cognate antigen by a specific T-cell receptor (TCR) in addition to costimulatory signaling via CD28 molecules[29,33]. Thus, the inability of BHB to activate T cells in the absence of physiological TCR stimuli is thoroughly preferable. A constant stimulation of immune cells in an TCR-independent manner could favor chronic pro-inflammatory settings promoting potentially harmful chronic autoreactive cells[4,41].

In contrast, under stimulating conditions, mimicking physiological antigen presentation, BHB did exert a substantial impact on human T-cell immunometabolism. In response to BHB, $CD8^+$ T cells displayed induced gene expression and secretion of their cytotoxic effector molecules such as perforin, granzyme B and TNFα[109–111]. In addition, BHB-conditioned $CD8^+$ T cells

expressed markedly enhanced levels of IFNγ, which facilitates antigen recognition and eradication of pathogenic cells[30,31]. Indeed, this was also functionally reflected in a significantly increased cell lysis capacity after incubation with BHB.

Stimulated T cells also displayed upregulated gene expression and respective protein secretion of $CD4^+$ T-cell cytokines IL-2 and IL-4 after being cultivated in the presence of BHB. IL-2, a pleiotropic cytokine, is generally known to be a potent regulator of T-cell expansion, particularly *in vitro*, but is also able to limit T-cell responses to self-antigens[36,37,112]. These tolerogenic properties seem to be based on the fact that IL-2 signaling is required for both expansion and maintenance of $CD4^+$ $CD25^+$ regulatory T cells (T_{reg})[42,113]. At the same time, IL-2 inhibits the polarization of $CD4^+$ T cells into pro-inflammatory Th_{17} cells[114,115]. Besides regulating humoral immunity, the anti-inflammatory cytokine IL-4 promotes differentiation of Th_2 cells and counteracts formation of pro-inflammatory Th_1 cells by suppressing IL-12 signaling but is also capable of abrogating Th_{17} maturation[116–118].

As BHB was able to enhance T-cell immunity and to modify cytokine secretion patterns, we next set out to investigate if ketone bodies might also affect differentiation of distinct T helper cell subsets. Upon BHB-incubation in Th_1 or Th_2-skewing media, Th_1 transcription factor was significantly downregulated, followed by a reduced frequency of pro-inflammatory Th_1 cells, while Th_2 transcription factor and cell count remained unaltered. However, BHB was able to exert a significant impact on CD4 T-cell differentiation beyond the long-established Th_1/Th_2 duality. Analysis of immunoregulating T_{reg} and inflammatory Th_{17} cells, which are considered to be meaningful functionally opposite T helper cell lineages, revealed BHB's substantial impact on their respective differentiation. An important aspect here is that Th_{17} cells also exhibit a substantial functional heterogeneity. Among them, $Th_{17.1}$ cells, display a specific pathogenic signature, secreting both, IL-17A and IFNγ and appear to be particularly associated with autoimmunological pathologies compared to $IL\text{-}17A^+$ $IFN\gamma^-$ "classical" Th_{17} cells[51,68,119,120]. Following 48 hours of incubation, no changes in T_{reg}-associated gene expression were detectable, while Th_{17} transcription factor RORc and master cytokine IL-17A were upregulated. Consistent with these results, frequency of Th_{17} cells was also elevated. However, prolongation of the incubation period up to five days led to significantly reduced cell numbers of total $IL\text{-}17A^+$ T cells and pathogenic $Th_{17.1}$ cells. Subset differentiation, using the respective polarizing cytokine milieu, revealed BHB^+ T cells to express increased levels of T_{reg} transcription factor FOXP3, consequently followed by an amplified fraction of $CD25^+$ $FOXP3^+$ regulatory T cells showing enhanced secretion of key cytokines IL-10 and TGFβ1. Conversely, BHB markedly attenuated the polarization of both, classical and $IL\text{-}17A^+$ $IFN\gamma^+$ $Th_{17.1}$ cells, which translated into dampened IL-17A secretion.

The heterogeneous pool of $CD4^+$ T helper cells yet not only differs functionally, but each lineage also relies on unique predominant metabolic pathways that are intimately linked to the differentiation, function, and maintenance of the respective subset[55,56,121]. Initially, regulatory T cells and Th_{17} cells share similar requirements, however, upon differentiated STAT activation, they diverge into the respective phenotypes with pronounced opposite functional properties[39,98,122]. This dichotomy is also reflected in a different antagonistic metabolic energy supply. Whereas T_{reg} meet their energy demands upon activation mostly via oxidative phosphorylation fueled by fatty acid oxidation (FAO), Th_{17} cells favor glycolysis[38,56,121]. Additionally, Th_{17} cells uniquely express high levels of pyruvate dehydrogenase kinase (PDHK), an enzyme that inhibits PDH-mediated transformation of pyruvate into acetyl-CoA, preventing the former from entering the mitochondrial tricarboxylic acid cycle (TCA). This results in enhanced pyruvate-to-lactate conversion for rapid but non-mitochondrial ATP generation[123,124].

As changes in nutrient availability and subsequent altered metabolic pathway usage can considerably affect T-cell development[39,57], we thus hypothesized that the observed changes in T_{reg} and Th_{17} cell frequencies might be a consequence of differential metabolic alterations in these opposing cell lineages upon incubation with BHB.

Recently, it was demonstrated that ketone bodies indeed markedly shift T-cell metabolism toward enhanced mitochondrial oxidative phosphorylation. Increased mitochondrial respiration was particularly pronounced in $CD8^+$ T cells, whereas $CD4^+$ T cells did not display enhanced OXPHOS to the same extent[83]. Therefore, we set out to investigate possible differential effects of BHB on the metabolism of human Th_{17} and T_{reg} cells. Upon incubation with BHB, T_{reg} displayed significantly increased basal, maximal, and spare capacity as well as a substantial gain in mitochondrial mass, while the glycolytic capacity of T_{reg} remained intact. In Th_{17}, conversely, ketone bodies reduced the mitochondrial mass and led to markedly decreased mitochondrial oxidative respiration. In contrast to regulatory T cells, cellular glycolysis in Th_{17} cells was also markedly compromised in response to BHB.

Previous studies have shown that enhanced OXPHOS in Th_{17} cells leads to the development of a more pathogenic Th_{17} cell signature, comprising increased capacity of IL-17A and IFNγ secretion. Conversely, drug-induced inhibition of oxidative respiration in these cells attenuates pro-inflammatory cytokine secretion which counteracts tissue inflammation and ablates autoimmunity[39,125–127]. Consistent with these findings, our *in vitro* results clearly suggest that by compromising oxidative phosphorylation in Th_{17} cells, ketone bodies lead to a less pathogenic Th_{17} phenotype, manifested in reduced levels of IL-17A and IFNγ secretion. Thus, opposite

immunometabolic reprogramming of T_{reg} and Th_{17} cells might be a new link for how ketone bodies shape the human T helper cell pool toward more anti-inflammatory lineages.

These cell lineage-dependent differential changes in OXPHOS may also explain why previous metabolic analyses of total $CD4^+$ T cells did not show such a pronounced effect upon BHB incubation compared to $CD8^+$ T cells, as the opposing responses of heterogeneous $CD4^+$ subsets might offset each other when being analyzed collectively.

Taken together, these data highlight the potent immunomodulatory effects of BHB on human T-cell immunity. Next, we initiated a prospective nutritional study enrolling healthy participants to conduct a three-week ketogenic diet in order to validate our findings.

6.2 KETOGENIC DIET SHAPES HUMAN T-CELL IMMUNE RESPONSE

Healthy participants performed a three-week ad libitum ketogenic diet (KD) with a restricted carbohydrate consumption of no more than 30 g per day. Immune cells were isolated prior to and after the dietary phase for T-cell focused immunological analyses. Blood ketone body levels were closely monitored throughout the study and ranged between 1.0 – 1,5 mM. This physiological and controlled metabolic state of dietary ketosis is harmless and must not be confused with ketoacidosis, a complication of type 1 diabetes, caused by uncontrolled production of ketone bodies due to a deficiency of insulin[86,128,129].

Transcriptome profiling after the three-week KD depicted considerable changes in gene expression patterns of $CD4^+$ and $CD8^+$ T cells. This KD-mediated reprogramming was also reflected in an enhanced T-cell immunity, depicted by increased expression of respective $CD4^+$ and $CD8^+$ key cytokines and an elevated cell lysis capacity after KD. T-cell activation after KD was also evident in upregulated expression of cytotoxic T-lymphocyte-associated protein 4 (CTLA4) in both lineages. CTLA4, a cell surface receptor, is primarily found on activated T cells and acts as an immune checkpoint that dampens T-cell responses[130,131]. As CTLA4 is essential for immunological self-tolerance by preventing uncontrolled activation of T cells, besides being a sign of enhanced T-cell activation, this demonstrates T-cell enhancement by KD not to be at the expense of an uncontrollable, potential harmful immune reaction[131–134].

In line with the *in vitro* results, carbohydrate restriction markedly enhanced human immunity in both $CD4^+$ and $CD8^+$ T cells. However, our previous *in vitro* findings have emphasized the need for in-depth subset analyses of the heterogenous $CD4^+$ T-cell compartment, as ketone bodies appear to exert opposing effects on immunometabolic processes depending on the T helper cell lineage.

Indeed, KD led to a pronounced differentiation of anti-inflammatory Th_2 cells, significantly decreasing the Th_1/Th_2 ratio. Carbohydrate restriction also had a substantial impact on the T_{reg}/Th_{17} balance. Here, flow cytometric analyses revealed significantly elevated frequencies of T_{reg} followed by increased concentrations of anti-inflammatory IL-10. Differentiation of pro-inflammatory IL-17^+ T cells, in contrast, was significantly attenuated. Of note, classical IL-$17A^+$ IFNγ^- Th_{17} cells remained unaltered, whereas IL-$17A^+$ IFNγ^+ $Th_{17.1}$ cells were markedly reduced. Concomitantly, this led to decreased secretion of Th_{17} master cytokines IL-17A and IL-22.

These findings are particularly pertinent because immunoregulatory T_{reg} and pro-inflammatory Th_{17} cells play antagonistic roles within human T cell-mediated immunity, and a distorted interplay between these two lineages has far-reaching implications for the pathogenesis of various autoimmune and inflammatory disorders[54,135–137]. Both Th_{17} master cytokines IL-17A and IL-22 drive synovial inflammation by inducing the secretion of pro-inflammatory cytokines in fibroblasts and macrophages, thereby aggravating joint inflammation in patients with rheumatoid arthritis (RA). Their concentrations also correlate with disease severity[61]. Likewise in psoriasis, pathologically activated dendritic cells (DC) promote polarization of Th_{17} cells. Subsequently, increased levels of IL-17A and IL-22 not only maintain the chronic inflammatory microenvironment but also act directly on keratinocytes causing aberrant hyperproliferation and hyperplasia which further exacerbates severe psoriatic skin lesions[62,63,65]. Recently developed, and approved antibodies against IL-17A have therefore emerged as an effective therapeutic option for psoriasis treatment counteracting the Th_{17}-driven inflammation[64,138].

Yet, carbohydrate restriction not only substantially tilted the T_{reg}/Th_{17} balance in favor of the anti-inflammatory phenotype, which in turn dampened the general secretion of potentially disease driving IL-17A and IL-22, but particularly reduced frequencies of pathogenic non-classical IFNγ/IL-17A double positive $Th_{17.1}$ cells. This Th_{17} subset is particularly found at sites of inflammation in various (auto-)inflammatory diseases and possesses distinct pathogenic properties[58]. This clearly emphasizes the potential of KD as a possible preventive and therapeutic measurement for a broad spectrum of diseases arising from a dysfunctional inflammatory environment.

Nonetheless, it must be kept in mind that Th_{17} cells do play an essential role in protection against extracellular bacterial and fungal pathogens. By promoting granulopoiesis, modulating chemokine gradients for neutrophil recruitment into infected tissue and inducing the production of antimicrobial peptides, these cells are indispensable for preserving barrier function and host defense[38,119,139,140]. As a total loss of Th_{17} cell function results in immunological disorders such

as Job's syndrome or chronic mucocutaneous candidiasis which both manifest in increased susceptibility to fungal infections[141,142], complete abolition of Th_{17} immunity is not beneficial and absolutely contraindicated.

In this context, differentiated analyses depicted KD-mediated regulation of IL-17A secretion to be dependent on initial baseline levels. IL-17A secretion in participants with comparatively higher concentration prior to KD was significantly reduced upon carbohydrate restriction, whereas cytokine secretion of those with lower baseline levels only slightly increased but generally remained unchanged. A similar response was also evident for IL-17A mRNA expression. Importantly, for no other cytokine this pattern was detectable upon KD, indicating a prominent immunomodulating role of KD in IL-17A homeostasis. Thus, carbohydrate-restriction might bear the potential of counteracting pathologically increased disease-driving cytokine secretion, which is of particular importance for patients with immunological disorders associated with pronounced IL-17A concentrations, while maintaining required immune functions under physiological conditions. In addition, stimulation with LPS proved that although KD shifts the adaptive immune response toward anti-inflammatory phenotypes, it still significantly enhances adaptive immune capacity in the presence of pathogens.

Taken together, this study provides the first evidence that a KD profoundly enhances the immune capacity of human $CD4^+$ and $CD8^+$ T cells, manifested by an elevated cell lysis capacity, augmented cytokine secretion and distinct changes in the composition of the heterogenous T helper cell pool. Beyond the classical Th_1/Th_2 paradigm, ketone bodies shift the reciprocally linked balance of T_{reg} and Th_{17} cells in favor of the anti-inflammatory immunoregulatory phenotype via differential immunometabolic reprogramming.

Hence, in today's society, with its surplus of carbohydrates, a ketogenic diet should be understood as an important component to counteract the development of lifestyle-related disorders, which are becoming more and more prevalent. Our study is a first step toward deciphering the underlying dietary effects in order to conceptualize nutritional interventions as powerful and feasible therapeutic tools in modern medicine.

7 Figures, tables, and abbreviations

7.1 LIST OF FIGURES

7.2 LIST OF TABLES

7.3 LIST OF ABBREVIATIONS

°C	Degree Celsius
2-DG	2-Desoxyglucose
APC	Antigen presenting cells
APC	Allophycocyanin (fluorophore)
ATP	Adenosine triphosphate
BDH1	β-hydroxybutyrate dehydrogenase
BHB	β-hydroxybutyrate
BMI	Body mass index
BSA	Bovine serum albumin

Calcein AM	Calcein acetoxymethyl
CD	Cluster of differentiation
cDNA	complementary DNA
CO_2	Carbon dioxide
CoA	Coenzyme A
CTLA4	Cytotoxic T-lymphocyte-associated protein 4
DAMPs	Danger-associated molecular patterns
DC	Dendritic cells
DGE	Deutsche Gesellschaft für Ernährung e.V. (German Nutrition Society)
dl	Deciliter
DMSO	Dimethyl sulfoxide
DNA	Deoxyribonucleic acid
dsDNA	double-stranded DNA
EAE	Experimental murine encephalomyelitis
ECAR	Extracellular acidification rate
ELISA	Enzyme-linked immunosorbent assay
et al.	And others (et alia)
ETC	Electron transport chain
FACS	Fluorescence-activated cell scanning
FAO	Fatty acid oxidation / ß-oxidation
Fc	Fragment crystallizable region (tail region of antibody)
FCCP	Carbonyl-cyanide-p-trifluoromethoxy phenylhydrazone
FCS	Fetal calf serum
FDR	False discovery rate
Fig.	Figure
FITC	Fluorescein isothiocyanate (fluorophore)
FOXO3	Forkhead box O3 (transcription factor)
g	Gram

GBM	Glioblastoma
GZMB	Granzyme B
h	hours
HDACs	Histone deacetylases
HEPES	4-(2-hydroxyethyl)-1-piperazineethanesulfonic acid (buffer)
HMG	β-hydroxy-β-methylglutaryl
HMGCS2	3-hydroxymethylglutaryl-CoA synthase
HRP	Horseradish peroxidase
IFN	Interferon
IL	Interleukin
KD	Ketogenic diet
l	Liter
LPS	Lipopolysaccharide
m	Milli
M / mol	Molar / Mole (unit)
MFI	Mean fluorescence intensity
mg	Milligram
MHC	Major histocompatibility complex
min	Minute
mpH	Milli-pH units
n	Total number of individuals
NAD	Nicotinamide adenine dinucleotide
NC	Control group
ng	Nanogram
NGS	Next-generation sequencing
NLRP3	NLR family pyrin domain containing 3 (inflammasome)
no.	Number
ns	Not significant
OCR	Oxygen consumption rate

OXPHOS	Oxidative phosphorylation
p	Pico
p-value	Level of statistical significance
PAMPs	Pathogen-associated molecular patterns
PBMC	Peripheral mononuclear cells
PBS	Phosphate-buffered saline
PDH	Pyruvate dehydrogenase
PDHK	Pyruvate dehydrogenase kinase
PE	Phycoerythrin (fluorophore)
PerCP	Peridinin-chlorophyll-protein complex (fluorophore)
PRF1	Perforin-1
qRT-PCR	Real-time quantitative reverse transcriptase polymerase chain reaction
R+A	Rotenone + antimycin A
RA	Rheumatoid arthritis
RFU	Relative fluorescence units
RNA	Ribonucleic acid
ROS	Reactive oxygen species
rpm	Revolutions per minute
RPMI medium	Roswell Park Memorial Institute medium
SCOT	Succinyl-CoA:3-ketoacid-CoA transferase
SD	Standard deviation
SEM	Standard error of mean
STAT	Signal transducer and activator of transcription (transcription factor)
T0	Prior to ketogenic diet
T1	After ketogenic diet
TBP	TATA-binding protein (transcription factor)
TCA	Tricarboxylic acid cycle / Krebs cycle
TCR	T-cell receptor

TGFβ	Transforming growth factor β
Th_x	T helper cells type x
TM	Trademark
TNFα	Tumor necrosis factor α
T_{reg}	Regulatory T cells
U	Units
UPL	Universal Probe Library
µ	Micro

8 References

1. Brown GC. Living too long. *EMBO Rep*. 2015;16(2):137-141. doi:10.15252/embr.201439518

2. Vaupel JW, Villavicencio F, Bergeron-Boucher MP. Demographic perspectives on the rise of longevity. *Proc Natl Acad Sci U S A*. 2021;118(9). doi:10.1073/pnas.2019536118

3. Aburto JM, Villavicencio F, Basellini U, Kjaergaard S, Vaupel JW. Dynamics of life expectancy and life span equality. *PNAS*. 2020;114(10):5250-5259. doi:10.1073/pnas.1915884117/-/DCSupplemental

4. Furman D, Campisi J, Verdin E, et al. Chronic inflammation in the etiology of disease across the life span. *Nature Medicine*. 2019;25(12):1822-1832. doi:10.1038/s41591-019-0675-0

5. Noncommunicable diseases. Accessed February 12, 2022. https://www.who.int/news-room/fact-sheets/detail/noncommunicable-diseases

6. Olshansky SJ, Passaro DJ, Hershow RC, et al. A Potential Decline in Life Expectancy in the United States in the 21st Century. *The New England Journal of Medicine*. Published online 2005. www.nejm.org

7. Harper S, Riddell CA, King NB. Declining Life Expectancy in the United States: Missing the Trees for the Forest. *Annual Review of Public Health*. 2020;42:381-403. doi:10.1146/ANNUREV-PUBLHEALTH-082619-104231

8. Myles IA. Fast food fever: Reviewing the impacts of the Western diet on immunity. *Nutrition Journal*. 2014;13(1). doi:10.1186/1475-2891-13-61

9. Christ A, Latz E. The Western lifestyle has lasting effects on metaflammation. *Nature Reviews Immunology*. 2019;19(5):267-268. doi:10.1038/s41577-019-0156-1

10. Ludwig DS, Ebbeling CB, Heymsfield SB. Discrepancies in the Registries of Diet vs Drug Trials. doi:10.1001/jamanetworkopen.2019.15360

11. Dhurandhar EJ, Raynor H, Hingle M, Archer E, Lavie CJ, Hill JO. The Failure to Measure Dietary Intake Engendered a Fictional Discourse on Diet-Disease Relations. *Frontiers in Nutrition | www.frontiersin.org*. 2018;5:105. doi:10.3389/fnut.2018.00105

12. Kearns CE, Schmidt LA, Glantz SA. Sugar industry and coronary heart disease research: A historical analysis of internal industry documents. *JAMA Internal Medicine*. 2016;176(11):1680-1685. doi:10.1001/jamainternmed.2016.5394

13. The sugar conspiracy | Sugar | The Guardian. Accessed February 19, 2022. https://www.theguardian.com/society/2016/apr/07/the-sugar-conspiracy-robert-lustig-john-yudkin

14. Kohlenhydrate - DGE. Accessed February 18, 2022. https://www.dge.de/wissenschaft/referenzwerte/kohlenhydrate-ballaststoffe/

15. Bundesministerium für Ernährung und Landwirtschaft. *Deutschland, Wie Es Isst - Der BMEL-Ernährungsreport 2021*.

16. Sugar projections: Consumption, per capita | OECD-FAO Agricultural Outlook 2021-2030 | OECD iLibrary. Accessed February 19, 2022. https://www.oecd-ilibrary.org/agriculture-and-food/sugar-projections-consumption-per-capita_4ad4cf3a-en

17. Christ A, Günther P, Lauterbach MAR, et al. Western Diet Triggers NLRP3-Dependent Innate Immune Reprogramming. *Cell*. 2018;172(1-2):162-175.e14. doi:10.1016/j.cell.2017.12.013

18. Guo H, Callaway JB, Ting JPY. Inflammasomes: Mechanism of action, role in disease, and therapeutics. *Nature Medicine*. 2015;21(7):677-687. doi:10.1038/nm.3893

19. Zheng D, Liwinski T, Elinav E. Inflammasome activation and regulation: toward a better understanding of complex mechanisms. *Cell Discovery*. 2020;6(1). doi:10.1038/s41421-020-0167-x

20. Sharma BR, Kanneganti TD. NLRP3 inflammasome in cancer and metabolic diseases. *Nature Immunology*. 2021;22(5):550-559. doi:10.1038/s41590-021-00886-5

21. Dror E, Dalmas E, Meier DT, et al. Postprandial macrophage-derived IL-1β stimulates insulin, and both synergistically promote glucose disposal and inflammation. *Nature Immunology*. 2017;18(3):283-292. doi:10.1038/ni.3659

22. Qu Q, Xuan W, Fan GH. Roles of resolvins in the resolution of acute inflammation. *Cell Biology International*. 2015;39(1):3-22. doi:10.1002/cbin.10345

23. Medzhitov R. Origin and physiological roles of inflammation. *Nature*. 2008;454(7203):428-435. doi:10.1038/nature07201

24. Wang D, DuBois RN. Immunosuppression associated with chronic inflammation in the tumor microenvironment. *Carcinogenesis*. 2015;36(10):1085-1093. doi:10.1093/carcin/bgv123

25. Shi Z, Wu X, Yu S, et al. Short-Term Exposure to a Western Diet Induces Psoriasiform Dermatitis by Promoting Accumulation of IL-17A–Producing γδ T Cells. *Journal of Investigative Dermatology*. 2020;140(9):1815-1823. doi:10.1016/j.jid.2020.01.020

26. Butler MJ. The role of Western diets and obesity in peripheral immune cell recruitment and inflammation in the central nervous system. *Brain, Behavior, & Immunity - Health*. 2021;16:100298. doi:10.1016/j.bbih.2021.100298

27. Walker LSK, Chang X, Zielinski CE, et al. The Impact of Dietary Components on Regulatory T Cells and Disease. *Frontiers in Immunology*. 2020;11:253. doi:10.3389/fimmu.2020.00253

28. Nagaraj S, Gupta K, Pisarev V, et al. Altered recognition of antigen is a mechanism of CD8+T cell tolerance in cancer. *Nature Medicine*. 2007;13(7):828-835. doi:10.1038/nm1609

29. Pennock ND, White JT, Cross EW, Cheney EE, Tamburini BA, Kedl RM. T cell responses: Naïve to memory and everything in between. *American Journal of Physiology - Advances in Physiology Education*. 2013;37(4):273-283. doi:10.1152/advan.00066.2013

30. Bhat P, Leggatt G, Waterhouse N, Frazer IH. Interferon-γ derived from cytotoxic lymphocytes directly enhances their motility and cytotoxicity. *Cell Death Dis*. 2017;8(6):e2836. doi:10.1038/cddis.2017.67

31. Ivashkiv LB. IFNγ: signalling, epigenetics and roles in immunity, metabolism, disease and cancer immunotherapy. *Nature Reviews Immunology*. 2018;18(9):545-558. doi:10.1038/s41577-018-0029-z

32. Chen X, Suzuki H, Moser M, et al. The Significance of Tumor necrosis Factor Receptor Type ii in CD8 + Regulatory T Cells and CD8 + effector T Cells. *Frontiers in Immunology*. 2018;9:22. doi:10.3389/fimmu.2018.00583

33. Gaud G, Lesourne R, Love PE. Regulatory mechanisms in T cell receptor signalling. *Nature Reviews Immunology*. 2018;18(8):485-497. doi:10.1038/s41577-018-0020-8

34. Geginat J, Paroni M, Maglie S, et al. Plasticity of human CD4 T cell subsets. *Frontiers in Immunology*. 2014;5(DEC). doi:10.3389/fimmu.2014.00630

35. Cosmi L, Maggi L, Santarlasci V, Liotta F, Annunziato F. T helper cells plasticity in inflammation. *Cytometry Part A*. 2014;85(1):36-42. doi:10.1002/cyto.a.22348

36. Ross SH, Cantrell DA. Signaling and Function of Interleukin-2 in T Lymphocytes. *Annual Review of Immunology*. 2018;36:411-433. doi:10.1146/annurev-immunol-042617-053352

37. Liao W, Lin JX, Leonard WJ. Interleukin-2 at the Crossroads of Effector Responses, Tolerance, and Immunotherapy. *Immunity*. 2013;38(1):13-25. doi:10.1016/j.immuni.2013.01.004

38. Knochelmann HM, Dwyer CJ, Bailey SR, et al. When worlds collide: Th17 and Treg cells in cancer and autoimmunity. *Cellular and Molecular Immunology*. 2018;15(5):458-469. doi:10.1038/s41423-018-0004-4

39. Shin B, Benavides GA, Geng J, et al. Mitochondrial Oxidative Phosphorylation Regulates the Fate Decision between Pathogenic Th17 and Regulatory T Cells. *Cell Reports*. 2020;30(6):1898-1909.e4. doi:10.1016/j.celrep.2020.01.022

40. Kitz A, Singer E, Hafler D. Regulatory t cells: From discovery to autoimmunity. *Cold Spring Harbor Perspectives in Medicine*. 2018;8(12). doi:10.1101/CSHPERSPECT.A029041

41. Duan L, Rao X, Sigdel KR. Regulation of inflammation in autoimmune disease. *Journal of Immunology Research*. 2019;2019. doi:10.1155/2019/7403796

42. Shevyrev D, Tereshchenko V. Treg Heterogeneity, Function, and Homeostasis. *Frontiers in Immunology*. 2020;10. doi:10.3389/fimmu.2019.03100

43. Shevach EM, Thornton AM. tTregs, pTregs, and iTregs: Similarities and Differences. *Immunol Rev*. 2014;259(1):88-102. doi:10.1111/imr.12160.tTregs

44. Tekguc M, Wing JB, Osaki M, Long J, Sakaguchi S. Treg-expressed CTLA-4 depletes CD80/CD86 by trogocytosis, releasing free PD-L1 on antigen-presenting cells. *PNAS*. 2021;118(30). doi:10.1073/pnas.2023739118

45. Lee GR. The Balance of Th17 versus Treg Cells in Autoimmunity. *International Journal of Molecular Sciences*. 2018;19(3):1-14. doi:10.3390/ijms19030730

46. Noack M, Miossec P. Th17 and regulatory T cell balance in autoimmune and inflammatory diseases. *Autoimmunity Reviews*. 2014;13(6):668-677. doi:10.1016/j.autrev.2013.12.004

47. McGeachy MJ, Cua DJ. Th17 Cell Differentiation: The Long and Winding Road. *Immunity*. 2008;28(4):445-453. doi:10.1016/j.immuni.2008.03.001

48. Taams LS. Interleukin-17 in rheumatoid arthritis: Trials and tribulations. *Journal of Experimental Medicine*. 2020;217(3). doi:10.1084/jem.20192048

49. Dubin PJ, Kolls JK. Interleukin-17A and Interleukin-17F: A Tale of Two Cytokines. *Immunity*. 2009;30(1):9-11. doi:10.1016/j.immuni.2008.12.010

50. Bhaumik S, Basu R. Cellular and molecular dynamics of Th17 differentiation and its developmental plasticity in the intestinal immune response. *Frontiers in Immunology*. 2017;8(MAR). doi:10.3389/fimmu.2017.00254

51. Yasuda K, Takeuchi Y, Hirota K. The pathogenicity of Th17 cells in autoimmune diseases. *Seminars in Immunopathology*. 2019;41(3):283-297. doi:10.1007/s00281-019-00733-8

52. Cerboni S, Gehrmann U, Preite S, Mitra S. Cytokine-regulated Th17 plasticity in human health and diseases. *Immunology*. 2021;163(1):3-18. doi:10.1111/imm.13280

53. Annunziato F, Cosmi L, Liotta F, Maggi E, Romagnani S. Defining the human T helper 17 cell phenotype. *Trends in Immunology*. 2012;33(10):505-512. doi:10.1016/j.it.2012.05.004

54. McGinley AM, Sutton CE, Edwards SC, et al. Interleukin-17A Serves a Priming Role in Autoimmunity by Recruiting IL-1β-Producing Myeloid Cells that Promote Pathogenic T Cells. *Immunity*. 2020;52(2):342-356.e6. doi:10.1016/j.immuni.2020.01.002

55. MacIver NJ, Michalek RD, Rathmell JC. Metabolic Regulation of T Lymphocytes. *Annual Review of Immunology*. 2013;31(1):259-283. doi:10.1146/annurev-immunol-032712-095956

56. Chapman NM, Boothby MR, Chi H. Metabolic coordination of T cell quiescence and activation. *Nature Reviews Immunology*. 2019;20(January). doi:10.1038/s41577-019-0203-y

57. Sukumar M, Liu J, Ji Y, et al. Inhibiting glycolytic metabolism enhances CD8+ T cell memory and antitumor function. *Journal of Clinical Investigation*. 2013;123(10):4479-4488. doi:10.1172/JCI69589

58. van Hamburg JP, Tas SW. Molecular mechanisms underpinning T helper 17 cell heterogeneity and functions in rheumatoid arthritis. *Journal of Autoimmunity*. 2018;87:69-81. doi:10.1016/j.jaut.2017.12.006

59. Nistala K, Adams S, Cambrook H, et al. Th17 plasticity in human autoimmune arthritis is driven by the inflammatory environment. *Proc Natl Acad Sci U S A*. 2010;107(33):14751-14756. doi:10.1073/pnas.1003852107

60. Yang P, Qian FY, Zhang MF, et al. Th17 cell pathogenicity and plasticity in rheumatoid arthritis. *Journal of Leukocyte Biology*. 2019;106(6):1233-1240. doi:10.1002/JLB.4RU0619-197R

61. Zhong W, Zhao L, Liu T, Jiang Z. IL-22-producing CD4+T cells in the treatment response of rheumatoid arthritis to combination therapy with methotrexate and leflunomide. *Scientific Reports*. 2017;7. doi:10.1038/srep41143

62. Furue M, Furue K, Tsuji G, Nakahara T. Interleukin-17A and Keratinocytes in Psoriasis. *Int J Mol Sci*. 2020;21. doi:10.3390/ijms21041275

63. Marinoni B, Ceribelli A, Massarotti MS, Selmi C. The Th17 axis in psoriatic disease: Pathogenetic and therapeutic implications. *Autoimmunity Highlights*. 2014;5(1):9-19. doi:10.1007/s13317-013-0057-4

64. Bugaut H, Aractingi S. Major Role of the IL17/23 Axis in Psoriasis Supports the Development of New Targeted Therapies. *Frontiers in Immunology*. 2021;12. doi:10.3389/fimmu.2021.621956

65. Kanda N, Hoashi T, Saeki H. The Defect in Regulatory T Cells in Psoriasis and Therapeutic Approaches. *Journal of Clinical Medicine*. 2021;10. doi:doi.org/10.3390/jcm10173880

66. Nussbaum Id L, Chen YL, Ogg GS, Ogg GS. Role of regulatory T cells in psoriasis pathogenesis and treatment Funding sources. *British Journal of Dermatology*. Published online 2020. doi:10.1111/bjd.19380

67. Ramesh R, Kozhaya L, McKevitt K, et al. Pro-inflammatory human Th17 cells selectively express P-glycoprotein and are refractory to glucocorticoids. *Journal of Experimental Medicine*. 2014;211(1):89-104. doi:10.1084/jem.20130301

68. Harbour SN, Maynard CL, Zindl CL, Schoeb TR, Weaver CT. Th17 cells give rise to Th1 cells that are required for the pathogenesis of colitis. *Proc Natl Acad Sci U S A*. 2015;112(22):7061-7066. doi:10.1073/pnas.1415675112

69. Ueno A, Jeffery L, Kobayashi T, Hibi T, Ghosh S, Jijon H. Th17 plasticity and its relevance to inflammatory bowel disease. *Journal of Autoimmunity*. 2018;87:38-49. doi:10.1016/j.jaut.2017.12.004

70. Zhao J, Lu Q, Liu Y, et al. Th17 Cells in Inflammatory Bowel Disease: Cytokines, Plasticity, and Therapies. *Journal of Immunology Research*. 2021;2021. doi:10.1155/2021/8816041

71. Maeda S, Osaga S, Maeda T, et al. Circulating Th17.1 cells as candidate for the prediction of therapeutic response to abatacept in patients with rheumatoid arthritis: An exploratory research. *PLoS ONE*. 2019;14(11). doi:10.1371/journal.pone.0215192

72. Georas, Steve N. TJC. Sarcoidosis and T-Helper Cells Th1, Th17, or Th17.1. *American Journal of Respiratory and Critical Care Medicine*. 2016;193(11):2014-2016.

73. van Langelaar J, van der Vuurst De Vries RM, Janssen M, et al. T helper 17.1 cells associate with multiple sclerosis disease activity: Perspectives for early intervention. *Brain*. 2018;141(5):1334-1349. doi:10.1093/brain/awy069

74. Wei M, Duan D. Efficacy and safety of monoclonal antibodies targeting interleukin-17 pathway for inflammatory arthritis: a meta-analysis of randomized controlled clinical trials. *Drug Design, Development and Therapy*. Published online 2016:10-2771. doi:10.2147/DDDT.S91374

75. de Cabo R, Mattson MP. Effects of Intermittent Fasting on Health, Aging, and Disease. *N Engl J Med*. 2019;381(26):2541-2551. doi:10.1056/NEJMra1905136

76. Bolla AM, Caretto A, Laurenzi A, Scavini M, Piemonti L. Low-carb and ketogenic diets in type 1 and type 2 diabetes. *Nutrients*. 2019;11(5). doi:10.3390/nu11050962

77. García-Rodríguez D, Giménez-Cassina A. Ketone Bodies in the Brain Beyond Fuel Metabolism: From Excitability to Gene Expression and Cell Signaling. *Frontiers in Molecular Neuroscience*. 2021;14. doi:10.3389/fnmol.2021.732120

78. White H, Venkatesh B. Introduction Clinical review: Ketones and brain injury. *Critical Care*. 2011;15(219). doi:doi:10.1186/cc10020

79. Cotter DG, Schugar RC, Crawford PA. Ketone body metabolism and cardiovascular disease. *Am J Physiol Heart Circ Physiol*. 2013;304:1060-1076. doi:10.1152/ajpheart.00646.2012.-Ketone

80. Goday A, Bellido D, Sajoux I, et al. Short-Term safety, tolerability and efficacy of a very low-calorie-ketogenic diet interventional weight loss program versus hypocaloric diet in patients with type 2 diabetes mellitus. *Nutrition and Diabetes*. 2016;6(9):e230. doi:10.1038/nutd.2016.36

81. Choi IY, Lee C, Longo VD. Nutrition and fasting mimicking diets in the prevention and treatment of autoimmune diseases and immunosenescence. *Molecular and Cellular Endocrinology*. 2017;455(1):4-12. doi:10.1016/j.mce.2017.01.042

82. Newman JC, Verdin E. β-hydroxybutyrate: Much more than a metabolite. *Diabetes Research and Clinical Practice*. 2014;106(2):173-181. doi:10.1016/j.diabres.2014.08.009

83. Hirschberger S, Strauß G, Effinger D, et al. Very-low-carbohydrate diet enhances human T-cell immunity through immunometabolic reprogramming. *EMBO Molecular Medicine*. Published online 2021:1-18. doi:10.15252/emmm.202114323

84. Ketonkörper - Kompaktlexikon der Biologie. Accessed February 23, 2022. https://www.spektrum.de/lexikon/biologie-kompakt/ketonkoerper/6343

85. Newman JC, Verdin E. β-Hydroxybutyrate: A Signaling Metabolite. *Annual Review of Nutrition*. 2017;37:51-76. doi:10.1146/annurev-nutr-071816

86. Puchalska P, Crawford PA. Multi-dimensional Roles of Ketone Bodies in Fuel Metabolism, Signaling, and Therapeutics. *Cell Metabolism*. 2017;25(2):262-284. doi:10.1016/j.cmet.2016.12.022

87. Veech RL, Bradshaw PC, Clarke K, Curtis W, Pawlosky R, King MT. Ketone bodies mimic the life span extending properties of caloric restriction. *IUBMB Life*. 2017;69(5):305-314. doi:10.1002/iub.1627

88. Veech RL. The therapeutic implications of ketone bodies: The effects of ketone bodies in pathological conditions: Ketosis, ketogenic diet, redox states, insulin resistance, and mitochondrial metabolism. *Prostaglandins Leukotrienes and Essential Fatty Acids*. 2004;70(3):309-319. doi:10.1016/j.plefa.2003.09.007

89. Shimazu T, Hirschey MD, Newman J, et al. Supression of oxidative stress and β-OHB as endogenous histone deactetylase. *Science (1979)*. 2013;339(6116):211-214. doi:10.1126/science.1227166.Suppression

90. Xie Z, Zhang D, Chung D, et al. Metabolic Regulation of Gene Expression by Histone Lysine β-Hydroxybutyrylation. *Molecular Cell*. 2016;62(2):194-206. doi:10.1016/j.molcel.2016.03.036

91. Rahman M, Muhammad S, Khan MA, et al. The b-hydroxybutyrate receptor HCA 2 activates a neuroprotective subset of macrophages. *Nature Communications*. 2014;5. doi:10.1038/ncomms4944

92. D'Andrea Meira I, Romão TT, do Prado HJP, Krüger LT, Pires MEP, da Conceição PO. Ketogenic diet and epilepsy: What we know so far. *Frontiers in Neuroscience*. 2019;13(JAN). doi:10.3389/fnins.2019.00005

93. Poff AM, Moss S, Soliven M, D'Agostino DP. Ketone Supplementation: Meeting the Needs of the Brain in an Energy Crisis. *Frontiers in Nutrition*. 2021;8. doi:10.3389/fnut.2021.783659

94. Youm YH, Nguyen KY, Grant RW, et al. The ketone metabolite β-hydroxybutyrate blocks NLRP3 inflammasome-mediated inflammatory disease. *Nature Medicine*. 2015;21(3):263-269. doi:10.1038/nm.3804

95. Goldberg EL, Asher JL, Molony RD, et al. β-Hydroxybutyrate Deactivates Neutrophil NLRP3 Inflammasome to Relieve Gout Flares. *Cell Reports*. 2017;18(9):2077-2087. doi:10.1016/j.celrep.2017.02.004

96. Choi IY, Piccio L, Childress P, et al. A Diet Mimicking Fasting Promotes Regeneration and Reduces Autoimmunity and Multiple Sclerosis Symptoms. *Cell Reports*. 2016;15(10):2136-2146. doi:10.1016/j.celrep.2016.05.009

97. Cell separation strategies using MACS® Technology | Deutschland. Accessed April 16, 2022. https://www.miltenyibiotec.com/DE-en/products/macs-cell-separation/macs-cell-separation-strategies.html#gref

98. Barbi J, Pardoll D, Pan F. Metabolic control of the Treg/Th17 axis. *Immunological Reviews*. 2013;252(1):52-77. doi:10.1111/imr.12029

99. https://www.istockphoto.com/de/7romawka7. Accessed May 9, 2022. https://www.istockphoto.com/de/7romawka7

100. GeneCards - Human Genes | Gene Database | Gene Search. Accessed May 20, 2022. https://www.genecards.org/

101. Liebmann M, Hucke S, Koch K, et al. Nur77 serves as a molecular brake of the metabolic switch during T cell activation to restrict autoimmunity. *Proc Natl Acad Sci U S A*. 2018;115(34):E8017-E8026. doi:10.1073/pnas.1721049115

102. Liu X, Wang Y, Lu H, et al. Genome-wide analysis identifies NR4A1 as a key mediator of T cell dysfunction. *Nature*. 2019;567(7749):525-529. doi:10.1038/s41586-019-0979-8

103. Afshin A, Sur PJ, Fay KA, et al. Health effects of dietary risks in 195 countries, 1990–2017: a systematic analysis for the Global Burden of Disease Study 2017. *The Lancet*. 2019;393(10184):1958-1972. doi:10.1016/S0140-6736(19)30041-8

104. Abderrazak A, Syrovets T, Couchie D, et al. NLRP3 inflammasome: From a danger signal sensor to a regulatory node of oxidative stress and inflammatory diseases. *Redox Biology*. 2015;4:296-307. doi:10.1016/j.redox.2015.01.008

105. Zinöcker MK, Lindseth IA. The western diet–microbiome-host interaction and its role in metabolic disease. *Nutrients*. 2018;10(3). doi:10.3390/nu10030365

106. Nassar MF, El-Gendy YGA, Hamza MT, Mohamed MN, Radwan N. Effect of ketogenic diet for drug-resistant epilepsy on immunological cells. *Neurological Sciences*. 2021;(0123456789). doi:10.1007/s10072-021-05574-8

107. Talib WH, Mahmod AI, Kamal A, et al. Ketogenic diet in cancer prevention and therapy: Molecular targets and therapeutic opportunities. *Current Issues in Molecular Biology*. 2021;43(2):558-589. doi:10.3390/cimb43020042

108. Ang QY, Alexander M, Newman JC, et al. Ketogenic Diets Alter the Gut Microbiome Resulting in Decreased Intestinal Th17 Cells. *Cell*. Published online 2020:1-13. doi:10.1016/j.cell.2020.04.027

109. Street SEA, Cretney E, Smyth MJ. Perforin and interferon-activities independently control tumor initiation, growth, and metastasis. *Blood*. 2001;97(1).

110. Osińska I, Popko K, Demkow U. Perforin: An important player in immune response. *Central European Journal of Immunology*. 2014;39(1):109-115. doi:10.5114/ceji.2014.42135

111. Thiery J, Keefe D, Boulant S, et al. Perforin pores in the endosomal membrane trigger the release of endocytosed granzyme B into the cytosol of target cells. *Nature Immunology*. 2011;12(8):770-777. doi:10.1038/ni.2050

112. Nelson BH. IL-2, Regulatory T Cells, and Tolerance. *The Journal of Immunology*. 2004;172(7):3983-3988. doi:10.4049/jimmunol.172.7.3983

113. Zorn E, Nelson EA, Mohseni M, et al. IL-2 regulates FOXP3 expression in human CD4+CD25+ regulatory T cells through a STAT-dependent mechanism and induces the expansion of these cells in vivo. *Blood*. 2006;108(5):1571-1579. doi:10.1182/blood-2006-02-004747

114. Laurence A, Tato CM, Davidson TS, et al. Interleukin-2 Signaling via STAT5 Constrains T Helper 17 Cell Generation. *Immunity*. 2007;26(3):371-381. doi:10.1016/j.immuni.2007.02.009

115. Stockinger B. Good for Goose, but Not for Gander: IL-2 Interferes with Th17 Differentiation. *Immunity*. 2007;26(3):278-279. doi:10.1016/j.immuni.2007.03.001

116. Cooney LA, Towery K, Endres J, Fox DA. Sensitivity and Resistance to Regulation by IL-4 during Th17 Maturation. *The Journal of Immunology*. 2011;187(9):4440-4450. doi:10.4049/jimmunol.1002860

117. Chatterjee P, Chiasson VL, Bounds KR, Mitchell BM. Regulation of the anti-inflammatory cytokines interleukin-4 and interleukin-10 during pregnancy. *Frontiers in Immunology*. 2014;5(MAY):1-1. doi:10.3389/fimmu.2014.00253

118. Guenova E, Skabytska Y, Hoetzenecker W, et al. IL-4 abrogates TH17 cell-mediated inflammation by selective silencing of IL-23 in antigen-presenting cells. *Proc Natl Acad Sci U S A*. 2015;112(7):2163-2168. doi:10.1073/pnas.1416922112

119. Stadhouders R, Lubberts E, Hendriks RW. A cellular and molecular view of T helper 17 cell plasticity in autoimmunity. *Journal of Autoimmunity*. 2018;87:1-15. doi:10.1016/j.jaut.2017.12.007

120. Karmaus PWF, Chen X, Lim SA, et al. Metabolic heterogeneity underlies reciprocal fates of TH17 cell stemness and plasticity. *Nature*. 2019;565(7737):101-105. doi:10.1038/s41586-018-0806-7

121. Bantug GR, Galluzzi L, Kroemer G, Hess C. The spectrum of T cell metabolism in health and disease. *Nature Reviews Immunology*. 2018;18(1):19-34. doi:10.1038/nri.2017.99

122. Shen H, Shi LZ. Metabolic regulation of Th17 cells. *Molecular Immunology*. 2019;109(March):81-87. doi:10.1016/j.molimm.2019.03.005

123. Kono M, Yoshida N, Maeda K, et al. Pyruvate dehydrogenase phosphatase catalytic subunit 2 limits Th17 differentiation. *Proc Natl Acad Sci U S A*. 2018;115(37):9288-9293. doi:10.1073/pnas.1805717115

124. Gerriets VA, Rathmell JC. Metabolic pathways in T cell fate and function. *Trends in Immunology*. 2012;33(4):168-172. doi:10.1016/j.it.2012.01.010

125. Kaufmann U, Kahlfuss S, Yang J, Ivanova E, Koralov SB, Feske S. Calcium Signaling Controls Pathogenic Th17 Cell-Mediated Inflammation by Regulating Mitochondrial Function. *Cell Metabolism*. 2019;29(5):1104-1118.e6. doi:10.1016/j.cmet.2019.01.019

126. Franchi L, Monteleone I, Hao LY, et al. Inhibiting Oxidative Phosphorylation In Vivo Restrains Th17 Effector Responses and Ameliorates Murine Colitis. *The Journal of Immunology*. 2017;198(7):2735-2746. doi:10.4049/jimmunol.1600810

127. Fuseini H, Cephus JY, Wu P, et al. ERα Signaling Increased IL-17A Production in Th17 Cells by Upregulating IL-23R Expression, Mitochondrial Respiration, and Proliferation. *Frontiers in Immunology*. 2019;10. doi:10.3389/fimmu.2019.02740

128. Manninen AH. Metabolic effects of the very-low-carbohydrate diets: Misunderstood "villains" of human metabolism. *J Int Soc Sports Nutr*. 2004;1(2):7-11. www.sportsnutritionsociety.org

129. Mohorko N, Černelič-Bizjak M, Poklar-Vatovec T, et al. Weight loss, improved physical performance, cognitive function, eating behavior, and metabolic profile in a 12-week

ketogenic diet in obese adults. *Nutrition Research*. 2019;62:64-77. doi:10.1016/j.nutres.2018.11.007

130. Oyewole-Said D, Konduri V, Vazquez-Perez J, Weldon SA, Levitt JM, Decker WK. Beyond T-Cells: Functional Characterization of CTLA-4 Expression in Immune and Non-Immune Cell Types. *Frontiers in Immunology*. 2020;11. doi:10.3389/fimmu.2020.608024

131. Klocke K, Sakaguchi S, Holmdahl R, Wing K. Induction of autoimmune disease by deletion of CTLA-4 in mice in adulthood. *Proc Natl Acad Sci U S A*. 2016;113(17). doi:10.1073/pnas.1603892113

132. Kolar P, Knieke K, Hegel JKE, et al. CTLA-4 (CD152) controls homeostasis and suppressive capacity of regulatory T cells in mice. *Arthritis and Rheumatism*. 2009;60(1):123-132. doi:10.1002/art.24181

133. Schmidt EM, Wang CJ, Ryan GA, et al. CTLA-4 Controls Regulatory T Cell Peripheral Homeostasis and Is Required for Suppression of Pancreatic Islet Autoimmunity. *The Journal of Immunology*. 2009;182(1):274-282. doi:10.4049/jimmunol.182.1.274

134. Chan D v., Gibson HM, Aufiero BM, et al. Differential CTLA-4 expression in human CD4+ versus CD8 + T cells is associated with increased NFAT1 and inhibition of CD4+ proliferation. *Genes and Immunity*. 2014;15(1):25-32. doi:10.1038/gene.2013.57

135. Sehrawat S, Rouse BT. Interplay of regulatory T cell and Th17 cells during infectious diseases in humans and animals. *Frontiers in Immunology*. 2017;8(APR). doi:10.3389/fimmu.2017.00341

136. Shan J, Jin H, Xu Y. T Cell Metabolism: A New Perspective on Th17/Treg Cell Imbalance in Systemic Lupus Erythematosus. *Frontiers in Immunology*. 2020;11. doi:10.3389/fimmu.2020.01027

137. Lee GR. The Balance of Th17 versus Treg Cells in Autoimmunity. *International Journal of Molecular Sciences*. 2018;19.

138. Sakkas LI, Zafiriou E, Bogdanos DP. Mini review: New treatments in psoriatic arthritis. Focus on the IL-23/17 Axis. *Frontiers in Pharmacology*. 2019;10(JULY). doi:10.3389/fphar.2019.00872

139. Mulcahy ME, Leech JM, Renauld JC, Mills KHG, McLoughlin RM. Interleukin-22 regulates antimicrobial peptide expression and keratinocyte differentiation to control Staphylococcus aureus colonization of the nasal mucosa. *Mucosal Immunology*. 2016;9(6):1429-1441. doi:10.1038/mi.2016.24

140. Littman DR, Rudensky AY. Th17 and Regulatory T Cells in Mediating and Restraining Inflammation. *Cell*. 2010;140(6):845-858. doi:10.1016/j.cell.2010.02.021

141. Ma CS, Chew GYJ, Simpson N, et al. Deficiency of Th17 cells in hyper IgE syndrome due to mutations in STAT3. *Journal of Experimental Medicine*. 2008;205(7):1551-1557. doi:10.1084/jem.20080218

142. McDonald DR. Th17 deficiency in human disease. *Journal of Allergy and Clinical Immunology*. 2012;129(6):1429-1435. doi:10.1016/j.jaci.2012.03.034

9 Publications and scientific presentations

9.1 PUBLISHED PARTS OF THESIS

Parts of this thesis have been published in:

Hirschberger, S., Strauß, G., **Effinger, D**., Marstaller, X., Ferstl, A., Müller, M. B., Wu, T., Hübner, M., Rahmel, T., Mascolo, H., Exner, N., Heß, J., Kreth, F. W., Unger, K. & Kreth, S. Very-low-carbohydrate diet enhances human T-cell immunity through immunometabolic reprogramming. EMBO Mol. Med. 13, e14323 (2021).

D. Effinger, S. Hirschberger, P. Yoncheva, S. Kreth
Eine ketogene Diät supprimiert den humanen Th17-Immunmetabolismus
Hauptstadtkongress der DGAI 2021
ePosterabstract, Anästhesie & Intensivmedizin 2021

9.2 ALL SCIENTIFIC PUBLICATIONS

Müller, M. B., Hübner, M., Li, L., Tomasi, S., Ließke, V., **Effinger, D.**, Hirschberger, S., Pogoda, K., Sperandio, M. & Kreth, S. Cell-crossing functional network driven by microRNA-125a regulates endothelial permeability and monocyte trafficking in acute inflammation. Front. Immunol. (2022)

Hirschberger, S., Strauß, G., **Effinger, D.**, Marstaller, X., Ferstl, A., Müller, M. B., Wu, T., Hübner, M., Rahmel, T., Mascolo, H., Exner, N., Heß, J., Kreth, F. W., Unger, K. & Kreth, S. Very-low-carbohydrate diet enhances human T-cell immunity through immunometabolic reprogramming. EMBO Mol. Med. 13, e14323 (2021).

Hübner, M.*, **Effinger, D.***, Wu, T., Strauß, G., Pogoda, K., Kreth, F.-W. & Kreth, S. The IL-1 Antagonist Anakinra Attenuates Glioblastoma Aggressiveness by Dampening Tumor-Associated Inflammation. Cancers 12, (2020).
*** both authors contributed equally**

Hübner, M., Moellhoff, N., **Effinger, D.**, Hinske, C. L., Hirschberger, S., Wu, T., Müller, M. B., Strauß, G., Kreth, F.-W. & Kreth, S. MicroRNA-93 acts as an 'anti-inflammatory tumor suppressor' in glioblastoma. Neurooncol Adv 2, vdaa047 (2020).

Rahmel, T., Hübner, M., Koos, B., Wolf, A., Willemsen, K.-M., Strauß, G., **Effinger, D.**, Adamzik, M. & Kreth, S. Impact of carbohydrate-reduced nutrition in septic patients on ICU: study protocol for a prospective randomised controlled trial. BMJ Open 10, e038532 (2020).

Hirschberger, S., Hübner, M., Strauß, G., **Effinger, D.**, Bauer, M., Weis, S., Giamarellos-Bourboulis, E. J. & Kreth, S. Identification of suitable controls for miRNA quantification in T-cells and whole blood cells in sepsis. Sci. Rep. 9, 15735 (2019)

Hübner, M., Tomasi, R., **Effinger, D.**, Wu, T., Klein, G., Bender, M., Kilger, E., Juchem, G., Schwedhelm, E. & Kreth, S. Myeloid-Derived Suppressor Cells Mediate Immunosuppression After Cardiopulmonary Bypass. Crit. Care Med. 47, e700–e709 (2019).

Hübner, M., Hinske, C. L., **Effinger, D.**, Wu, T., Thon, N., Kreth, F.-W. & Kreth, S. Intronic miR-744 Inhibits Glioblastoma Migration by Functionally Antagonizing Its Host Gene MAP2K4. Cancers 10, (2018).

10 Acknowledgements

Throughout the preparation and writing of this dissertation I have experienced a great deal of support and assistance. Therefore, I would like to take this opportunity to thank all those who have accompanied me over the past years and without whose support this work would not have been possible.

First and foremost, I would like to thank my supervisor Prof. Dr. Dr. med. Simone Kreth. Only her enthusiasm for the subject made this project possible in the first place. With her passionate interest in science, she was able to inspire me to pursue research and the field of nutritional medicine well beyond this dissertation.

Likewise, I would also like to thank Prof. Dr. med. Bernhard Zwißler for the ongoing support and the opportunity to conduct research to this extent.

Once again, I thank Gabriele Strauß, Annika Schmid, Simon Hirschberger, Max Hübner, Martin Müller, Gabriele Gröger, Gudrun Prangenberg, Jessica Drexler, Katja Gieseke, Florian Gosselin, Bärbel Reincke and the entire research group. The constant support not only in technical matters and the unique familiar atmosphere are far from self-evident. I consider it a great privilege to have the opportunity to work not only with colleagues but with friends.

Finally, I wish to express my sincere gratitude toward my family whose constant support and continuous encouragement kept me motivated and confident throughout all these years.

11 Affidavit

LMU LUDWIG-MAXIMILIANS-UNIVERSITÄT MÜNCHEN

Dekanat Medizinische Fakultät
Promotionsbüro

Affidavit

Effinger, David

Surname, first name

Marchioninistraße 15, 81377 München

Address

I hereby declare, that the submitted thesis entitled

Ketogenic diet enhances human T-cell immunity and reprograms the immunometabolism of Th17 and regulatory T cells

is my own work. I have only used the sources indicated and have not made unauthorised use of services of a third party. Where the work of others has been quoted or reproduced, the source is always given.

I further declare that the dissertation presented here has not been submitted in the same or similar form to any other institution for the purpose of obtaining an academic degree.

Munich, 18.11.22

Place, Date

David Effinger

Signature doctoral candidate

Affidavit 18.11.2022

12 Confirmation of congruency

LMU LUDWIG-MAXIMILIANS-UNIVERSITÄT MÜNCHEN

Dekanat Medizinische Fakultät
Promotionsbüro

Confimation of congruency between printed and electronic version of the doctoral thesis

Doctoral Candidate: David Effinger

Address: Marchioninistraße 15, 81377 München

I hereby declare that the electronic version of the submitted thesis, entitled

Ketogenic diet enhances human T-cell immunity and reprograms the immunometabolism of Th17 and regulatory T cells

is congruent with the printed version both in content and format.

Munich, 18.11.2022
Place, Date

David Effinger
Signature doctoral candidate

Congruency of submitted versions Date: 18.11.2022